Gross Motion Planning—A Survey

YONG K. HWANG

Sandia National Laboratories, Albuquerque, New Mexico 87185

NARENDRA AHUJA

Beckman Institute and Coordinated Science Laboratory, University of Illinois, Urbana, Illinois 61801

Motion planning is one of the most important areas of robotics research. The complexity of the motion-planning problem has hindered the development of practical algorithms. This paper surveys the work on gross-motion planning, including motion planners for point robots, rigid robots, and manipulators in stationary, time-varying, constrained, and movable-object environments. The general issues in motion planning are explained. Recent approaches and their performances are briefly described, and possible future research directions are discussed.

Categories and Subject Descriptors: I.2.8 [**Artificial Intelligence**]: Problem Solving, Control Methods, and Search—*graph and tree search strategies*; *heuristic methods*; I.2.9 [**Artificial Intelligence**]: Robotics; I.2.10 [**Artificial Intelligence**]: Vision and Scene Understanding—*motion*

General Terms: Algorithms, Theory

Additional Key Words and Phrases: Collision detection, computational geometry, implementation, motion planning, obstacle avoidance, path planning, spatial representation

INTRODUCTION

Until recently, robots were primarily employed for carrying out programmed, repetitious tasks. Methodologies and algorithms for autonomous functioning were examined, but their implementation was hindered by the slow computing hardware. With the rapid advances in semiconductor and computing technology, it has become feasible to build robots that can function at reasonable speeds. Much research has been done to develop theories and algorithms needed for robots to process information and interact with the environment. Examples of such capabilities include perception, reasoning, planning, manipulation, and learning.

This paper is concerned with the state of the art of the research done on autonomous motion planning.

Consider a highly automated factory where mobile robots pick up parts and deliver them to assembly robots (Figure 1). The robots must find their way to parts, pick them up, and move to the assembly stations. All these motions have to be executed without colliding with objects and other robots. Paths of the robots have to be short, and the pickup operations should not include unnecessary movements. Without a motion planner for the robots and arms, human operators have to constantly specify the motions. An automatic motion planner will relieve the operators from this
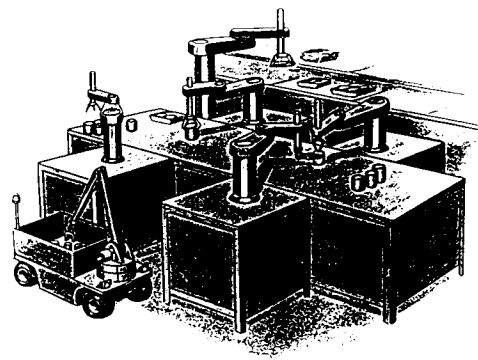
CONTENTS

Figure 1. Robots in an automated factory. Mobile robots deliver parts from the warehouse to assembly robots. Mobile robots need to find short paths while avoiding objects and other robots. The assembly robots also need to avoid collisions during their assembly motions.

tedious job and enable them to control at a supervisory level. In turn, this increases efficiency by eliminating human errors. The need for collision avoidance and efficient motion leads to the problem of motion planning (MP). Motion planning can be broadly classified as either *gross-* or *fine-*motion planning.

Gross-motion planning is concerned with the problems involving free space much wider than the objects' sizes plus the positional error of the robot. This ensures that positional error will not cause unexpected collisions while executing the collision-free paths generated by gross motion planners. Fine-motion planning deals with the problem of moving objects when the space is so narrow that the required accuracy of motion exceeds a robot's positional accuracy. Each problem requires a different approach to plan motion.

This paper presents a survey of recent developments in gross-motion planning. It summarizes the past work, mostly in computational geometry and robotics, and discusses possible directions for future research. It is directed toward people interested in motion-planning

research or in implementing an algorithm on real robots. There are several different classes of motion-planning problems. Motion planning can be static or dynamic, depending on whether the information on the robot's environment is fixed or updated. If obstacles are stationary (moving), it is called time invariant (time varying). If robots can move some objects, it is called the movable-object problem. If motions of more than one robot are planned, it is called the multimovers problem. If the robot can change its shape it is conformable. Motion planning is either constrained or unconstrained, depending on whether there are constraints on a robot's motion other than the geometric interference. These include bounds on a robot's velocity and acceleration and constraints on the curvature of a robot's paths.

In order to review the past work in these categories, a classification scheme is developed in Section 1. Complexity of motion planning is also discussed in Section 1. Section 2 discusses the basic issues and steps common to all motion-planning approaches. Section 3 surveys work on motion planning following the classification scheme presented in Section 1, and for each class surveying different approaches according to how they address the issues described in Section 2. Section

4 concludes this paper with suggestions for developing efficient MP algorithms.

1. NATURE OF MOTION-PLANNING PROBLEM

This section introduces the definitions of terms used in MP. The complexity of MP is then discussed to show how hard MP is. Readers not interested in complexity analysis may skip this part (Section 1.2). Next, classification of the different gross-motion-planning problems and algorithms are presented, which are used to survey the MP work in Section 3.

1.1 Definitions of Terms

We will give definitions of terms and illustrate concepts using Figure 2. *Robots* are the things that are moving, whether points, polytopes, or manipulators. A *manipulator* is a mechanical arm consisting of links and joints. *Polytopes* are polygons in two dimensions (2D) or polyhedra in three dimensions (3D). The shapes of rigid robots or links of manipulators are typically given as polytopes or by formula using constructive solid geometry. The *world space* refers to the physical space in which robots and obstacles exist. The *configuration* of an object of a given shape is a set of independent parameters that characterizes the position of *every* point in the object. Six numbers are needed to specify the configuration of a rigid body in three dimensions (three for position, three for orientation specification). Given the shape of each link of a manipulator, the configuration of the manipulator can be specified by the angles at its joints (Figure 2a). The number of parameters specifying the configuration of an object is called the *degrees of freedom* (dof) of the object. The set of all configurations are called the *configuration space* (*Cspace*). The *free space* refers to parts of the world space not occupied by obstacles or parts of the Cspace for which the robot does not collide with any obstacle. We use the term *feasible* to mean collision free. The *path* of an object is a curve in

the configuration space. The manipulator motion in Figure 2b corresponds to the path in Figure 2c. The curve is represented either by a mathematical expression or by a sequence of points along the curve. The *trajectory* is the path along with an assignment of time—the time assigned to a point along the path denotes the time instant at which the object assumes the configuration associated with that point. Motion planning is a general term that refers to either path planning or trajectory planning.

For complexity analysis, m and n denote the complexities of robots and obstacles, respectively. For polygonal (polyhedral) objects, m and n denote the number of edges (faces and edges) unless stated otherwise. The number of degrees of freedom of a robot is denoted by d; $\Omega(\ )$ denotes a lower bound. The terms describing the hardness of problems are briefly explained. If there is a polynomial-time algorithm to solve a problem, the problem is said to be in P. A problem is in NP (nondeterministic polynomial) if there is a polynomial-time algorithm to verify a solution to the problem (thus $P \subseteq NP$). This means that a problem in NP can be solved in polynomial time if we have an infinite number of computers to verify in parallel all possible branches of the search tree of possible solutions to the problem. In other words, an NP problem requires a very long computation time to solve if the problem size is large. A problem is NP-hard if it is at least as difficult as any NP problem. NP-hardness of a problem is proved by transforming the problem to one of the known NP-hard problems. A problem is NP-complete if it is in NP and NP-hard, and there are several known NP-complete problems. The question of whether or not P = NP is still open. Since it is not known if there is an NP problem that has an exponential lower bound, one cannot conclude that an NP-hard problem has an exponential lower bound. A problem is in PSPACE if it requires a (memory) space polynomial in the problem size. Similar definitions apply to
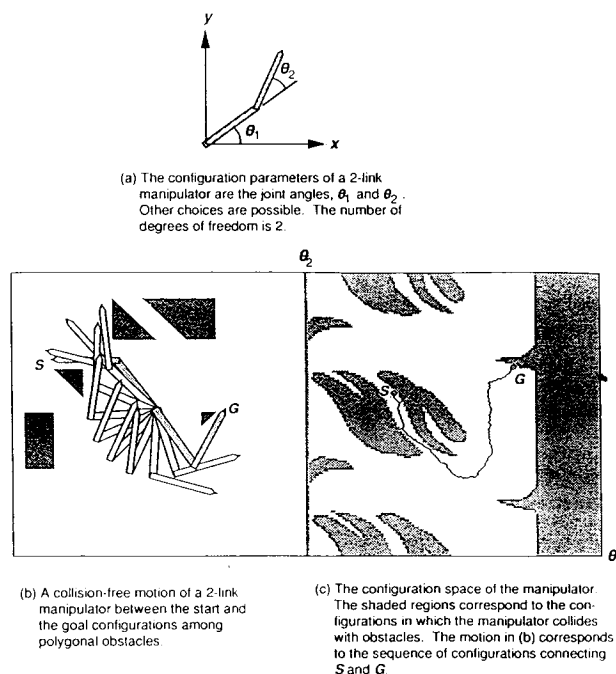
(a) The configuration parameters of a 2-link manipulator are the joint angles, θ_1 and θ_2. Other choices are possible. The number of degrees of freedom is 2.

(b) A collision-free motion of a 2-link manipulator between the start and the goal configurations among polygonal obstacles.

(c) The configuration space of the manipulator. The shaded regions correspond to the configurations in which the manipulator collides with obstacles. The motion in (b) corresponds to the sequence of configurations connecting S and G.

Figure 2. Configuration of a robot.

PSPACE-hardness and PSPACE-completeness. A more detailed discussion about the hardness can be found in Cormen et al. [1990].

Complexity of a problem is analyzed by giving an upper bound or a lower bound on the number of elementary computations or the size of memory space required to solve a problem. An upper bound is obtained by showing an algorithm for the problem having a complexity bounded above by some function of the input size, say $O(u(n))$. A lower bound is obtained by showing a family of example problems whose only solutions are bounded below by some function of the size of the example, say $O(l(n))$. If a problem has matching upper and lower bounds, i.e., $u(n) = l(n)$, then it can be said that the problem has complexity $u(n)$.

1.2 Complexity of Motion Planning

To study the complexity of motion planning, the generalized mover's problem is defined as follows. Given a robot with d degrees of freedom in an environment with n obstacles, find a collision-free path connecting the current (start) configuration of the robot to a desired (goal) configuration. The size of the input is d and n. The complexity of description of the robot, m, is either fixed or incorporated in the complexity of the environment. A historical account of the generalized mover's problem given in Canny [1988] is summarized here; see Canny [1988] for details.

The generalized mover's problem can be solved as follows. The set of robot configurations where the robot does not intersect any obstacles is called the *free configuration space*. Since the shapes of most robots and obstacles can be expressed with semialgebraic sets (unions and intersections of algebraic, e.g., polynomial inequalities), the boundaries of the free configuration space can also be represented with semi-algebraic sets. It may seem that when rotation is included, use of transcendental functions (sine and cosine) is necessary. There is,

$Q = (s, v), \quad s = scalar, \quad v = 3vector.$

$Q^* = (s, -v)$

$Q_1 + Q_2 = (s_1 + s_2, v_1 + v_2)$

$Q_1 Q_2 = (s_1 s_2 - v_1 v_2, s_1 v_2 + s_2 v_1 + v_1 \times v_2)$

Representation of a Point

$p = (0, v)$

Transformation

translation of point p by t

$(0, v + t)$

rotation of point p about vector n by an angle θ

$Q p Q^*, \quad$ where $Q = (cos(\theta/2), n \; sin(\theta/2))$

Figure 3. Quaternion representation of a rotation. The coordinates of a rotated point is a polynomial function of the quaternion coordinates.

however, a representation of rotation, e.g., quaternions, that enables us to relate a rotated position of a point to its original position with an algebraic expression (Figure 3). The free configuration space can then be broken into simpler pieces or *cells*, and the cell adjacency relations are computed. Finding a collision-free path between the start and goal configurations of the robot is equivalent to finding the cells containing the start and goal configurations and then finding a connected sequence of cells representing the free configuration space. This way of solving the generalized mover's problem reduces the problem to that of deciding the satisfiability of formulae in the first-order theory of reals. A formula in this theory is built from boolean combinations of polynomial inequalities, and both existential and universal quantifiers are allowed. A sample formula looks like $\exists x \forall y (y \geq x)$ and $(-y^3 \leq x)$. Tarski [1951] showed that sets defined by such a formula also have a defining formula free of quantifiers, proving that the theory of reals is decidable.

The first upper bound on the complexity of the generalized mover's problem is reported in Schwartz and Sharir [1981]. Using the decomposition method of Collins [1975] to compute cells of the free configuration space, they developed an algorithm that has a double exponential

time complexity of $O(n^{2^{d+6}})$. This double exponential complexity is improved in Canny [1987] and Canny [1988] to a single exponential time. Rather than computing the cells representing the free Cspace, one-dimensional boundary curves of the free Cspace are constructed by projecting the free Cspace in higher dimensions to two dimensions. A collision-free path connecting two robot configurations is found from this network of boundary curves.

The first lower-bound result on the complexity of MP appears in Reif [1979]. The generalized mover's problem in a 3D space is shown to be PSPACE-hard with an example of a many-jointed object constrained to move within a complex system of narrow channels. Reif [1979] also presents a polynomial-space algorithm, proving that the generalized mover's problem is PSPACE-complete. In Hopcroft et al. [1984a], the reachability problem for planar linkages (determining whether the linkage can reach a point) is shown to be PSPACE-hard. The proof consists of showing that there are linkages that are capable of simulating linear-bounded automaton (LBA) computations and that the size of the description of a linkage that simulates a given LBA on input length n is linear in n and the size of the description of LBA. The PSPACE-hardness follows from the fact that the acceptance problem for LBAs is PSPACE-complete (see Hopcroft and Ullman [1979] for LBA and PSPACE).

The planning of coordinated translational motions of iso-oriented rectangles inside a rectangular boundary (see Figure 4a) is shown to be PSPACE-hard in Hopcroft et al. [1984b] by reducing the PSPACE-hard symbol transposition problem to the motion planning of the rectangles described above. The symbol transposition problem is the problem of transforming a given finite string of symbols into another string by a sequence of moves changing the position of a symbol, subject to a set of adjacent rules which constrain the symbols that can stand next to each other. The five darker rectangles at the top in Figure 4a, called *dominoes*,
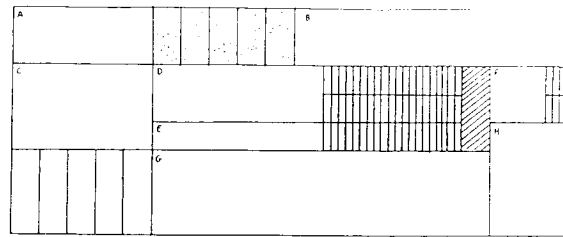
(a) Feasible motions of the five dotted rectangles, called *dominoes*, in the almost full box simulate the *symbol transposition* problem. The hatched region is the only empty space.
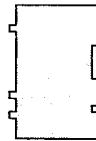
(b) The dominoes have different patterns on their sides
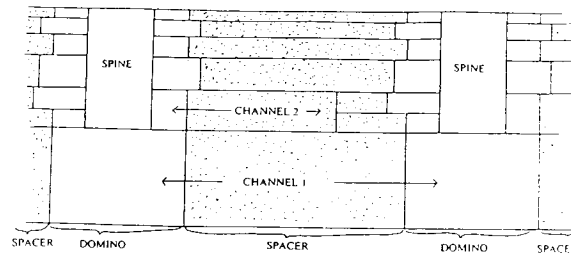
(c) Dominoes are further decomposed into rectangles

Figure 4. Planning coordinated motions of multiple rectangles is PSPACE-hard. Reprinted from *International Journal of Robotics Research*, vol. 3, no. 4, pp. 76–88, Hopcroft, J., Schwartz, J. T., and Sharir, M, "On the complexity of motion planning for multiple independent objects: PSPACE-hardness of the 'warehouseman's problem'," by permission of the MIT Press, Cambridge, Mass., Copyright, © 1984 MIT Press.

represent a string of symbols. Each domino has a pattern of extrusions and indentations on its vertical sides so that only dominoes with matching patterns can be next to each other (see Figure 4b). This encodes the adjacency rules in the symbol transposition problem. The dominoes are further decomposed into rectangles, completing the reduction of the transposition problem to the motion planning of the rectangles (see Figure 4c). This problem is later shown to be in PSPACE in Hopcroft and Wilfong [1986], thus proving its PSPACE completeness. This is shown by analyzing the connected set of the free Cspace. Note the configuration space has dimension $2n$, where n is the number of rectangles, since each

rectangle has 2 degrees of freedom in this problem. The connected set forms a polytope in the $2n$-dimensional space and consists of faces of various dimensions. They show that if there is a collision-free motion of rectangles between two configurations in the connected set, then there is also a collision-free motion along the one-dimensional faces, i.e., edges, of the polytope representing the connected set. Motion planning is reduced from a search of a high-dimensional space to a graph-searching problem, and such motions can be described in polynomial space.

There are many other complexity analyses on various versions of MP, including the shortest-path problem for a point

robot among polygons [Asano et al. 1985], among polyhedral obstacles [Canny and Reif 1987], MP of a line segment in three dimensions [Ke and O'Rourke 1987], and MP among moving obstacles [Reif and Sharir 1985]. These are described in appropriate subsections of Section 3.

Tannenbaum and Yomdin [1987] have shown that the maximal number of the connected components of the semi-algebraic set $\mathbb{R}^d \setminus \cup \{f_i = 0\}$, where $i = 1, \ldots, m$ and $\{f_i = 0\}$ are of degree n, is polynomial in m and n and exponential in the number of degrees of freedom d. This bound is derived from results of algebraic geometry, namely, the Harnack Inequality and the Bezout Theorem, which give upper bounds on the number of intersection points of polynomial curves of degree n. Their result shows that it is likely to take an exponential time in d to compute a description of the entire configuration space. This does not imply that MP has an exponential-time lower bound, since we do not have to compute *all* parts of the configuration space to plan a motion, and there is yet no family of motion-planning problems whose configuration spaces have exponentially many connected components. In summary, the current status of the known complexity bounds on the generalized mover's problem is that it is PSPACE-hard, but has an upper bound which is exponential in the number of degrees of freedom.

1.3 Classification of Motion-Planning Problems

We first explain the distinction between path planning and trajectory planning. Path planning typically refers to the design of only geometric (kinematic) specifications of the positions and orientations of robots, whereas trajectory planning includes the design of the linear and angular velocities as well. Therefore, path planning is a subset of trajectory planning, wherein the dynamics of robots is unimportant or neglected. A case where trajectory planning must be used is the design of walking motion for a biped since the dynamics of balance cannot be neglected. Path planning is also used as the first step in the design of trajectories. When designing a complex sequence of motions, it is often easier to devise the path first and then assign the velocity along the path. We now introduce several variations of the motion-planning problem and establish a framework for classification.

Motion planning can be **static** or **dynamic**, depending on the mode in which the obstacle information is available. In a static problem, all the information about obstacles is known a priori, and the motion of the robot is designed from the given information. In dynamic planning, only partial information is available about the obstacles, e.g., the visible parts of the obstacles. To achieve a given goal, the robot plans a path based on the available information. As the robot follows the path, it discovers more obstacle information. This is used to update the internal representation of the robot's environment, and the robot replans a path from the updated representation. The process of updating the representation and planning paths is continued until the robot accomplishes its goal. Most papers in MP have dealt with the static case.

When there is more than one robot it is called a **multimovers problem**. If objects can change shape then the motion-planning problem is **conformable**. Otherwise it is **nonconformable**. An important subclass of conformable problems concerns motion planning of linked bodies since most robots and manipulators are made of jointed limbs. When the environment or the configurations of obstacles change it is a **time-varying** problem. Otherwise it is a **time-invariant** problem. If robots can move a subset of objects, it is the **movable-object** problem.

Motion planning is either **constrained** or **unconstrained**, according to whether there are inherent restrictions on the motion of robots, i.e., restrictions arising due to reasons other than colli-

sions with obstacles. These include bounds on a robot's velocity and acceleration and constraints on the curvature of robot's paths. Trajectory planning of any physical system is constrained since the actuators (motors) have finite power. Another example is the task of carrying a cup of coffee, which has a severe restriction on the movement of the cup so as not to spill the coffee.

1.4 Classification of Motion-Planning Algorithms

There are two aspects to the classification of MP algorithms: the completeness (*exact* or *heuristic*) and the scope (*global* or *local*). Exact algorithms either find a solution or prove that there is no solution. Exact algorithms are usually computationally expensive. In contrast, heuristic algorithms are aimed at generating a solution in a short time. They may fail to find a solution for difficult problems, or they may find a poor solution. Heuristic algorithms are important in engineering applications, while exact algorithms determine complexities of problems and algorithms. There are two other types of completeness: *resolution completeness* and *probablistic completeness* (we will consider these as exact also). The resolution completeness is related to discretization. When continuous quantities such as obstacle dimensions or configuration parameters are discretized, the associated algorithm is inherently approximate. However, its accuracy can be arbitrarily improved by increasing the resolution of discretization. If an algorithm is exact in the limit as the discretization approaches a continuum it is called resolution complete. An algorithm is probabilistically complete if its probability of finding a solution (if one exists) can be made to approach 1. This characteristic is typical of algorithms using a random search such as simulated annealing. These algorithms need a long computation time to make the probability close to 1.

Global algorithms take into account all the information in the environment, and

they plan a motion from the start to the goal configuration. Local algorithms are designed to avoid obstacles in the vicinity of the robot and thus use information about nearby obstacles only. They are used when the start and goal configurations are close together. Local methods are used as a component in a global planner or as a safety feature to avoid unexpected obstacles not present in the model of the environment but detected by sensors during motion execution.

2. BASIC ISSUES AND STEPS IN MOTION PLANNING

This section describes the basic issues and steps that any MP formulation must involve. These issues include configuration space, object representation, approaches to motion planning, search methods, and local optimization of motion. Motion planning is done in the following steps. First, the configuration parameters of the robot need to be determined. The concept of the Cspace is fundamental to motion planning, since it is the space of all possible motions of a robot. A detailed explanation of the Cspace and methods of computing the set of feasible configurations are given. Second, the robot and objects have to be represented. Several available representation schemes are explained and compared. Third, an MP approach suitable to the MP problem at hand needs to be selected. There are four different approaches developed for MP, and different problems require different approaches. Fourth, a search method must be selected to find a solution path. The choice is determined by the required optimality of the solution and available computing resources. Several search methods are reviewed. Finally, the solution path is locally optimized to yield a shorter and smoother path. Most MP algorithms find a path that contains sharp corners, which cause jerky motions of the robot. Unless the robot is moving at a very slow speed, these corners must be smoothed out. The following subsections discuss these five steps in detail.
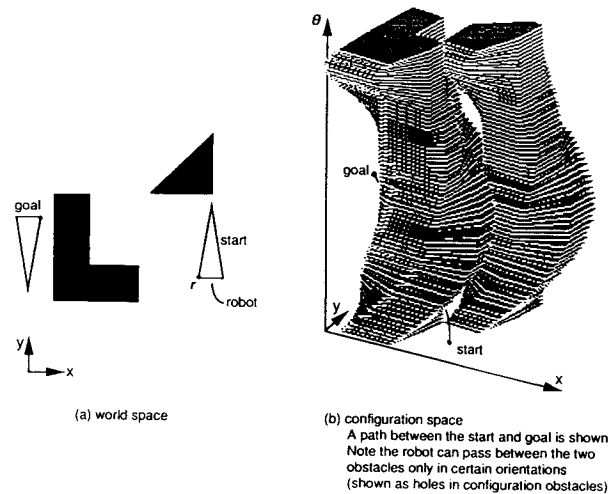
Figure 5. A triangular robot among polygonal obstacles. The configuration parameters are the position of robot vertex r and the rotation about this point. Configuration obstacles are shown in (b).

2.1 World-Space vs. Configuration Space

The world space refers to the physical space robots and obstacles exist in. A configuration of an object or a robot is a set of independent parameters completely specifying the position of *every* point of the object or robot. The space of all possible configurations, the configuration space (Cspace), of an object represents all possible motions of the object and plays a fundamental role in motion planning. It was first used in motion planning in the influential paper by Lozano-Pérez and Wesley [1979]. In essence, all motion-planning problems are equivalent once they are formulated in the configuration space; they reduce to the problem of finding a connected sequence of points between the start and the goal configurations in the Cspace. The dimension of the Cspace is the number of the parameters representing a configuration, also called degrees of freedom.

For a point robot, the Cspace is identical to the world space and has the same number of dimensions. The triangle in Figure 5a needs 3 parameters to specify its configuration, 2 for the position of an arbitrarily chosen reference point of the triangle, and 1 for the orientation of

the triangle about the reference point. The corresponding Cspace has dimension 3. Likewise, a rigid object in 3D world space requires 6 parameters for configuration specification: 3 for the position of the reference point and 3 for the orientation.

Configurations that result in collisions between the robot and obstacles are called the configuration obstacles. A point inside a configuration obstacle corresponds to a situation where the robot overlaps with one or more obstacles (a physically impossible state) and a point on the boundary of a configuration obstacle to a situation where the robot is just touching (in contact with) one or more obstacles. (Methods of computing configuration obstacles are discussed below.) Figure 5b shows the configuration obstacles corresponding to the world space in Figure 5a along with the start and the goal configurations of the robot.

What makes MP hard is the dimensionality of the Cspace, i.e., the space of all possible motions of the robot. For a single rigid robot in 3D world space, the Cspace is 6-dimensional, and representing it with a grid requires 10^{12} points for a resolution of 100 points per dimension. Use of a grid is unrealistic for MP involv-

ing multirobots. To complicate the matter, configuration obstacles do not usually have compact representations, as seen in Figure 2c and 5b. MP is thus a challenging research problem.

Computation of configuration obstacles

There are seven basic ways to compute configuration obstacles: point evaluation, Minkowski set difference, boundary equation, needle, sweep volume, template, and a Jacobian-based method. All of these can be used for any type of robot. Point evaluation is the simplest but most inefficient of them. It places the robot in a configuration and determines whether the robot intersects any obstacles. If the robot does, the configuration belongs to a configuration obstacle.

Minkowski set difference of two sets A and B are the set of points $Mdiff(A, B)$ = $\{a - b | a \in A, b \in B\}$. For a rigid object without rotation, the configuration obstacles are the union of Minkowski set differences between areas occupied by obstacles and the robot. In Figure 6, the reference point of the robot cannot be placed in the shaded region, which is $Mdiff(obstacle, robot)$. If the robot and obstacle are convex polytopes, then the Minkowski set difference of them is the convex hull of the Minkowski set difference of their vertices. This method is most used for polytopes.

In the boundary equation method, one derives the constraints on the configuration variables that bring the robot in contact with obstacles. Such equations of contact constraints define the boundaries of configuration obstacles. For a polyhedral representation, the equations are derived from the vertex/face and edge/ edge contacts between the robot and an obstacle (see Figure 7). These equations can simply be evaluated to determine whether a point is in the configuration obstacles or not. Representing configuration obstacles as a union of nonoverlapping semi-algebraic cells is very difficult (especially for dof > 3).

In the needle method, all but one of the configuration parameters are fixed, and
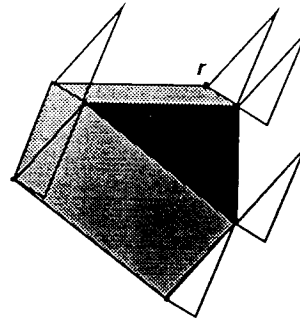
Figure 6. The shaded region is the Minkowski set difference. The reference point of the robot in this orientation cannot be placed in this region.

$x + cos(\theta) = 3$
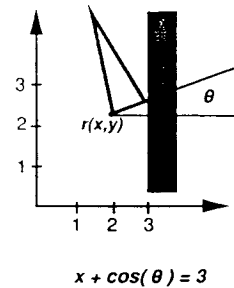
Figure 7. A boundary equation of a configuration obstacle.

the values of the variable parameter that bring the robot in contact with all the obstacles are computed, usually using the boundary equations. From these values, intervals (or needles) that are in configuration obstacles can be computed. This method is commonly used to generate a two-dimensional slice of the Cspace by computing the needles for each value of one of the fixed parameters (Figure 8), but not for any higher-dimensional slice because of the large number of needles needed.

The sweep volume method computes the volume in the world space swept by a robot as the robot configuration is varied over a set in the Cspace. If the sweep volume does not intersect any obstacle, the set in the Cspace is outside of configuration obstacles. This is an effective way

(a) a 2-link manipulator   (b) configuration obstacles

Figure 8. Needle method. For each value of the first joint angle, feasible ranges of the second joint angle are computed. Reprinted from *IEEE Journal of Robotics and Automation*, vol. RA-3, no. 3, pp. 224–238, Lozano-Pérez, T., "A simple motion planning algorithm for general robot manipulators," by permission of IEEE, Piscataway, N.J., Copyright, © 1987 IEEE.
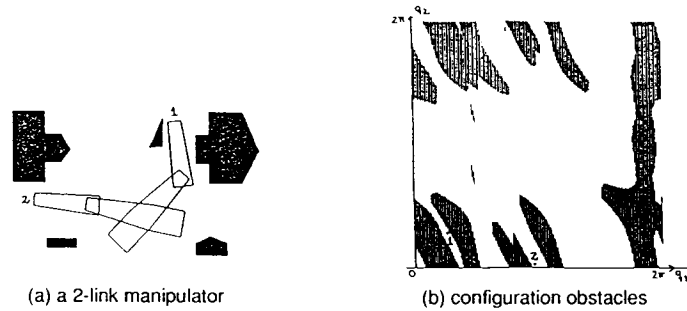

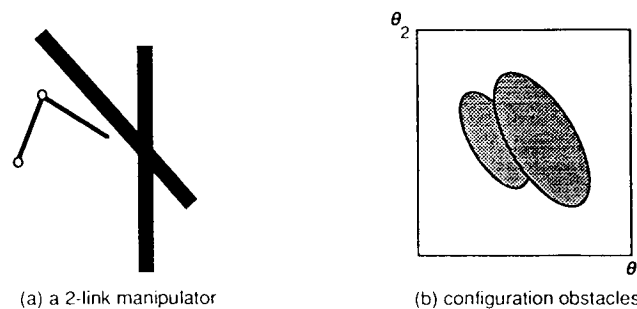(a) a 2-link manipulator   (b) configuration obstacles

Figure 9. Template method. For a 2-link manipulator, the configuration obstacle corresponding to an infinite wall is similar to an ellipse. The configuration obstacles for two walls are the union of two templates (of different sizes and locations).

to compute free parts of the Cspace, but the sweep volume is hard to compute if the set has a high dimension.

The template method computes the configuration obstacles due to features of world obstacles. These features are typically points and lines, and the corresponding configuration obstacles are called templates. The shape and position of a template can be parameterized by the position of the obstacle feature. For example, for a 2-link robot and one of the line obstacles in Figure 9a the configuration obstacle due to the line is similar to an ellipse (Figure 9b). The templates for each set of values of the parameters are computed in a grid form and then stored in the memory. The world obstacles are represented as a union of features for which the templates are computed. The whole configuration obstacles are then computed by "stamping" the template for each feature on the grid representing the whole Cspace. This method was developed in Branicky and Newman [1990] and works well for dof ≤ 4. For MP with a higher dof, it suffers from a huge memory requirement due to the use of grid.

Finally, the Jacobian-based method is very elegant in computing a "block" of free or obstacle-occupied Cspace. The Jacobian J of a robot is a matrix that relates the displacement, dx, of a point on the robot to the change in the robot configuration, dq. In equation form, this is $dx = J(q)^*dq$. Note J is a function of q. For a robot in a configuration q, the maximum of $|J(q)|$ over all the points on

the robot, called the bound $B(q)$ on $J(q)$, is computed. If the minimum distance between the robot in q and all the obstacles is D, then it follows that the sphere centered at q with radius $D/B(q)$ is contained in the free Cspace. Likewise, if we define a negative distance D^- between two overlapping objects as the minimum distance by which one of the objects has to translate to separate the two objects, we can compute a sphere of radius $D^-/B(q)$ that is contained in a configuration obstacle. Instead of $B(q)$, one can use the maximum of $B(q)$ over all q, which is called the uniform bound, UB on the Jacobian. This is a constant and needs to be computed once. But it is much larger than $B(q)$ for most q, and the sizes of computed spheres are much smaller. This method, developed in Paden et al. [1989], is the simplest way to compute "chunks" of free or occupied Cspace, but the chunks are very small for a long object or for a manipulator in an extended configuration. By fixing some of the configuration variables, spheres of lower dimensions can be computed. Also, different choices of distance measure in the Cspace result in different kinds of spheres. For example, l_∞ distance, i.e., $l_x(p, q) = \max|p_i - q_i|$, results in a cuboid. Cuboids have a nice property that they can fill the Cspace without cracks, which Euclidean spheres cannot do.

There are many variations of the above methods to compute configuration obstacles more efficiently, and when combined with a search strategy, they result in an MP algorithm. These variations are discussed with the algorithms.

A detailed complexity analysis of generating configuration obstacles is presented in Sharir [1987] for the case of translating only, that is nonrotating, robots moving in two and three dimensions. The objects are assumed to be polytopes. If curved objects are allowed, the algebraic degrees of the curves must be considered in the complexity analysis since the number of intersection points between curves depends on the degrees. This unnecessarily complicates the complexity analysis of MP, and thus objects are represented by curves of degree 1, i.e., planes. In 2D, the configuration obstacles have $O((mn)^2)$ edges where m and n are the numbers of edges of the robot and obstacles, respectively. The configuration obstacles can be generated in $O((mn)^2 \log(mn))$ time for arbitrary polygons and in $O(mn \log(mn))$ time for convex polygons. In 3D, configuration obstacles have $O((mn)^3)$ faces where m and n are the number of faces of the robot and obstacles, respectively. It is conjectured that for a translating convex robot the configuration obstacles can be generated in $O((mn)^2\alpha(mn))$ time, where $\alpha(k)$ is the extremely slowly growing inverse Ackermann's function which is less than 5 for all practical values of k.

2.2 Object Sensing and Representation

A robot has to have a model of objects in its environment before it can plan a collision-free motion. In an unknown environment or a dynamic environment, the robot has to sense objects at an appropriate time interval. Typically used are visual sensors, e.g., stereo cameras, or range sensors based on sonar, infrared, or laser light. Both types of sensors yield a depth map of the environment. These data are often converted to a polyhedral representation to save memory space and to speed up subsequent computations. In a well-known and well-controlled environment such as in a robotic assembly workcell, object data are available from the part design in the form of CAD data. These data are created using solid modelers, which represent objects as unions and intersections of basic solid primitives (cuboids, spheres, cylinders, and cones) or by specifying the boundaries of objects (called B-rep). In this case, sensors are needed only to verify the position and orientation of objects.

Once the information about shapes and configurations of objects is acquired, it can be represented in a number of ways. Commonly used representations are grid, cell tree, polyhedra, constructive solid geometry (CSG), and boundary representation (B-rep). These can be used to rep-
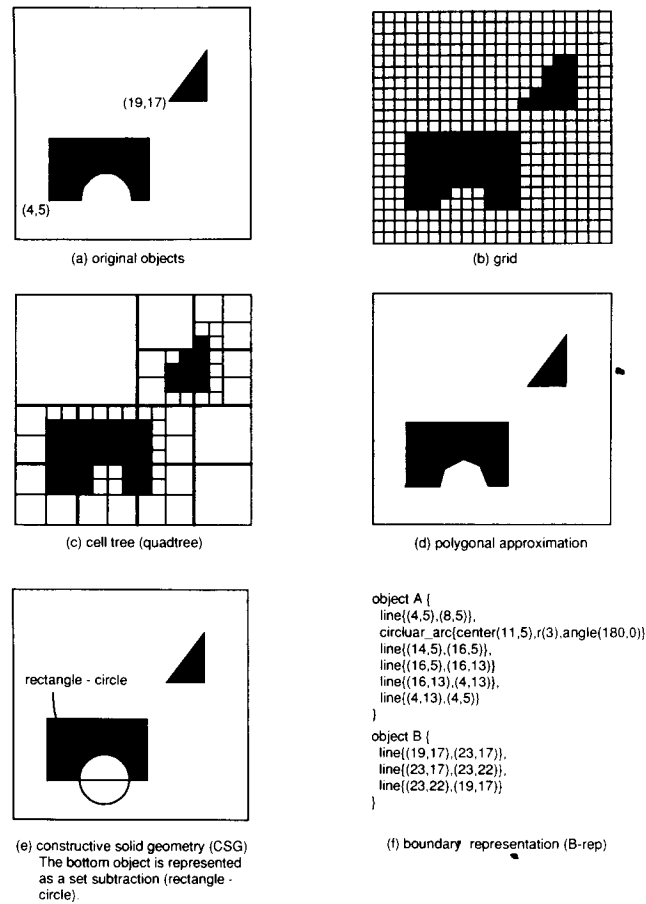
(a) original objects

(b) grid

(c) cell tree (quadtree)

(d) polygonal approximation

(e) constructive solid geometry (CSG)
The bottom object is represented
as a set subtraction (rectangle -
circle).

object A {
  line{(4,5),(8,5)},
  circluar_arc{center(11,5),r(3),angle(180,0)}
  line{(14,5),(16,5)},
  line{(16,5),(16,13)}
  line{(16,13),(4,13)},
  line{(4,13),(4,5)}
}

object B {
  line{(19,17),(23,17)},
  line{(23,17),(23,22)},
  line{(23,22),(19,17)}
}

(f) boundary representation (B-rep)

Figure 10. Object representations.

resent objects in the world space or in the configuration space. The objects in Figure 10a are shown in these representations in Figures 10b–f.

A grid is an array of (usually rectilinear) identical cells, and the cells are marked as 1 (dark) if it is occupied by an obstacle, or else marked as 0 (white) (Figure 10b). One might think this is an inefficient way to represent an object, but its simplicity has many computational advantages, especially on a massively parallel computer. For example, the volume of an irregularly shaped object is best computed by this representation. (Volume computation is needed to compute the center of mass to assess stability, which is an important consideration in some MP problems).

The cell tree representation is developed to overcome the disadvantage of grid when representing a large object. This representation divides the space into a small number of big cells. Cells completely inside or outside of objects are marked as such, and the cells partially occupied by the objects are further divided. This process is repeated until the size of the cells reaches a resolution limit. Figure 10c shows an example called the quadtree in 2D (called octree in 3D). The number of cells in this representation is proportional to the surface area of an object. Its main disadvantage compared to the grid is the overhead of computing adjacency between cell.

Polyhedral representation is one of the most used ones, since many objects can

be closely approximated with unions of polyhedra (Figure 10d). There exist many efficient algorithms for computing the intersection of and distance between two polyhedra. Computations of intersection and distance are the two most important computations in motion planning.

CSG and B-rep are mostly used in solid modeler. The CSG represents objects as unions, intersections, and set differences of primitive shapes (Figure 10e), and the B-rep explicitly lists boundary features of objects (Figure 10f). One of their advantages is that they can represent curved objects with a small number of parameters specifying the curves. A polyhedral representation needs many faces to accurately approximate a curved surface. Commercial solid modelers presently offer sophisticated geometric computation routines such as intersection, volume, and center of mass. If one is designing a motion planner for assembly planner, the CAD modeler used for part designing must be used for the motion planner as well.

An object representation scheme should be selected such that it is readily computable from the sensed or available data. To expedite MP, one might consider converting one representation to that in which intersection and distance computation can be done efficiently.

2.3 Approaches to Motion Planning

Numerous methods have been developed for MP; some are applicable to a wide variety of MP problems, whereas others have a limited applicability. These methods are variations of a few general approaches: skeleton, cell decomposition, potential field, and mathematical programming. Most classes of MP problems can be solved using these approaches. These approaches are not necessarily mutually exclusive, and a combination of them is often used in developing a motion planner.

2.3.1 Skeleton

In the skeleton approach, the free Cspace, i.e., the set of feasible motions, is

retracted, reduced to, or mapped onto a network of one-dimensional lines. This approach is also called the retraction, roadmap, or highway approach. The search for a solution is limited to the network, and MP becomes a graph-searching problem. In this approach, MP is done in three steps. First, the robot is moved from its starting configuration to a point on the skeleton, using a canonical method. Second, the robot is moved from the goal configuration to a point on the skeleton likewise. Then the two points on the skeleton are connected using lines in the skeleton. The skeleton must represent all topologically distinct feasible paths in Cspace. Otherwise, the MP algorithm is not complete, i.e., may miss a solution.

The well-known skeletons are the *visibility graph* and the *Voronoi diagram*, commonly used ones for 2D, the *silhouette* and the *subgoal network*. The visibility graph is the collection of lines in the free space that connects a feature of an object to that of another. Figure 11 shows the visibility graph of polygons in the plane, where vertices are used as the feature. The shortest path for a point robot between point S and G (the bold lines) can be found from the visibility graph if the point S and G are included as features. There are $O(n^2)$ edges in the visibility graph, and it can be constructed in $O(n^2)$ time and space in 2D [Asano et al. 1985], where n is the number of features.

If the robot is required to stay away from obstacles, the *nearest-site* Voronoi diagram can be used (referred as Voronoi diagram from now on). It is defined as the set of points that are equidistant from two or more object features. A comprehensive survey of the Voronoi diagram is presented in Aurenhammer [1991]. Figure 12 shows the Voronoi diagram for polygons when the polygons themselves are taken as features (the square boundary is counted as one obstacle). If edges of the polygons are taken as features, a different Voronoi diagram results. The Voronoi diagram partitions the space into regions, where
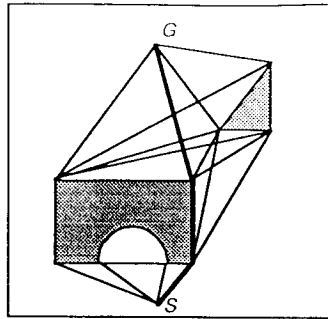
Figure 11. The visibility graph is formed by lines connecting visible vertices. A solution path is shown in bold lines.
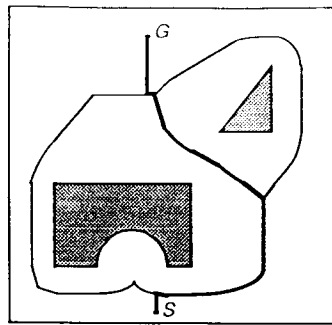

Figure 12. The Voronoi diagram is the set of points equidistant from two or more objects.

each region contains one feature. For each point in a region, this feature is the closest feature to the point than any other feature. A path from S and G can be found by first moving the robot on the diagram, along the diagram, and then to the goal G (the bold curves). The Voronoi diagram is attractive in two respects: there are only $O(n)$ edges in the Voronoi diagram, and it can be efficiently constructed in $\Omega(n \log n)$ time, where n is the number of features [Preparata and Shamos 1985]. See Ahuja and Schachter [1983], Kirkpatrick [1979], Lee and Drysdale [1981], Preparata and Shamos [1985], Shamos and Hoey [1975], and Yap [1985] for computing the Voronoi diagram. The Voronoi diagram contains curves when edges of polygons are used as features. A different Voronoi diagram

containing only straight lines is developed [Canny and Donald 1987]. It uses a measure of distance that is not a true metric instead of the usual Euclidean distance to determine equidistant points.

For higher-dimensional spaces than 2D, both the visibility graph and the Voronoi diagram have higher complexities, and it is not obvious what to select for the features. For example, the Voronoi diagram among polyhedra is a collection of 2D faces, which is not a 1D skeleton. The visibility graph can be constructed from the vertices of polyhedra, but the shortest path then no longer lies in the visibility graph. Therefore, the visibility graph and the Voronoi diagram are mostly used for 2D motion planning.

In Canny [1987, 1988], a general method of constructing a skeleton in arbitrary dimensions is presented. It projects an object in a higher-dimensional space to a lower-dimensional space and then traces out the boundary curves of the projection, which is called *silhouette*. The silhouette curves are recursively projected to a lower-dimensional space, until they become one-dimensional lines. Then the.curves are connected at places where new silhouette curves appear or disappear using linking curves (Figure 13). This method is developed to find a path from a graph of one-dimensional curves, which has a lower complexity than the original space containing the objects. It is mostly used in theoretical algorithms analyzing complexity, rather than developing practical algorithms. A path found from the silhouette curves makes the robot slide along obstacle boundaries. A variation of this algorithm is implemented in Canny and Lin [1990].

The subgoal network method does not build an explicit representation of the configuration obstacles. Instead, the list of reachable configurations from the start configuration is maintained. When the goal configuration is reachable the MP is solved. The reachability of one configuration from another is decided by a rather simple local-MP algorithm called *local operator*, such as that moving the robot in a straight line between the configura-
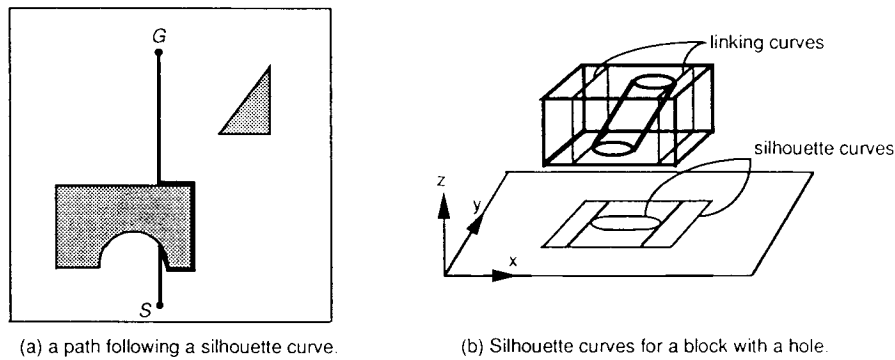
(a) a path following a silhouette curve.

(b) Silhouette curves for a block with a hole.

Figure 13. Silhouette curve.

tions. In the beginning, this approach finds a candidate sequence of intermediate configurations called *subgoals* and uses the local operator to successively move the robot through the subgoals in the sequence. A heuristic is usually used to find the sequence, but a sequence of random configurations can be used. If the robot cannot reach the goal configuration, the reached subgoals are stored in the list, and another candidate sequence is found between the goal and any one of the reached subgoals. The local operator is used again to check the existence of a feasible motion through the sequence, and this process is repeated. Note that the feasible motion between two reachable configurations need not be stored, as it can be readily recovered by the local operator. The main advantage of this algorithm is the small memory requirement. The visibility graph is an example of a subgoal network, where subgoals are object features and where the local operator is *go-straight*. Figure 14 shows a subgoal network generated using a local operator that moves the robot diagonally. When the robot collides, new subgoals are generated by sampling a few points on the path.

The choice of the local operator determines the completeness of this approach. In one extreme, one can use the go-straight algorithm, which often fails to find a feasible motion between two configurations which are far apart. Consequently, the adjacent subgoals must be
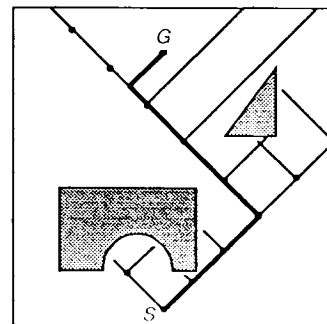
Figure 14. Subgoal network.

close by, which increases the number of subgoals. On the other extreme, one can use an exact global-motion planner as the local operator, in which case only one sequence of subgoals containing the start and goal need to be tested. This local operator approach is a systematic way to decompose an MP problem into a number of simpler MP problems. It was introduced in Faverjon and Tournassoud [1987] and completed in Chen and Hwang [1992]. It is our experience that this approach is most efficient when a potential-field method is used as the local operator.

2.3.2 Cell Decomposition

In this approach, the free Cspace is decomposed into a set of simple cells, and the adjacency relationships among the cells are computed. A collision-free path

between the start and the goal configuration of the robot is found by first identifying the two cells containing the start and the goal and then connecting them with a sequence of connected cells. Cells can be object dependent or independent. In an object-dependent decomposition, boundaries of obstacles are used to generate the cell boundaries, and the union of free cells exactly defines the free space. The number of cells is small, but the complexity of decomposition is high; and the computations of containment, intersection, connectivity, and adjacency of the cells are difficult. Note that adjacency information is needed to find a sequence of connected cells from the start to the goal configuration. For example, it is NP-hard to decompose into convex polygons a polygon with polygonal holes [Keil and Sack 1985]. Object-dependent decompositions usually result in semi-algebraic cells. An example of object-dependent cell decomposition is shown in Figure 15 with a solution sequence of cells between S and G. In an object-independent decomposition, the Cspace is prepartitioned into cells of a simple shape, and each cell is tested for whether it is inside or outside of configuration obstacles. Since the cell shape and location are independent of the object shape and location, the cell boundaries do not tightly enclose the object. The representation error can be made small, however, by increasing the number of cells. The MP computations mentioned above are, however, much easier if not trivial. Examples of object-independent cell decompositions are the grid and the quadtree (Figures 10b and c).

2.3.3 Potential Field

A historical review of the potential-field approach can be found in Koditschek [1989]. The idea of using potential functions for obstacle avoidance was used in Khatib and Mampey [1978] and in Hogan [1985] for force control. It was also developed independently in Miyazaki and Arimoto [1984] and Pavlov and Voronin [1984]. This approach constructs a scalar
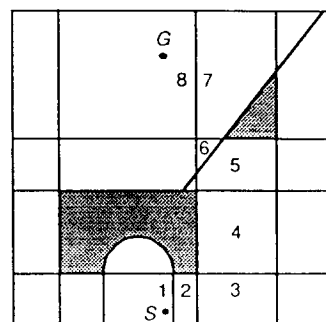

Figure 15. Object-dependent cell decomposition.

function called the potential that has a minimum, when the robot is at the goal configuration, and a high value on obstacles. Everywhere else, the function is sloping down toward the goal configuration, so that the robot can reach the goal configuration from any other configuration by following the negative gradient of the potential. The high value of the potential prevents the robot from running into obstacles.

Figure 16 illustrates this approach. First, an *obstacle potential* is constructed that has a high value on the obstacles, and it decreases monotonically as the distance from obstacles increases (Figure 16a). Note the inverse of distance to obstacles can be used for this purpose. Added to the obstacle potential is a *goal potential* that has a large negative value at the goal and increases monotonically as the distance from the goal increases (Figure 16b). The negative of the inverse of distance to the goal is a commonly used goal potential. The sum of the two potentials is computed (Figure 16c), and the path from the start to the goal configuration is found by putting a small marble at the start and following its movement.

An obstacle potential constructed in this way resembles the electrostatic potential generated by obstacles made of positively charged matter, hence the name of this approach. The potential is most often assigned to obstacles in the world space. It is redundant to compute
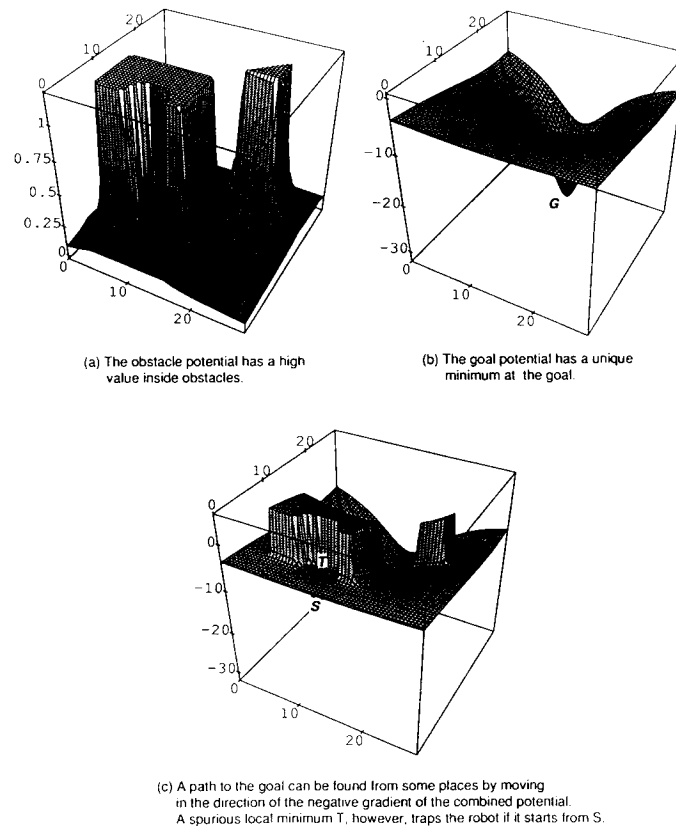
(a) The obstacle potential has a high value inside obstacles.

(b) The goal potential has a unique minimum at the goal.

(c) A path to the goal can be found from some places by moving in the direction of the negative gradient of the combined potential. A spurious local minimum T, however, traps the robot if it starts from S.

Figure 16. The potential-field approach.

configuration obstacles and then assign a potential to them. If the robot is not a point, the total potential on the robot is computed by adding the potential values on a set of points sampled from the surface of the robot.

This approach is simple, but the potential function usually has several local minima at configurations other than the goal. (point T in Figure 16c). These spurious local minima often trap the robot. One other disadvantage is that the expression for the potential becomes very cumbersome when there are many concave objects. Unless the robot is a point and unless obstacles are nonoverlapping convex objects, the potential field approach alone cannot be used as a global algorithm. This is expected since no detailed shape analysis is done unlike other approaches. The best way to use

the potential-field approach is to use it as a submodule for global-motion planners that decompose the original MP problem into many local problems solvable by the potential-field approach. Although such algorithms may not be exact, they are attractive due to their low computational costs.

2.3.4 Mathematical Programming

This approach represents the requirement of obstacle avoidance with a set of inequalities on the configuration parameters. Motion planning is formulated then as a mathematical optimization problem that finds a curve between the start and goal configurations minimizing a certain scalar quantity. Since such an optimization is nonlinear and has many inequality constraints, a numerical method is used to find the optimal solution.

2.4 Search Methods

Given a way of describing the free space, and thus the capability of identifying feasible configurations, MP reduces to finding a connected sequence of feasible configurations between the start and goal from the representation. There are several search methods developed in artificial intelligence such as depth-first, breadth-first, best-first, A*, and bidirectional searches [Barr and Feigenbaum 1981]. Random-search techniques such as simulated annealing are also used for MP [Barraquand and Latombe 1990]. Dijkstra's shortest-path algorithm for graphs is also useful for MP [Dijkstra 1959]. We will only give brief overviews of these here.

Search methods are best explained using a grid. Consider a grid in Figure 17a where infeasible configurations are marked dark, and the start and goal configurations of the robot are marked with *S* and *G*, respectively. The robot is allowed to move either horizontally or vertically only. At each configuration, the robot has at most four possible moves. When the robot moves from configuration q_p to q_c, q_p is called a parent of q_c, and q_c the child of q_p (obviously, q_p and q_c must be adjacent). During the search, each configuration is allowed to have only one parent; otherwise, the robot may keep moving in a cycle. To retrieve a solution path, each reached configuration must remember its parent configuration. Solution paths are denoted by bold lines in Figure 17a-e.

The depth-first search moves the robot from *S* to configurations in the order shown in Figure 17a. The depth-first search always generates a child of the most recently reached configuration. Note that the solution is not the shortest. In contrast, the breadth-first search generates the children of the earliest reached configuration first, resulting in Figure 17b. This method is also called *brushfire*, since it resembles the way fire progresses in a dry grassland. The brushfire method can find the shortest path, but it examines a large part of the space. It is obvious that both of these are not very efficient.

Without an easily computable criterion that indicates a better direction to move, this is all one can do. Such is the case when the robot has to select the next cell to move to among irregular overlapping cells representing the free space.

If the distance from a configuration to the goal is computed, one can generate the children of the current configuration and move to the child nearest to the goal. This is the best-first search, sometimes called hill climbing, and works well in many cases (Figure 17c). If there is a blind alley between configuration obstacles (often occurs in practical problems), the best-first search can also take a long time to reach the goal.

The A* search is used when a solution with a minimum cost (typically the shortest path) is desired. For A* to be used, there must be an underestimate of the cost from the current configuration to the goal (called cost-to-go). A straight-line distance gives such an underestimate (obstacles only increase the path length). The total cost, which is the sum of the cost from the start configuration to the current configuration (called cost-so-far) and the cost-to-go, gives a lower bound on the actual cost. A* search generates the children of the reached configurations whose total cost is the smallest. When a solution is found, it does not generate the children of any reached configurations whose total cost is greater than the total cost of the solution. The better the cost-to-go approximates the actual cost, the more A* can prune out partially generated paths, making it more efficient. Figure 17d shows the process of A* search.

The bidirectional search generates the children of both the start and the goal configurations and can be used with any one of the above search methods. Figure 17e shows the bidirectional search combined with the depth first. The robot switches the direction when it cannot get any closer to the other side. It is particularly efficient when the goal is in a narrow channel between obstacles, making it hard to reach from the start configuration.
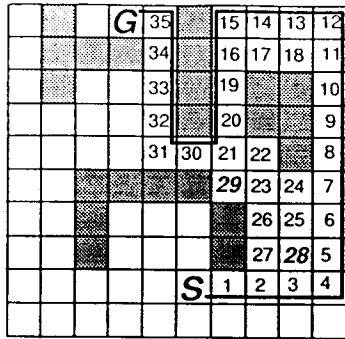
(a) Depth first searh. The robot favors the motion to the east, north, west, and then south, in that order. Note at cell 28, the robot has no cells to go, and the search resumes from the highest numbered cell with an empty adjacent cell.
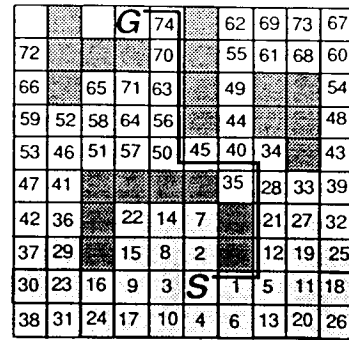
(b) Breadth first search (brush fire). The robot goes from the lowest numbered cell to an adjacent cell. The dotted cells are visited cells at an intermediate stage of search.
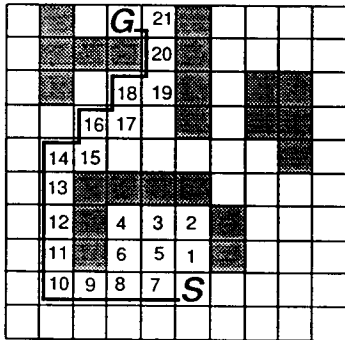
(c) Best first search (hill climb). The robot goes to the empty cell closest to G.
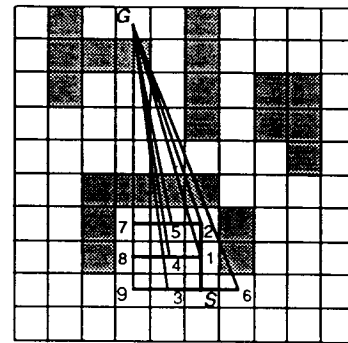
(d) A* search. The robot goes to the cell for which the sum of the path length from S (bold lines) and the estimate of the path length to G (the straight line distance is used here) is the smallest.
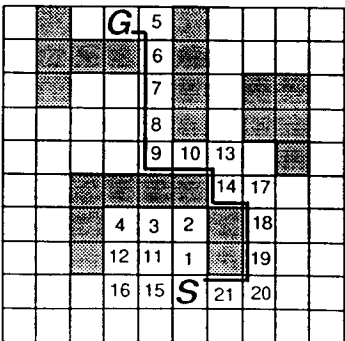
(e) Bi-directional search. Whenever the robot cannot get any closer to the other side, it switches the direction of search.

Figure 17. Search strategies.

All of the above search methods eventually explore all parts of the search space. If this is not possible, a random-search technique can be used, e.g., a highly redundant manipulator with many degrees of freedom. Random search can be used in a variety of ways. Suppose we have a local-motion planner which blindly

moves the robot in the direction toward the goal (and the robot gets stuck after sometime). We randomly pick a point m_0 in the Cspace and try to move the robot from the start to m_0, and from m_0 to the goal using the local-motion planner. If the robot cannot reach m_0, we decrease the probability of point selection in a neighborhood of m_0. Then, we pick another point m_1 according to the modified probability. If the local planner moves the robot from the start to m_1, but fails to move to the goal, we put m_1 in the reachable set. When another point m_2 is selected, the local planner tries to move the robot from any reachable point to m_2, and then to the goal. This approach is probabilistically complete, but may take a long time to find a solution. See Barraquand and Latombe [1990] for an example of this method.

When searching for the shortest path between two nodes in a graph with weighted edges, Dijkstra's algorithm of $O(n^2)$ is the most efficient. Beginning from the goal node, it finds the nodes connected to the goal, puts them in a queue, and assigns each of them the cost-to-goal, which is the weight of the edge connecting it to the goal. The expanded goal node is marked as the parent of the nodes in the queue. Among the nodes in the queue, it selects the node with the smallest cost-to-goal, deletes it from the queue, finds nodes connected to it, and computes the cost-to-goal for each node by adding the weight of the connecting edge to the cost-to-goal of the parent node. If any of the children nodes has a previously computed cost-to-goal greater than the newly computed one, its cost is changed to the new one, and the costs of all its descendants are updated. This process is repeated until all the nodes are assigned a cost. The minimum-cost sequence of edges between the start and the goal is then retrieved by following the parents beginning from the start node.

The efficiency of a search method depends on the particular MP problem at hand. Of course, several search strategies described above could be combined.

The following guidelines can be used to develop a customized search method.

Selection of Search Methods

(1) If there is a criterion for selecting a good moving direction, then use best-first rather than depth-first or breadth-first search.

(2) If the problem is easy in the sense that the free space is wide and allows many motion solutions, and any solution is adequate instead of an optimal solution, then a depth-first or best-first search will suffice.

(3) If the shortest path is desired, use A* search or Dijkstra's algorithm.

(4) If a massively parallel computer is used, breadth-first search can be effective.

(5) Use bidirectional search whenever possible. To connect two configurations, always move from the cluttered side, since it is easier for the robot to move from a cluttered space to an open space, rather than to achieve a particular configuration in a cluttered space.

(6) The MP is difficult since it is computationally intensive to generate a spatial representation of *all* collision-free configurations. If many MP problems are to be solved with different start and goal configurations within the same environment, it is useful to compute once in the beginning a more-or-less complete spatial representation and search in this representation paths connecting many pairs of start and goal configurations.

(7) If just one MP problem is to be solved in an environment, do not generate a complete representation of the Cspace. Interleave the representation computation and the search. That is, try to find a solution from a partial representation of the Cspaces. If there is no solution, incrementally refine the representation and search for a solution again. In many situations, a solution will be found before the

complete representation is computed. We call this paradigm *ICORS*, which stands for Interleaved Computations Of Spatial Representation and Search of a solution.

(8) If the environment is marginally changing, use an updating scheme to avoid complete recomputation of the representation.

2.5 Local Optimization of Motion

Once a collision-free path is found, it can be further optimized by a numerical method. Two commonly used optimality criteria are the length of the path and safety clearance between the robot and obstacles. The resulting performance index to be minimized can be expressed as

$$J = \int_{q_{start}}^{q_{goal}} (1 + w^* D^{-1}(q)) \, dq,$$

where $D(q)$ is the distance between the robot and obstacles; w is the relative weighting factor, and the integral is over the path connecting q_{start} and q_{goal}. Note the minimization of $D^{-1}(q)$ prevents the robot from colliding with obstacles. Several numerical methods can be used to find a path with the minimum J with the path found by an MP algorithm as the initial guess [Bryson and Ho 1975]. It is our experience that a simple gradient method performs satisfactorily. One can also include dynamics of robot actuators (motors) to optimize quantities such as the travel time, energy expended during the motion, etc. The resulting path is smooth and thus easier to execute on a real robot, but it is optimal only in the vicinity of the initial guess. One can use a straight-line path between the start and goal involving collisions as the initial guess and get a collision-free path with numerical optimization. But this happens only in simple cases where the obstacles are convex and disjoint, and it is not recommended.

An efficient-distance algorithm for polytopes is developed and used for numerical optimization in Gilbert and

Johnson [1985]. With polygonal robot and obstacles, and robot dynamics included in J, the numerical algorithm took 300–600 iterations to converge. See Gilbert et al. [1988] and Gilbert and Foo [1990] for algorithms for computing the distance between polytopes or curved objects. Another procedure for computing distance between polyhedra is reported in Lin and Canny [1991], which is about three times faster than Gilbert's algorithm to our estimation. In Hwang and Ahuja [1989] an obstacle-potential function is used in place of $D^{-1}(q)$ in optimization. Their potential function is simpler to compute than distance, and using J that includes just the path length and safety clearance their algorithm converges to an optimum in 20–30 iterations. For an example of an optimized manipulator motion see Figure 36 (later).

3. SURVEY OF RECENT WORK

A brief history of motion planning between the 1940's and early 1980's is found in Schwartz and Yap [1987], along with a review of their work. The June, 1987, issue of the *IEEE Journal of Robotics and Automation* also gives a selection of eight papers on motion planning from various disciplines such as mathematics, computer science, and electrical/mechanical engineering. The book *Robot Motion Planning* [Latombe 1991], intended as a graduate-level textbook, defines various MP problems and approaches. It gives detailed explanations of landmark papers along with a comprehensive list of references up to 1990. This section surveys many papers published between 1979 and 1989, and some papers published after 1989. It also discusses future research directions on various MP problems.

Algorithms are surveyed according to the type of environments: stationary, time varying, movable obstacles, and environments with constraints. Figure 18 shows our taxonomy. Because there are many more papers on MP in stationary environments than other environments, these are further classified by the types
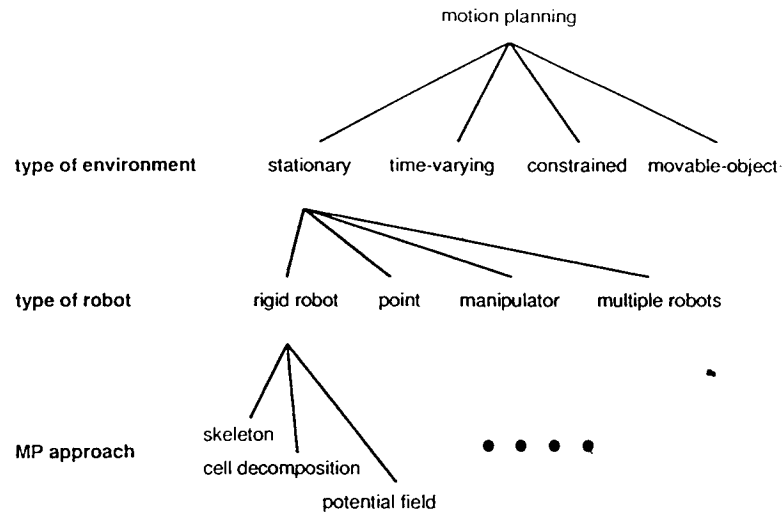
Figure 18. Taxonomy of motion planning.

of robots (rigid or linked robots, single or multiple robots) and surveyed in four subsections. First, the work on MP of a single rigid robot is presented. Section 3.1.2 surveys the work on MP of a point robot. Although a point robot is a special case of rigid robots, a large number of results have been reported for this problem because (1) the problem space is lower dimensional and (2) the results are useful for navigation planning. Section 3.1.3 presents the work on MP of a manipulator. Motion planning of multiple robots is surveyed in Section 3.1.4. Since there is a relatively small number of papers dealing with time-varying environments, environments with constraints, and movable-obstacle cases, the survey for these categories is presented without further classification according to the robot type. Algorithms in each section are grouped according to the approaches used. Each algorithm is explained briefly, and its efficiency, applicability, and amenability to implementation are discussed. The pros and cons of each algorithm can be found in the comparison tables in Section 3.5. The tables highlight features of the algorithms such as degrees of freedom of robots, shapes of robots and obstacles,

degrees of exactness, and actual speeds of execution.

Comparing the actual running times of algorithms is difficult due to the fact that different computers are used to solve different examples. If an example problem is included, we give the computation time along with the speed of the computer in MIPS (millions of instructions per second). If the MIPS are not available, we interpret the result as the running time on a typical computer available in the published year.

3.1 Stationary Environments

A stationary environment is the simplest type of environment to plan motion, and algorithms for this problem are often used as ingredients of MP algorithms for other environments. Much of MP research has been concerned with stationary environments, and this work is surveyed in the following four subsections.

3.1.1 Classical Mover's Problem

The classical mover's problem refers to the problem of moving a rigid robot among stationary obstacles of fixed shapes. Figure 5 shows a typical classical mover's problem. It is the most studied

version of the motion-planning problem. This problem has important applications in vehicle navigation on land, on sea, underwater, in air, and in outer space. For the task of moving an object with a manipulator, the existence of a collision-free motion for the object to be moved is a necessary condition for a feasible manipulator motion.

Skeleton Approach

The idea of the configuration space is introduced in Lozano-Pérez and Wesley [1979]. To plan motions for a translating polygonal robot among polygonal obstacles, configuration obstacles are computed using Minkowski set difference. The resulting configuration obstacles are polygons, and the visibility graph is computed using polygon vertices as features. The shortest path is found from the visibility graph.

In Kedem and Sharir [1985, 1988], an exact and efficient algorithm is presented for a polygonal robot among polygonal obstacles. It has $O(mn\lambda_6(mn)\log mn)$ worst-case time complexity ($\lambda_6(r)$ is again the maximum length of an $(r, 6)$ Davenport-Schinzel sequence). This algorithm computes a skeleton, called an *edge graph*, consisting of curved edges of configuration obstacles, and feasible motion is found from the skeleton. The edge graph is built in two steps. First, for a fixed orientation θ of the robot, Minkowski set difference is used to compute the configuration obstacles, say $CO(\theta)$, which are polygons. When θ is slightly varied, the topology of $CO(\theta)$ does not change unless θ is one of the finitely many *critical orientations*, θ_c. Therefore, we partition the robot orientation dimension into a finite number of intervals using θ_c and compute $CO(\theta)$ once for each interval. The θ_c occur when the robot vertices touch three obstacle edges, one obstacle vertex and an edge, etc. As θ is varied, the vertices of $CO(\theta)$ trace out curved edges of the 3D configuration obstacles. These curved edges either branch or merge only when θ is one of the θ_c (see Figure 19). Two curved

edges are connected if they meet at one of the θ_c or if they are connected by an edge of polygons of $CO(\theta)$ for some θ. Second, the traced curved edges are stored in the nodes of the edge graph, and an edge is created between two nodes if the curved edges are connected. A canonical procedure is then used to move the robot to the edge graph from the start and goal configurations, and the rest of the path is found from the edge graph. It is implemented on a real robot and takes a few minutes to find a solution.

A similar algorithm is developed for a polygonal robot among polygonal obstacles in 2D in Avnaim et al. [1988]. Since the robot and obstacles can be represented as unions of line segments, the boundary equations for 3D configuration obstacles are derived from the intersection conditions between two line segments. The boundary equations are computed in $O(m^3n^3 \log(mn))$ time. Two different path-planning algorithms are presented. One algorithm finds in $O(m^3n^3)$ time a path along the boundaries of the configuration obstacles. The robot makes single point, edge, or surface contacts when following such a path. The robot goes from the start location to an obstacle surface, travels on a number of obstacle surfaces making occasional jumps among surfaces, and goes to the goal location (similar to the motion planned in Kedem and Sharir [1985]). The other algorithm computes a path away from obstacles using a decomposition of the free Cspace. The decomposition is done in $O(m^6n^6\alpha(mn)\log(mn))$, and finding a path from the decomposition takes $O(m^6n^6\alpha(mn))$ time. It is faster to compute motion when the robot is in contact with obstacles because the robot follows the boundaries of obstacles, thus avoiding the need for an explicit representation of the free space.

Cell Decomposition Approach

Cell Decomposition in world space. The first algorithm polynomial in the number of obstacles for the classical

(a) Edges of the configuration obstacles in Figure 3.1(b). Critical orientations are where the edges meet.

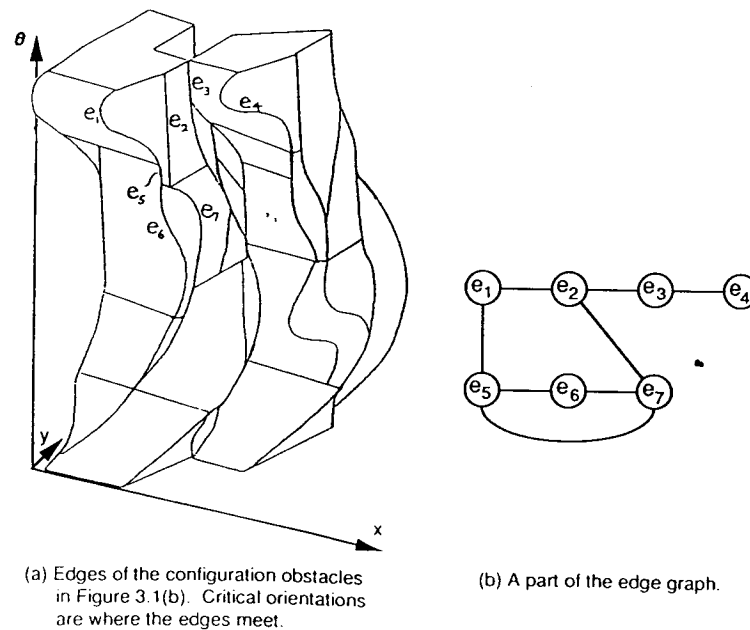(b) A part of the edge graph.

Figure 19. The edge graph of configuration obstacles.

mover's problem in 2D is reported in Schwartz and Sharir [1983a]. All objects are assumed to be polygons. The basic idea of this approach is to partition the free space into regions, each having qualitatively different sets of feasible orientations. When the reference point of a robot is at a certain location, the set of feasible orientations changes drastically. In Figure 20a, for example, the feasible orientation of the white rectangle changes drastically depending on whether the reference point, P, is above or below the line. Such a line is called a *critical curve*, and is used to partition the free space into regions called *noncritical regions*. (A point belongs to either critical curves or a noncritical region.) A critical curve is defined as the curve that the reference point of the robot traces while the robot maintains a *critical* contact with obstacles. Critical contacts are defined in many ways. For example, a vertex or an edge of the robot touches a vertex or an edge of an obstacle, or the robot touches two obstacles simultaneously. It is shown that for a polygonal

object moving among polygonal obstacles in the plane there are eight types of critical curves (Figure 20). If the reference point of the robot lies in a noncritical region, the feasible orientations of the robot can be expressed as a finite union of open sets of angles associated with the noncritical region. Each open set is bounded by the angles at which the robot is making contacts with some obstacles. The open sets are represented by the pair of edges/vertices in contact. The pairs of edges denoting the open sets of the feasible orientations stay the same as long as the reference point of the robot stays in the same noncritical region. This implies that the robot can move from a point to another in the same noncritical region if the orientations of the robot at the two points are in the same open set. The robot can move from one noncritical region to another if at a point on the boundary of the two regions there exists an orientation of the robot feasible in both regions. Two regions are said to be connected if such a point is found. The connectivity of the regions is then repre-

(a) Type I
P is translating with a VE contact while
staying maximally away from the obstacle.

(b) Type II
P is rotating with a VV or EV contact.

(c) Type III
P is translating with two vertex contact
with the same obstacle edge.

(d) Type IV
P is moving with two vertex contact
with two different obstacle edges.

(e) Type V
P is moving with a VE and an EV contact.

(f) Type VI
P is moving with an edge contact with
two different obstacle vertices.

(g) Type VII
P is moving with two EV contacts.

(h) Type VIII
P is translating with an EE contact.

Figure 20. Eight types of critical curves. The robot is the white polygon, and obstacles the black. P is the reference point of the robot, and Q is the robot vertex making a contact. A $VE(EV)$ contact denotes a contact between robot vertex (edge) and an obstacle edge (vertex). $VV(EE)$ denotes a vertex-vertex (edge-edge) contact.

sented in a graph called the connectivity graph, and the MP problem is transformed to one of finding a sequence of connected noncritical regions in the connectivity graph. The time complexity of this 2D algorithm is $O(n^5)$. A general framework for the MP algorithm with an arbitrary number of degrees of freedom is given in Schwartz and Sharir [1981]. The time complexity of the algorithm is $O(n^{(2^{d+6})})$, where n denotes the total

number of obstacle edges, and d is the number of degrees of freedom. In three dimensions ($d = 6$), this becomes $O(n^{4096})$. This algorithm serves as the existence proof of a polynomial-time algorithm in the number of obstacles.

Brooks [1983] represents 2D free space as a union of possibly overlapping generalized cones. A generalized cone has an axis of a certain length and a boundary on each side of the axis (Figure 21). The

(a) free space decomposition (b) A solution found for a rectangular robot

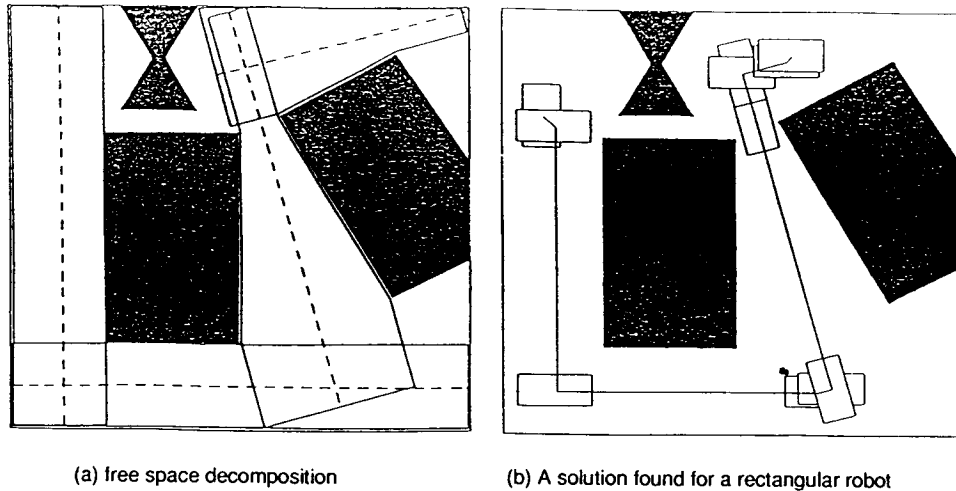**Figure 21.** Cell decomposition using generalized cones. Reprinted from *IEEE Transactions on Systems, Man, and Cybernetics*, vol. SMC-13, March/April, pp. 190–97, Brooks, R. A., "Solving the findpath problem by good representation of free space," by permission of IEEE, Piscataway, N.J., Copyright, © 1983 IEEE.

algorithm translates a polygonal moving body along the axes or spines of the generalized cones and rotates it at the intersections of the generalized cones. This algorithm is fast and yields paths that avoid obstacles generously. Kuan et al. [1985] improve the quality of the paths by representing the 2D free space as a union of generalized cones and convex polygons [Kuan et al. 1985]. There are two potential problems with this algorithm: the paths found may not be short if the free space is wide, and the algorithm may not find a solution when the robot has to translate and rotate simultaneously to avoid obstacles.

A similar but more elaborate algorithm is presented in Nguyen [1984]. The 2D free space is described as a network of linked cones. Feasible positions and orientations of the robot within each cone are computed. Feasible path segments are derived by local algorithms that use adjacency information about the cones. Four local algorithms are used, namely, traversing a free convex region, sliding along an edge, circumventing a corner, and going through a star-shaped region.

A* search is used to find global paths from local segments. The three algorithms above can be used when the free space is wide and when generous avoidance of obstacles is desired.

A heuristic algorithm based on a quadtree is presented in Noborio et al. [1989]. A candidate path is searched from the quadtree representation of the free space, and the corner points on the paths are labeled as intermediate goals (Figure 22a). The minimum width of a robot is used in the search process to eliminate paths that are too narrow. The candidate path would be a solution if the robot is a point. For a polygonal robot, the candidate path must be modified to avoid possible collisions. The robot is moved along the candidate path, and at each instant, the closest distance to obstacles and the direction to the intermediate goal is computed. This information is used to compute the robot's moving direction that avoids obstacles and moves the robot closer to the intermediate goal. The algorithm will fail if the robot has a complicated shape, but it seems to be efficient for mobile robots with simple shapes such
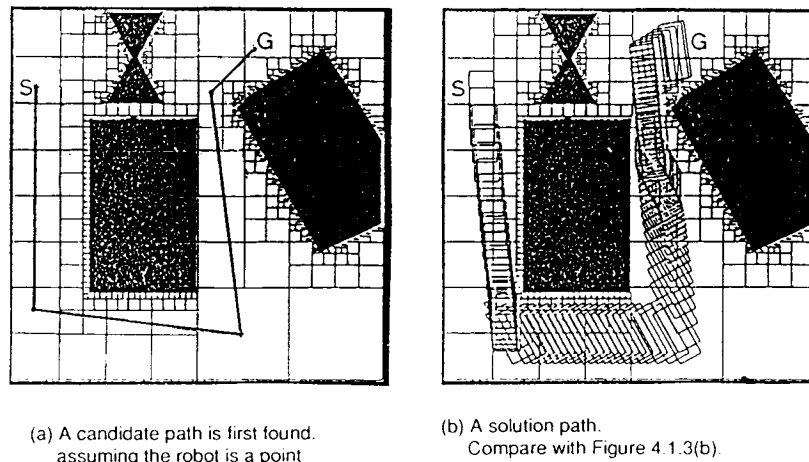
(a) A candidate path is first found.
assuming the robot is a point

(b) A solution path.
Compare with Figure 4.1.3(b).

Figure 22. Motion planning using a quadtree. Reprinted from *Proc. of IEEE Int. Conf. on Robotics and Automation*, pp. 484–489, Noboria, H., Naniwa, T., and Arimoto, S., "A feasible motion planning algorithm for a mobile robot on a quadtree representation," by permission of IEEE, Piscataway, N.J., Copyright, © 1989 IEEE.

as rectangles or circles. The algorithm takes a few minutes to solve the problem in Figure 22b.

Cell decomposition in configuration space. The octree is used to represent 3D configuration obstacles for a polygonal robot among polygonal obstacles in a 2D world [Brooks and Lozano-Pérez 1983]. The 3D configuration space is divided into 8 cuboids, and each cuboid is labeled either full, mixed, or empty depending on whether the cuboid is completely, partially, or not occupied by the configuration obstacles. A search is done on the cuboids to find a connected sequence of empty cuboids between the start and goal configurations. When no such sequence is found, the cuboids that are most likely to yield a sequence of empty subcuboids are divided. The process of searching and dividing (an ICORS scheme) continues until a solution is found or until the size of the divided cuboids reaches a preset limit. This algorithm is exact up to the resolution of the cuboid size. The configuration obstacles can also be computed in a 2^d-tree using the algorithm in Paden et al. [1989]. This algorithm can also be used for MP of

manipulators and is covered in Section 3.1.3.

The generalization of the configuration space approach to the three-dimensional world is carried out in Donald [1984]. Objects are assumed to be polyhedral. The corresponding Cspace has six dimensions. A six-dimensional lattice of points is laid over this space, where each point represents a small neighborhood in the Cspace. Equations representing boundaries of configuration obstacles are then derived from the contact conditions between the vertices/edges/faces of the robot and obstacles. These equations are evaluated when determining whether a point is inside or outside the configuration obstacles. The algorithm searches for a connected sequence of lattice points outside the configuration obstacles. Because the search space is very large, it uses several heuristics to speed up the search. This algorithm is complete at a given resolution of the lattice and will probably run in a few minutes on current *supercomputers*.

In Guibas et al. [1988], an $O(\lambda_s(n)\log^2 n)$ algorithm is presented for the generalized MP with two degrees of freedom, where n is the number of colli-

sion constraints, s the maximum algebraic degree of these constraints, and $\lambda_s(n)$ the (almost linear) maximum length of an (n, s) Davenport-Schinzel sequence. This algorithm is based on the $O(\lambda_s(n))$ upper bound they established for the complexity of a single connected component of the free configuration space, which is computed as follows. A set of curves Γ representing collision constraints partitions the Cspace into cells C, and we are interested in finding a single connected cell c^* that contains the start configuration s of the robot. A solution exists if the goal is in the same cell. To compute the cell, Γ is split into two subsets Γ_1, Γ_2 of equal size. Γ_1 and Γ_2 result in a different set of cells, C_1 and C_2. The cells, c_1^* and c_2^*, that contain s are selected from C_1 and C_2, respectively. Finally, the cell c^* of C containing s is computed by intersecting c_1^* and c_2^*. For MP of a rectangle in a polygonal environment, there is an algorithm of $O(((a/b)^* \epsilon^{-1} + 1)n \log^2 n)$, where $a \geq b$ are the dimensions of the rectangle, and ϵ denotes the tightness of the free space [Alt et al. 1990].

A sweep volume method is used to efficiently approximate configuration obstacles for a polygonal robot among polygons [Zhu and Latombe 1990]. This algorithm partitions the robot orientation into a set of intervals. For each interval, it computes two types of rectangular cells: *bounding* cells that contain the configuration obstacles and *bounded* cells that are contained in the configuration obstacles. The set difference between the two types of cells are further decomposed into smaller bounding and bounded cells until a satisfactory resolution is achieved. A path is found by connecting the empty cells, i.e., those in the complement of the set of bounding cells. This algorithm generates 5–10 times fewer cells than the octree method [Brooks and Lozano-Pérez 1983] and runs in less than 10 minutes on a Macintosh II computer.

Configuration obstacles are computed with Minkowski set difference using a graphics hardware in Lengyel et al. [1990]. This algorithm uses a standard graphics hardware to rasterize configuration obstacles into a series of bitmap slices and then uses the brush fire search to find a shortest path in this rasterized space. It takes about 25 seconds to compute obstacles in a 3D configuration space (raster size of 8 million points) and about 50 seconds to plan a path. This algorithm is near real time, but works well for dof $\leq$ 4 due to a huge memory space requirement.

Potential-Field Approach*

The potential-field is used not only to avoid obstacles locally but also to design a globally optimal path in the sense of path length for the classical mover's problem [Hwang and Ahuja 1989, 1992]. In this 2D and 3D heuristic algorithm, a computationally efficient potential function is defined in terms of the boundary equations of polyhedral obstacles. The topological structure of the free space is captured by the valleys of minimum potential (MPV), which consist of local minimum and saddle points of the potential. It is similar to the Voronoi diagram. The shortest path with the minimum chance of collision is selected from MPV, and narrow regions of free space along the initial path causing collisions are identified. Motion-planning problems are classified as having three different levels of difficulty in this algorithm. For the problems with the lowest level of difficulty, the free space between obstacles is quite wide for the robot, and there are no narrow regions. An optimal path is obtained by minimizing a weighted sum of the potential on the robot, change in robot's orientation, and travel distance as the robot moves along the path. The second level of difficulty is characterized by the existence of narrow regions. Feasible configurations of the robot in these regions are found by locally minimizing the potential on the robot. Each narrow region leads to two subproblems: one of moving the robot from the previous narrow region (or the source location), so it assumes a feasible configuration in the current narrow region, and another of
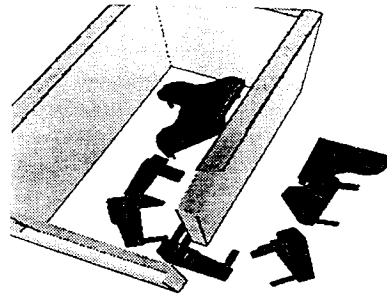
(a) Moving a grand piano into a room.
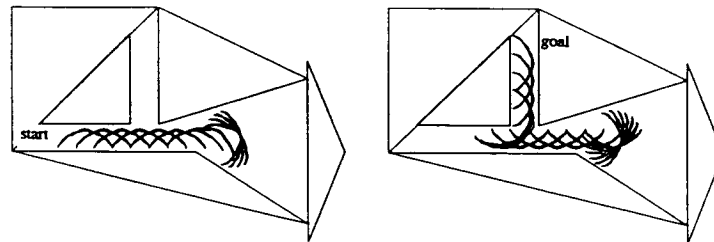
(b) The arc has to sidetrack twice to get the necessary orientation changes to reach the goal.

Figure 23. Potential-field-based motion planning.

moving the robot from the current narrow region, so it assumes a feasible configuration in the next narrow region (or the destination location). The robot moves from one feasible configuration in a narrow region to that in an adjacent region by following the initial path while minimizing the potential on it. Figure 23a shows the motion of moving a grand piano into a room, where a narrow region is at the doorway. For the most difficult class of problems considered, a narrow region has multiple feasible configurations, none of which can be connected to the feasible configurations on both sides. This leads to an additional third problem, that of connecting two feasible configurations in the same region, each of which is connected to only one side. Since the robot cannot easily move from one configuration to another in a narrow region, this problem is solved by moving the robot into an open space to get a necessary orientation change and moving back into the narrow region. Figure 23b shows an

arc-shaped robot making two excursions from the T junction to get the necessary orientation changes. Their algorithm finds near-optimal paths (in terms of path length) for a variety of 2D and 3D problems. The computation times are less than 5 minutes for 2D problems and 30 minutes for 3D problems with 5-10 obstacles on a 4-MIPS SUN computer. There are several notable features of this potential-field approach. It leads to smooth object motion; coarse topological planning is separated from cost minimization for detailed planning using a coarse-to-fine computation; it can be extended to solve problems in higher dimensions with a marginal increase in complexity; and computation of potential field is highly amenable to parallel and analog computing.

In Chuang and Ahuja [1991a], a closed-form expression of the electrostatic potential of a line segment is derived, assuming it is electrically charged. It is more smooth than those developed
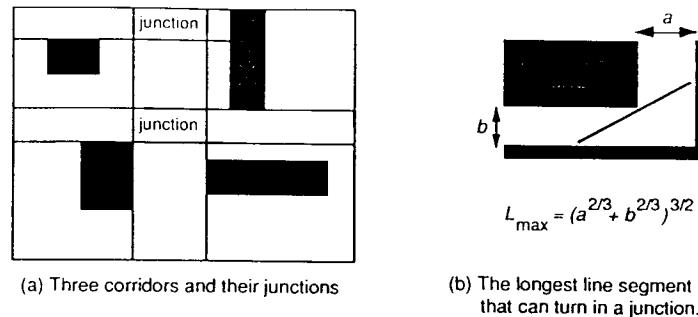
(a) Three corridors and their junctions

(b) The longest line segment that can turn in a junction.

$$L_{max} = (a^{2/3} + b^{2/3})^{3/2}$$

Figure 24. Moving a line segment among iso-oriented rectangles. Figure (b) reprinted from *Proc. of IEEE Int. Conf. on Robotics and Automation*, pp. 1413–1418, Maddila, S. R., "Decomposition algorithm for moving a ladder among rectangular obstacles," by permission of IEEE, Piscataway, N.J., Copyright, © 1986 IEEE.

by others and is used to plan paths for polygonal robots among polygons. In this algorithm, a global planner identifies narrow bottlenecks in the free space by computing *minimum-distance* links between obstacles. A collision-free path in each of these regions is computed using the potential field. These paths are connected to yield a solution. This algorithm generates a very smooth motion for the robot, since it uses the differentiable Newtonian potential function to avoid obstacles. This algorithm takes a few minutes on a 4-MIPS SUN computer to solve 2D problems with 5–10 obstacles.

A global-path-planning algorithm applied to both rigid robots and manipulators is presented in Warren [1989]. This algorithm generates configuration obstacles first and then assigns potential functions to the configuration obstacles. The potential function has a truncated conical shape; it has a maximum value at the center, decreases linearly as the distance from the center increases, and is zero beyond a preset distance from the configuration obstacles. The center of conical potential is located at the approximate center of each configuration obstacle. The algorithm initially plans a straight-line path from the start to the goal in the configuration space. Then this initial path is modified in the direction of minimizing potential. Since the potential has a conical shape, it will converge to a

curve contained in the free configuration space. This algorithm is significant in that it combines the idea of configuration space and potential functions. The overhead of computing connected components of configuration obstacles and their centers limit this algorithm to cases with dof < 3.

Motion Planning of Line Segment

The MP of a line segment, called a ladder, is simpler than MP of a polytope. The MP of a line segment has limited applicability in the real world, but it serves as a good reference to gauge the complexities of more general versions of the classical mover's problem.

Moving a ladder among iso-oriented rectangular obstacles is considered in Maddila [1986]. We mean by *iso-oriented* that sides of rectangles are parallel to the coordinate axes (Figure 24a). The problem is decomposed into several local-motion-planning problems. The free space is divided into corridors and junctions. Corridors are the "hallways" between rectangular obstacles, and junctions are the areas where corridors meet. The movement of the ladder is either horizontal or vertical, and rotations are performed at L-shaped junctions. Because of the iso-oriented nature of the rectangular obstacles, the maximum length of the ladder that can move through an L-

shaped channel is easily calculated (Figure 24b). A weighted graph called a motion graph is constructed from the solutions of the local subproblems. The weights represent the longest ladder that can be moved between the nodes of the motion graph. The algorithm finds a path in $O(n \log n)$ time and is also capable of finding the longest length of the ladder movable between two positions in the free space. This algorithm is useful in environments such as factory floors, where most obstacles are rectangular and iso-oriented.

The complexity of moving a ladder in three dimensions is studied in Ke and O'Rourke [1987, 1988]. An $\Omega(n^4)$ lower bound is established by constructing an example with a complex arrangement of polygons in space that force a ladder to make $\Omega(n^4)$ distinct moves, where n is the total number of obstacle vertices (Figure 25). They show an $O(n^6 \log n)$-time algorithm for moving a ladder using the cell decomposition approach of Schwarts and Sharir [1981].

Future Research Directions

Algorithms for the classical mover's problem have applications such as in assembly planning and navigation in cluttered environments. These algorithms are repeatedly used by task planners to check the feasibility of object transfer and placement. There is yet no 3D algorithm that matches the human MP capability. A brute-force way of computation using *supercomputers* or massively parallel computers is a possibility, but it is very expensive and still takes minutes. More efficient algorithms for the classical mover's problem in 3D are hence needed. The complexity analyses show that exact-motion planners for the 3D classical mover's problem will take a high-degree polynomial time. Since object models are not exact in most cases, future research should concentrate on heuristic algorithms that run in a few seconds at the expense of failing to find a solution to very hard, pathological, puzzle-like problems (humans, too, perform poorly in such

cases). Knowledge-based methods seem promising since many objects manipulated by robots are manmade and highly regular.

3.1.2 Point or Circular Robots

The shape of a point or a circular robot is independent of its orientation. It is useful to develop efficient algorithms for this problem since a robot can be treated as a point or a circle in many navigational situations. Many fast algorithms have been developed using representations such as visibility graph, quadtree (octree), or grids. The shortest-path problem for a point among polygons in 2D can be solved in $O(n^2)$ time with the visibility graph algorithm [Asano et al. 1985]. It is shown that the shortest-path problem among polyhedral obstacles in 3D is NP-hard [Canny and Reif 1987], and only exponential-time algorithms are known [Canny 1987], [Reif and Storer 1988], [Sharir and Schorr 1986]. Thus, an exact polynomial-time algorithm for 3D is unlikely, although there is an *approximate* polynomial-time algorithm Papadimitriou [1985].

There are two interesting special cases for a point robot. In the *weighted-region* problem, the world space consists of regions with different traveling costs, and the minimum-cost path between two points is not a straight line even if there are no obstacles (Figure 26). MP in a partially known environment assumes that the robot knows only those parts of the world that it has seen. For example, information about the space behind an obstacle is unknown until the robot acquires that data. Motions are planned based on partial information. The robot can construct a more complete representation of the world space as it explores the world. Algorithms for these two problems are presented at the end of this section.

Skeleton Approach

The visibility graph and the Voronoi diagram are prime candidates for a skeleton
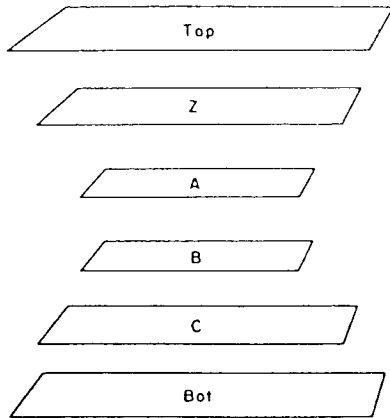
(a) a line segment is moving through equally spaces planes Z, A, B and C, which are between hole-less Top and Bottom planes. The length of the line segment is the same as the distance between plane Top and C.
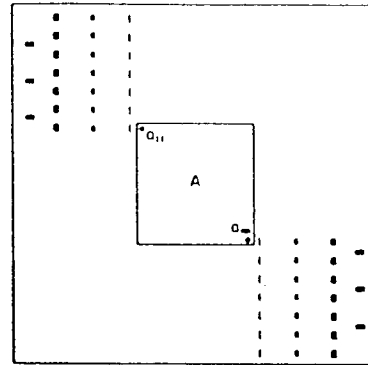
(b) Holes in Plane Z.
Plane A is drawn to establish scale.
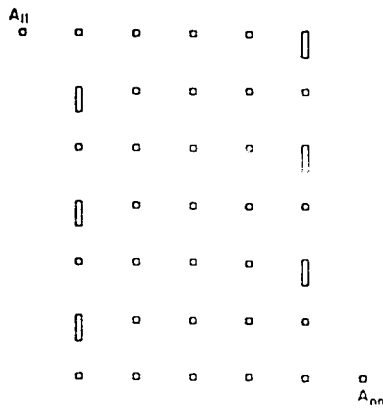
(c) Holes in Plane A
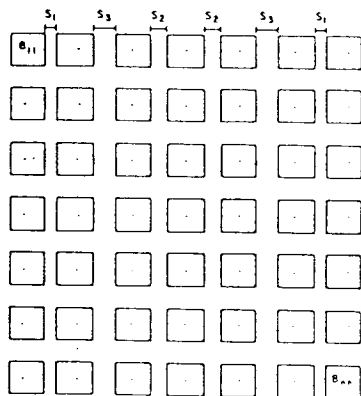
(d) Holes in Plane B
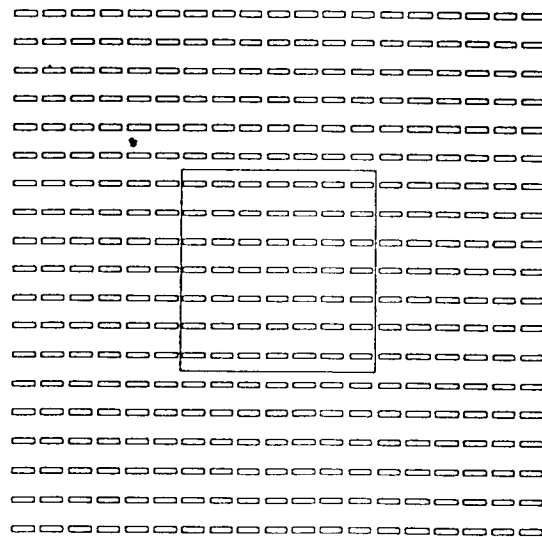
(e) Holes in Plane C.
Plane A is shown to establish scale.

Figure 25. A set of obstacle planes that forces a line segment to make $\Omega(n^4)$ moves to go from one hole to another. Reprinted from *Discrete and Computational Geometry*, vol. 3, pp. 197–217, Ke, Y. and O'Rourke, J., "Lower bounds on moving a ladder in two and three dimensions," by permission of Springer-Verlag New York, Inc., Copyright, © 1988 Springer-Verlag New York, Inc.
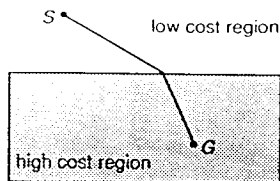
Figure 26. The minimum-cost path in a weighted region obeys the Snell's Law of refraction at the boundary.
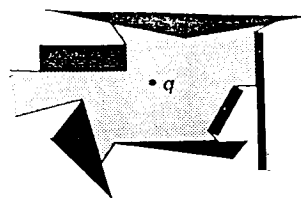
Figure 27. The visibility polygon (shaded region) from point q.

for finding a path among polygons in 2D. To be used for MP of a point robot, the feature set of the visibility graph has to include the start and goal points in addition to obstacle features. For the Voronoi diagram, a canonical procedure that moves the robot from the start and the goal points onto edges of the Voronoi diagram is needed. A straight line movement in one of the coordinate axes of the Cspace usually suffices. There are not many MP algorithms for point robots using the Voronoi diagram, since the algorithms generating the Voronoi diagram can be directly used for MP. (An $O(n \log n)$ algorithm to move a disc among polygons using the Voronoi diagram is reported in O'Dúnlaing and Yap [1982].) In contrast, the visibility graph is used in a variety of ways to solve many different MP problems.

The visibility graph takes $O(n^3)$ time to construct with the following trivial method, where n is the number of vertices. There are $O(n^2)$ possible line segments between every pair of polygon vertices, and testing of each line segment for intersection with the polygons takes $O(n)$ time. This time is improved to $O(n^2 \log n)$ [Lee 1978], to $O(n^2)$ [Asano et al. 1985; Sharir and Schorr 1984; Welzl 1985], and then to $O(nk + n \log n)$ time where k is the number of disjoint simple polygons [Reif and Storer 1985].

The *visible-polygon* idea is used to compute the visibility graph in Asano et al. [1985]. Given a query point q and a set of edges intersecting only at their endpoints, the visible polygon is the set of points p on the edges such that the line segment pq does not intersect any

other edge. The visibility polygon is computed by setting the origin of a polar coordinate system at the query point, ordering the endpoints of edges according to the polar angles, and finding the closest edge to the query point for each polar angle of the endpoints (Figure 27). This $O(n)$ visible-polygon algorithm is repeated for each of the n vertices, computing the visibility graph in $O(n^2)$ time. The $O(n^2)$ of Dijkstra's algorithm is used to find the shortest path in the visibility graph, giving the overall complexity of $O(n^2)$.

Rather than generating the whole visibility graph in the beginning, it is incrementally generated while searching for a solution path using A* search (ICORS) [Montgomery et al. 1987]. This algorithm makes use of pruning rules and a hierarchical set of visibility tests to minimize the size of the visibility graph, and thus speeds up the A* search. For example, the occlusion information among obstacles is used to generate only those paths to the visible vertices from the robot's current position. Although it has $O(n^2)$ worst-case time complexity, it runs much faster in average cases. Parallel implementation can be used to compute the costs of reaching vertices and to do the search.

de Rezende et al. [1985] consider the problem of finding a shortest path in the Manhattan or L_1 distance. The obstacles are disjoint rectangles with sides parallel to the coordinate axes. Motions of the robot can be restricted to either horizontal or vertical, since we are using the L_1 metric. The essence of the algorithm is the fact that the shortest

path between two points in this space is monotone in either vertical or horizontal direction. Assume without loss of generality that the start point has smaller x and y coordinates than those of the goal point. Move the robot in $+y$ direction, whenever possible, and in $+x$ direction only if $+y$ motion is blocked by a rectangle. If the robot passes under the goal point during this motion, an optimal solution is monotone in y direction (in x direction if it passes above). Note that the robot does not get stuck since the rectangles are disjoint. Once the direction of monotone motion is determined (let us assume it is $+x$), a type of scan line algorithm is used to find the shortest path. The scan line is moved from the start point in $+x$ direction and stopped at an x coordinate of a rectangle vertex, and the L_1 distance from the start to the vertex is computed. This vertex is stored in a list containing vertices that may lie on the shortest path. The scan line is moved to a next vertex of a rectangle in $+x$ direction, adding vertices to the list. A rule is used to delete vertices in the list that can no longer lie on the shortest path. This algorithm runs in $O(n \log n)$ and is useful for planning bus routes in cities or finding paths for electrical connections on circuit boards.

If the rectangles are weighted, i.e., the robot is allowed to go through them at extra costs, an $O(n \log^2 n)$-time and $O(n \log n)$-space (or $O(n \log^{3/2} n)$ time and space) algorithm is available [Lee et al. 1990]. The L_1 shortest path among polygons is studied in Clarkson et al. [1987]. It is of $O(n \log^2 n)$ and plans paths by constructing a weighted visibility graph whose vertices are the start, goal, vertices of the polygons, and some additional points called *Steiner* points. It also shows an $O(n^2 \log^3 n)$ algorithm for the L_1 shortest path among rectilinear obstacles in 3D.

There is a family of algorithms for the shortest paths on the surface of a single polyhedron. The algorithm in Hwang et al. [1989] computes a representation of a convex polyhedron in $O(n^6 \log n)$ time, which is used to find the shortest

path on the polyhedron between any pair of points on the edges of the polyhedron in $O(k + \log n)$ (k is the number of edges the shortest path crosses). This version of the problem is called the *all-pair* shortest-path problem. For the single-source problem (one of the points is fixed) for a single convex polyhedron, an $O(n^3 \log n)$ algorithm is presented in Sharir and Schorr [1984]. The time is later improved to $O(n^2 \log n)$ in Mount [1985]. For a nonconvex polyhedron, an $O(n^5)$ algorithm is developed in O'Rourke et al. [1984] and improved to $O(n^2 \log n)$ using the technique called *continuous Dijkstra* (Dijkstra algorithm applied to a finite number of continuous regions) in Mitchell et al. [1987, 1990], again to $O(n^2)$ in Chen and Han [1990]. We also note that there are $O(n)$-time algorithms for the minimum-link path problem inside a polygon [Suri 1986; Ke 1989] and an $O(E\alpha(n)\log^2 n)$-time algorithm for the same problem among polygons (E is the size of the visibility graph, and $\alpha(\,)$ denotes the extremely slowly growing inverse of Ackermann's function). Minimum-link paths are found by first computing the visible polygon (Figure 27) from the start point and then by recursively computing the visible polygons from the vertices of the computed visible polygons, until the goal point is visible.

Some parallel algorithms for solving visibility and shortest-path problems for simple polygons exist. Atallah et al. [1989] show an algorithm to compute visible portions of the plane from a point in a collection of line segments in $O(\log n)$ time with $O(n)$ processors. The number of processors for this problem is improved in Atallah and Chen [1989] to $O(n/\log n)$ for the case when the line segments form a simple polygon. The shortest path between two points in a simple polygon can be determined in $O(\log n)$ time with $O(n)$ processors [ElGindy and Goodrich 1988], and the shortest-path tree from a vertex to all other vertices can be computed in $O(\log^2 n)$ time using $O(n)$ processors. Goodrich et al. [1990] present an algorithm of $O(\log n)$ time with $O(n)$ ($O(n/\log n)$ with preprocessing) proces-
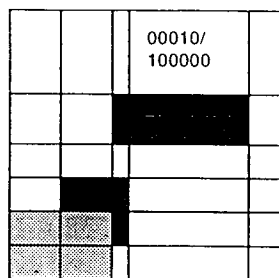
Figure 28. Rectangular cell decomposition and the coding of the cells. A cell has two strings that represent the horizontal/vertical position of the cell. The shaded region is a prime convex area.

sors for the shortest path in a simple polygon and an algorithm of $O(\log n)$ time with $O(n \log n + k/\log n)$ processors for the construction of the visibility graph for a simple polygon (k is the number of edges in the graph).

Cell Decomposition Approach

Overlapping iso-oriented rectangles are used as cells in decomposing the world space filled with polygons in Singh and Wagh [1987]. Polygons are first approximated with the smallest iso-oriented rectangles, and the rectangle edges are used to partition the free space into rectangles. Each free rectangle is coded with a pair of binary strings which has a 1 at the bit positions representing the horizontal and vertical locations of the rectangle (Figure 28). Unions of these free rectangles that form larger rectangles are computed, and only maximal unions are used for path planning. A maximal rectangular union is called a prime convex area because it has the binary strings that correspond to the prime implicant of the strings of the rectangles forming the union. Two overlapping prime convex areas are considered connected. The connectivity graph (with $O(n^2)$ nodes and $O(n^4)$ edges in the worst case) of the prime convex areas is constructed to carry out the search for near-minimum-length paths. This algorithm finds near-optimal solutions in less than a minute for problems containing 30 rectangular obstacles.

The free space among polygons is decomposed by using the lines containing edges of the polygons in Rueb and Wong [1987]. The resulting polygonal cells in the free space are joined to form overlapping maximal convex regions, and overlaps among these regions are found. The roadmap of the free space is formed with the overlaps as nodes and common convex regions joining the overlaps as edges. The roadmap is similar to the Voronoi diagram and constructed in $O(n^2)$ time in the worst case and in approximately linear time for common problems. Dijkstra's algorithm is used to find the shortest path in the roadmap. This algorithm takes about 200 seconds to solve the problem in Figure 29. This seems to be reasonably fast and can be used for a robot moving in a warehouse or a building.

A probabilistic approach is taken in Jun and Shin [1988] to plan a path for a point robot. The 3D space is represented with a 3D grid of points, and each point is marked as either free or occupied by obstacles. The probability of each point becoming a dead end is iteratively computed based on the obstacle shapes and locations. A probability of 1 is initially assigned to points occupied by obstacles, and 0 to those in the free space. The probability for each point is then modified in parallel by examining the probabilities of the adjacent points, increasing the probabilities of the points in blind alleys and narrow regions. The best-first search is then used to find the shortest path instead of the expensive A*. They report a speedup by a factor of 10 compared to using A* search. This algorithm is fast enough to be online if the environment does not change often and if only the start and goal positions of the robot change. If the obstacle information is in a grid form, this method can be used directly. If obstacles have a more compact representation, a smaller number of bigger cells should be used in the free-space decomposition.

An algorithm for a mobile robot moving on curved surfaces is developed in Gaw and Meystel [1986]. The surface is
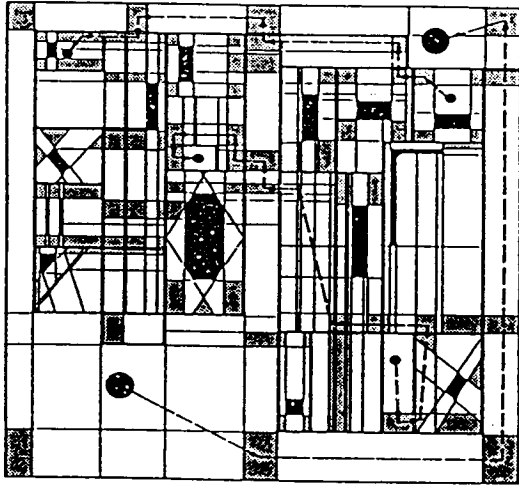
tains only a few small obstacles is denoted as a gray cell. When a gray cell is selected as a part of an optimal path, it is refined into black (obstacle occupied) and white (free) cells. This multiresolution approach speeds up the search process by 2-10 times. It takes 10-20 seconds to solve problems involving about 10 obstacles. This algorithm is very efficient when both the path length and the clearance are important and when the number of obstacles is large.

Potential-Field Approach

Thorpe has used a potential function based on distance to design an optimal path for a circular robot in 2D [Thorpe 1984]. A grid of points is laid over the world space, and each point on the grid is assigned a cost inversely proportional to the minimum of the distances to all obstacles. Then the A* search is used to compute the path on the grid having the minimum length and cost. The points on this path are then allowed to move to further decrease the cost of the path. Krogh and Thorpe [1986] later include a dynamic steering control in their formulation. Dynamic steering of the robot is done by minimizing a potential function which is the sum of a goal potential and an obstacle potential. The goal potential is formulated so that the robot is attracted to the next corner (turning point) along the path. The obstacle potential is defined as the inverse of the minimum time necessary to avoid obstacles, which can be computed from the maximum acceleration of the robot, the current velocity, and the distance to the approaching obstacle. A similar obstacle potential is used in Faverjon and Tournassoud [1987]. This algorithm is useful for a mobile robot that can control its acceleration in x and y direction independently. The grid search in this algorithm becomes expensive (especially for A*) if a solution with high spatial resolution is required. A parallel implementation, however, can greatly speed up this grid-based algorithm.

Koditschek [1987] has constructed a

Figure 29. Motion planning with object-dependent cell decomposition. Motions of circular robots are shown in dashed lines. Reprinted from *IEEE Trans. on Pattern Analysis and Machine Intelligence*, vol. PAMI-9, no. 2, pp. 263-273, Rueb, K. D. and Wong, A. K. C., "Structuring free space as a hypergraph for roving robot path planning and navigation," by permission of IEEE, Piscataway, N.J., Copyright, © 1987 IEEE.

represented by a set of iso-elevation lines (isolines), each of which consists of a set of points. The gradient vectors (of heights) are then computed at each point, and A* search is used to plan a path using a cost function that depends on the vehicle model and the elevation gradient vector. Obstacles are avoided by assigning an infinite cost to the points inside obstacles. It took five minutes for a three-obstacle problem with 100 vertices representing the isolines. This algorithm is very practical for mobile robots on uneven terrains.

A quadtree-based algorithm for a point robot is presented in Kambhampati and Davis [1986]. An optimal path in the sense of minimum length and maximum clearance is found from the quadtree using A* search. Search on a quadtree is much faster than that on a grid due to a smaller number of cells. To further speed up the search, the number of cells in the quadtree is reduced by using a multiresolution representation. A cell which con-

potential function for point robot navigation among disk obstacles, and Rimon and Koditschek [1988] have extended it to n-dimensional Euclidean space (E^n) for a point robot moving among disjoint E^n spheres. The potential function, called a navigation function by the authors, is 1 at the obstacle boundaries, a unique globally minimum value of 0 at the goal position, and has no local minima in the free space. Thus, no matter where the initial position is, the robot can follow the negative gradient of the potential to reach the goal position. The navigation function has the form $(\gamma(\gamma^k + \beta))^{-k}$, where γ is the distance to the goal and β is the product of the distances to all the spheres, with k sufficiently large. It is 1 at the boundary of one of the spheres since β is 0. It is 0 at the goal since γ is 0. A sufficiently large value of k makes the downhill slope of the potential toward the goal steep enough to remove all local minima. Notice that the disjointness of the obstacles is a critical assumption.

This navigation function has been extended to the disjoint *star* world in Rimon and Koditschek [1989]. A star is a set which has a point in its interior such that the set contains the line segment connecting the point and any point of the set. The algorithm deforms star shapes to spheres and uses the navigation function defined above. These algorithms are very attractive since they not only guarantee solutions, but also give the forces to control the robot in the form of the gradient of the navigation function. It is unlikely, however, that the approach could be generalized to nonpoint robots, since such robots result in configuration obstacles that are very concave and not disjoint.

A real-time strategy for a point robot to avoid elliptical obstacles in 2D is developed in Kheradpir and Thorp [1987]. Elliptical obstacles are used as state- (position and velocity) dependent constraints on the control variables. These constraints are used with the hard actuator limits in the optimal decision strategy to follow desired trajectories while avoiding obstacles. This algorithm is a *local*

planner since the desired trajectories to follow must be given. The main contribution of this paper is the real-time implementation. Its extension to manipulators will be very valuable for local avoidance of obstacles. Such local avoidance is necessary even with a global-path planner because of errors in obstacle models and uncertainties in sensors and actuators.

Two commonly used object representations in computer vision, the medial axis transform (MAT) and the generalized cylinder representation, can also be used for MP of a point robot. The MAT of a region is the Voronoi diagram where each point on the diagram is labeled with the distance to the region boundary. (So the region can be reconstructed by taking the union of all circles centered at each point with the radius equal to the distance labeling the point.) The generalized cylinder representation of an object consists of a (possibly curved) axis and a radius labeling each point on the axis. The object volume is then defined by the union of disks centered at the points on the axis and perpendicular to the axis. An approach to efficient derivation of the MAT and the generalized cylinder representations of a two-dimensional region is reported in Chuang and Ahuja [1991b]. Instead of using the shortest distance to the region border, a potential-field model is used for computational efficiency. The region border is assumed to be charged, and the valleys (saddle points and minima) of the resulting potential field are used to obtain preliminary estimates of the axes for the two representations. The potential valleys are found by following the negative gradient of the potential, thus avoiding two-dimensional search. The simple Newtonian potential is shown to be inadequate for deriving accurate representations. A higher-order potential is defined which decays faster with distance than as inverse of distance. It is shown that as the potential order becomes arbitrarily large, the axes approach those computed using the shortest distance to the border. An algorithm is presented to efficiently compute the MAT skeleton. This algorithm is then

modified to obtain the generalized cylinder axis of a polygonal region. These algorithms for polygonal regions are used to perform a multiresolution coarse-to-fine computation of the MAT and generalized cylinder axes of arbitrarily shaped regions. This algorithm can be used to compute the MAT of the free space and plan the motion of a point robot in 2D.

Weighted-Region Problem

The weighted-region problem has important applications in terrain navigation and the least-risk watchman route problem (a watchman route is such that each point in some set is visible from at least one point along the route). There are two approaches to solve this problem. Approximate algorithms discretize the space with a grid of points and assign a weight (cost) to each point. A shortest-path algorithm such as Dijkstra's algorithm is then used to find a sequence of points minimizing the total cost [Jones 1980; Kiersey and Mitchell 1984; Quek et al. 1985]. An exact approach is to use Snell's Law (the law of refraction in optics) as a local-optimality condition in planning globally optimal paths. It is well known that the path of a light ray traveling in different mediums obeys Snell's Law and results in the minimum-time path. An exact algorithm that runs in $O(n^7 L)$ time and $O(n^3)$ space is presented in Mitchell and Papadimitriou [1987]. (L denotes the precision of problem specification.) This algorithm uses the *continuous Dijkstra* introduced in Mitchell et al. [1987] and Snell's Law to plan paths. More efficient algorithms for various special cases are presented in Gewali et al. [1988].

In Richbourg et al. [1987], the plane is represented by a ternary map, i.e., the regions are labeled as either impossible to traverse, high cost, or low cost. The algorithm first treats high-cost regions as if they have the low cost and finds the shortest path. The actual cost of traveling on this path in the original ternary map is computed. This gives an upper bound of the costs for possible solutions

and also bounds the parts of the plane to be examined. Only those points whose distances to the start and the goal sum up to less than the upper bound need to be considered (these points form an ellipse; see Figure 30a). Wedges are used to represent the ranges of light rays that go through the same sequence of the boundary segments. Instead of using A* search on a static graph, the wedges are dynamically generated during the A* search process (ICORS). Figure 30b shows a minimum-cost path. Time complexity is not given and is likely to be high in the worst case. The authors point out that a brush fire search using a grid is likely to run faster if many high-cost polygonal regions are concentrated in a small region.

Partially Known Environment

The work on path planning in partially known environments has been restricted to point robot navigation in 2D [Chatila 1982; Chatila and Laumond 1985; Chattergy 1985; Koch et al. 1985; Oommen et al. 1987]. All these algorithms use world maps that are updated as the robot explores the environment. Heuristic strategies are used to plan paths from the partial information of the world using the world map. The robots often avoid unknown terrains by assigning a large cost to such areas.

Rao et al. [1988] have studied the problem of visiting a sequence of points in a partially known 2D polygonal world. Only those obstacles visible to the robot are known to the robot. Two algorithms, LNAV and GNAV, are developed based on the visibility graph. LNAV is used to move the robot between two vertices, say the current and the goal vertex. From the current vertex, the robot scans the world and obtains visible vertices. It then goes to one of the visible vertices that is not yet visited and closest to the goal. If at some point all visible vertices are visited, it backtracks until there is an unvisited vertex. This is repeated until the goal is reached. GNAV visits the sequence of vertices by repeated applica-
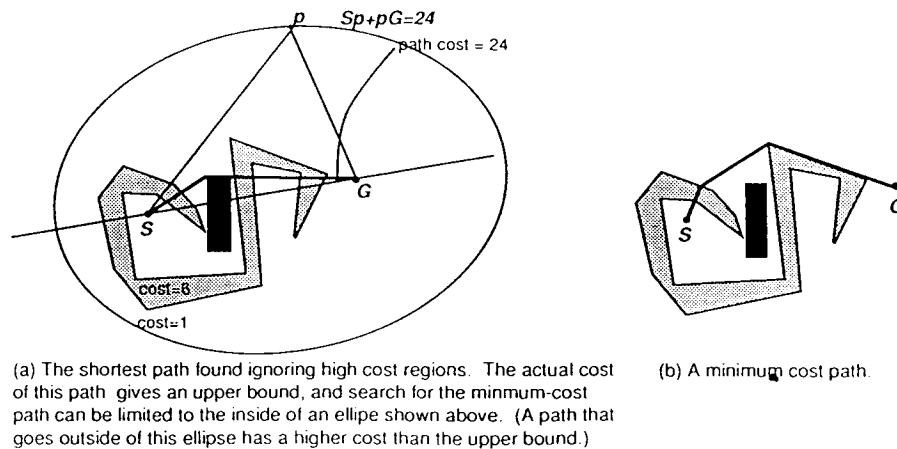
(a) The shortest path found ignoring high cost regions. The actual cost of this path gives an upper bound, and search for the minmum-cost path can be limited to the inside of an ellipe shown above. (A path that goes outside of this ellipse has a higher cost than the upper bound.)

(b) A minimum cost path.

Figure 30. Weighted-region problem. Reprinted from *Proc. of IEEE Int. Conf. on Robotics and Automation*, pp. 1631–1636, Richbourg, R. F., Rowe, N. C., Zyda, M. J., and McGhee, R. C., "Solving global two-dimensional routing problem using Snell's Law and A* search," by permission of IEEE, Piscataway, N.J., Copyright, © 1987 IEEE.

tion of LNAV with a restricted form of learning. The global-vertex graph is updated as the robot moves, and the path is planned in the global-vertex graph. The time complexity of LNAV is $O(n^2)$, which is typical of the visibility-based algorithms. GNAV is $O((n + m)^3)$ where m is the number of vertices to be visited.

Lumelsky [1987] describes algorithms in which the robot (*bug*) knows the goal location and can only feel obstacles. An interesting feature of this algorithms is that it does not use any explicit representation of the free space. All the information about obstacles comes from direct contact between the bug and obstacles. The bug goes directly toward the goal in a straight line *Ml*. When it encounters an obstacle, it follows the obstacle boundary while maintaining contact with the obstacle. When it meets the line *Ml* on the other side of the obstacle, it leaves the obstacle and heads for the goal again. Lumelsky [1987] proves the convergence of such a bug algorithm. The path found is not optimal in general. The bug algorithm has also been extended to the motion planning of manipulators (Section 3.3). In Lumelsky and Skewis [1988], the bug is equipped with finite-range vision to improve the efficiency of the paths. It plans the shortest path within its visual range while using the bug algorithm described above. It is proven that having vision always results in shorter paths than no vision, but longer-range vision does not necessarily result in shorter paths than shorter-range vision. Because of the inefficiency of the solutions obtained by the bug algorithms, they are applicable to cases where obstacle information is available only through touch sensors.

Future Research Directions

Path planners for a point robot in 2D have time complexities of $O(n \log n)$ to find a feasible path and $O(n^2)$ to find the shortest path. The 3D shortest-path problem is not discrete, i.e., the solution cannot be obtained in a finite number of steps, and exact polynomial algorithms are unlikely. See Sharir and Schorr [1984] for a double-exponential procedure for determining the sequence of obstacle edges that the shortest path passes through. The power of computers, however, has reached a stage where the point navigation in 3D can be done in near real-time by brute force using a brush fire search in a three-dimensional grid.

Motion planning of a point robot in static environments is well understood, and we suggest the following areas for future research. The first area is the kinodynamic planning, where dynamic constraints such as bounded acceleration are considered (see Section 3.3). Second, path planning of multiple robots with conflicting/common objectives has applications in planning of battlefield strategies and construction of large structures with multiple robots. This requires research in representing task requirements in terms of robot motions, formulating optimality criteria for various tasks, and efficient search methods for a very high-dimensional space (the Cspace dimension of multiple robots is the sum of the dof of all the robots). Third, more work is needed for sensor-based path planning in uncertain and partially known environments. This research will address the issue of uncertainty handling, sensing planning, and efficient representations for information updating. Some work in these areas can be found in Donald and Jennings [1991].

3.1.3 Manipulators

A manipulator is a robotic arm consisting of links joined together. Joints are either rotary or prismatic (translational), and actuators, e.g., motors, are used to change joint angles or link lengths. The configuration parameters are the joint angles and link lengths controlled by prismatic joints, and the dof is equal to the number of independently controlled actuators. In this section, the word "robot" refers to manipulator, and joint angles refer to configuration parameters. Links and joint angles are indexed from the base of the manipulator. For example, link 0 is connected to an object in the world space, e.g., the floor, and the ith joint angle controls the movement of the ith link. The type of manipulator is specified by a string of "R" and "P," where the ith character represents the type of ith joint. Figure 31 shows an Adept robot, whose joints are rotary except for the third joint (RRPRRR), and a PUMA robot with a

hand which has all rotary joints (RRR-RRR).

Kinematics of a manipulator refers to the computation of the position and orientation of a part of the manipulator (usually the tip) from the configuration. It involves *sines* and *cosines* if the manipulator has a rotary joint. *Inverse kinematics* is the computation of the configuration from the position and orientation of the tip. Note that this problem often needs to be solved for manipulation. For example, to pick up an object, we need to find a configuration of the manipulator that will place its gripper where the object is. For 3D world space, it is described as a set of 6 simultaneous nonlinear equations in *dof* variables. The inverse kinematics often has multiple solutions even for a simple 2-link planar manipulator. If dof > 6, an infinite number of solutions exist, and such manipulators are called *redundant*. There is no closed-form solution for most manipulators. The *dynamics* refers to the relationship between the position/velocity of the manipulator and the force/torques applied by the actuators.

The *Jacobian J* refers to the relationship between differential changes of the manipulator tip configuration dx and differential changes of the configuration of manipulator dq. In equation form, $dx = J(q)\,dq$. J is a $6 \times dof$ matrix whose elements are functions of q. If we want to compute dq from dx, the inverse of J is computed. J is singular, however, for a certain set of q, and the inverse does not exist. Such a set is said to consist of *singular* configurations of the manipulator. The physical interpretation is that there is no dq that will move the tip in dx direction. For example, the singular configurations of a two-link robot in Figure 32 are those for which the two links are parallel, since no differential changes in the configuration will move the tip in the radial direction. Special care is needed when solving an inverse kinematics problem using the Jacobian.

Because most manipulators have nonlinear kinematics, the design of *globally* and *dynamically* optimal motions among

(a) An Adept manipulator

(b) A PUMA manipulator
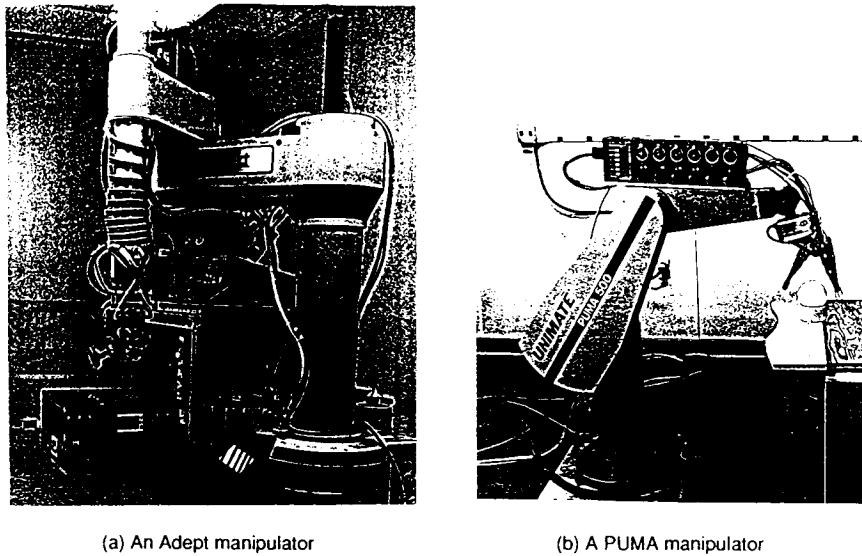
Figure 31. Commercial manipulators.

Figure 32. Singular configurations of a 2-link manipulator. The tip cannot move in the radial direction.

obstacles is difficult, and most global planners consider kinematics only. In algorithms that include dynamics, it is usually assumed that an initial path is given and that dynamic optimization is done *locally* in the vicinity of the path [Bobrow et al. 1985; Shin and McKay 1984]. This section will concentrate on kinematic global planners. Even for this case, a motion planner for manipulators having six degrees of freedom that runs at practical speeds has not been reported. Commercially available robots such as PUMA, Adept, and Gantry come with only a position controller, which basically make the robots follow specified trajectories. Only one graphics package for robot

simulation includes the path planner of Lozano-Pérez [1987]. With these definitions we now survey MP algorithms for manipulators.

Skeleton Approach

The MP of a planar d-link system confined in an obstacle-free circular region is studied in Hopcroft et al. [1985]. The bounding circle is the only obstacle. The algorithm first moves the linkage to a certain *normal form* and then puts each link into place, correcting its orientation if necessary using only *simple motions*. A simple motion involves monotone changes in at most four joint angles. It is defined so that the manipulator can move to any reachable point using only these motions, and it still retains the polynomial-time complexity of the MP algorithm. In a normal form, all the joints up to joint i lie on a radius of the bounding circle, and the rest of the joints touch the circle. Correcting orientation of a link involves destroying and restoring the positions of previous links, which takes $O(d^2)$ time. Orientation correction is done once for each link in the worst case, resulting in an $O(d^3)$ overall complexity.

This algorithm is a form of subgoal network, with the normal form and simple motion being the subgoal and local operator, respectively.

Faverjon and Tournasoud [1987] report a global-path planner for manipulators with many degrees of freedom. A subgoal network method is first developed in this paper. The global planner divides the Cspace into cells and assigns to the cells the probabilities that the local algorithm would succeed in them. All regions have the same probability initially and are then modified subsequently as the local algorithm is applied. The A* search is used to find a sequence of regions with the highest probability of success. A local operator is then applied to the sequence of cells. If the local operator finds (fails to find) a feasible motion in a cell, the probability of the cell is increased (decreased). The process of sequence generation and search for a feasible motion along the sequence is repeated. The local operator is based on a potential field called the *velocity damper*, i.e., constraints on the velocity with which the obstacles may be approached. This has an advantage over other potential fields in that it allows the robot to approach obstacles very closely. Other potential fields consider only the position of the robot and repel the robot away from the obstacles even if there is enough braking distance between them. The local planner moves the manipulator toward the goal by including a goal potential $|q - q_{goal}|^2$ in the minimization criterion while enforcing velocity damper constraints and uniformity of velocity for each joint. This offline algorithm is developed for a manipulator with a high number of degrees of freedom (10 links and 8 dof), for which exact algorithms have a very high complexity.

A randomized search technique is developed for the generalized mover's problem and is used for MP of high-dof manipulators [Barraquand and Latombe 1990]. This algorithm incrementally builds a graph connecting the local minima of a potential function defined in the Cspace and concurrently searches this graph until the goal is attained. A local minimum is connected to another one by executing a random motion to escape the potential well of the first one, followed by a gradient descent to reach the second one. This algorithm is probabilistically complete and is useful for a manipulator with high dof. The computation times for stick figure robots in polygonal/polyhedral environments are 2, 3, 15 minutes for $d = 8$, 10, 31, respectively. This algorithm is a combination of the potential-field and subgoal network approaches.

In Chen and Hwang [1992], a very efficient and resolution-complete motion planner is presented using a subgoal network method (Section 2.3.1). The efficiency and completeness of this algorithm are made possible by three things: defining subgoals in a hierarchical and multiresolution manner, bidirectional search, and the use of ICORS paradigm. A subgoal in this algorithm is defined by a rectangular cell of various dimensions s in the Cspace, where $0 \leq s \leq dof$. The cell of dimension dof is the whole Cspace, whereas a zero-dimensional cell is a point in the Cspace. A cell of dimension s is a set of configurations where the first $dof - s$ joint angles are specified, and the rest are unspecified. A set of cells of dimension s is obtained from an $s + 1$-dimensional cell by copying the values of the specified joint angles and by specifying the values of the $(dof - s)$th joint angle as follows. Place the first $dof - s - 1$ links in the configuration specified for the $(s + 1)$-dimensional cell. Move the $(dof - s)$th link by varying the $(dof - s)$th joint angle, and pick the values of the joint angle that put the link maximally away from the obstacles. For each of such values, an s-dimensional cell is created. This process is called *cell refinement*, and the resulting cells represent sets of configuration for which the first $d - s$ links are in *safe* locations. Note that a point cannot be refined. A cell is considered reached if the robot can reach any point in the cell. Two cells are considered adjacent if the L_1 distance between them is less than a preset threshold (the same definition holds

between a point and a cell). Imbedding the bidirectional search in the subgoal network method, this algorithm keeps two lists of reached points: the *s-reached* list containing the points reached from the start (initially only the start) and the *g-reached* list containing points reached from the goal (initially only the goal). Initially, there is only one subgoal, the whole Cspace C_0. The shortest sequence of subgoals between any point in s-reached list and g-reached list is found using Dijkstra's algorithm (initially start-C_0-goal is the only sequence). A local operator is used to check the existence of a feasible path along the chosen sequence by trying to move the robot from both ends of the sequence. The distance between the robot and obstacles is computed at the points at both ends of the sequence, and the robot is moved from the point with the smaller distance to the other. If there is no path, the last subgoal reached from each end is refined into several subgoals each having one less dimension. The refined subgoals are removed from the subgoal network, and the newly generated subgoals are entered in the subgoal network. The adjacency of subgoals is then updated in the subgoal network. The shortest sequence of subgoals between any s-reached points and g-reached points is computed again and subsequently checked by the local operator. This process is iterated until a path is found or until there is no sequence to examine. The local operator is based on the potential field and moves the robot toward the subgoal while maximizing the distance between the robot and obstacles. Figure 33a shows the subgoal network generated in the Cspace for the problem in Figure 2. Because the ICORS paradigm is used, this algorithm solves *easy* problem fast and *harder* problems with a gradual increase of computation time. It has an average computation time of 10 minutes on a 17-MIPS computer for 6-dof manipulators in polyhedral environments. This algorithm requires about 10,000 distance computations to solve the example in Figure 33b.

Lumelsky also applied the *bug* algorithm to manipulators of various types. In all of these algorithms, the robot is equipped only with touch sensors, and global information about *all* obstacles is not available a priori. Path planning for a Cartesian manipulator in 3D is described in Lumelsky [1986], in which the completeness of the algorithm is proved. The tip of the manipulator moves in the plane connecting the start and the goal positions and parallel to the last link. In Lumelsky [1987], the kinematics of 5 useful types of planar 2-link manipulators are analyzed. They are RR, PP, two RP, and PR types. The RP type has two kinds, depending on whether the sliding link is in the radial or angular direction. Obstacles in work space are transformed into configuration obstacles, and the bug algorithms are used in the Cspace. Although the topology of the joint space is more complicated than the Euclidean space, the bug algorithms are still shown to converge. Path planning of 2-link manipulators in 3D is described in Lumelsky and Sun [1987]. An implementation of the algorithm is reported in Cheung and Lumelsky [1988] in which infrared sensors are used on the PUMA 562 arm to detect contact. Using only the second and third degrees of freedom of PUMA (thus making the robot planar), the algorithm plans paths in real time with two Motorola 68020 microprocessors. The above algorithms have the same advantages and drawback as described earlier for other bug algorithms. Although these algorithms do not need all obstacle information a priori, the extension of the bug algorithm to 3D manifolds seems to necessitate the storage of obstacle information. This is because in 2D there are only two choices for the bug when it encounters an obstacle, turning right or left. In 3D, however, there are an infinite number of choices, and the storage of examined and unexamined choices is needed.

Cell Decomposition Approach

Brooks [1983] developed a 3D global planner for a PUMA robot arm. The
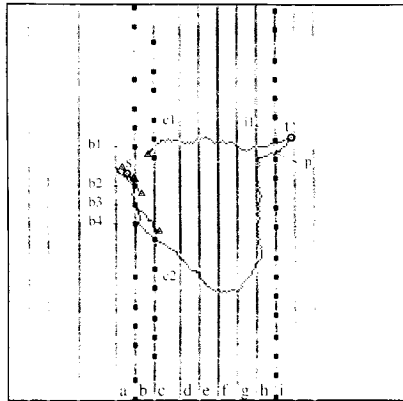
(a) The search process of SANDROS motion planner for the problem in Figure 2.1.
triangle : collision point, vertical bar: one-dimensional subgoal, square: point subgoal
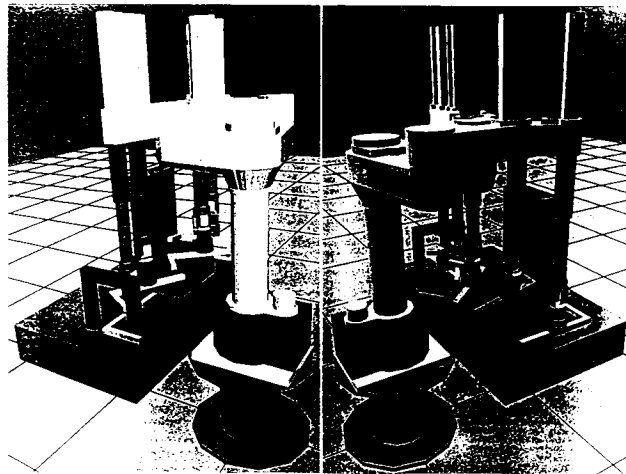
(b) A solution found for a 5-dof Adept manipulator.

Figure 33. SANDROS motion planner.

obstacles are vertical polygonal prisms. This simplifies the computation of intersection between the robot and obstacles, since with the first joint angle fixed, the movements of the second and third links are confined inside a vertical disk. Conservative approximation of configuration obstacles is derived using the geometry at the contact between the PUMA arm and the prisms. The configuration obstacles are represented by rectangles, and a path is found from the spines of the freeways between configuration obstacles. For an example with 6 obstacles, it takes less than one minute on a Lisp machine. This algorithm is useful in a table top environment.

Lozano-Pérez [1987] describes the first resolution-complete planner for general manipulators that has been implemented. Configuration obstacles are computed using the needle method, and the free Cspace is decomposed into regions. A graph specifying the connectivity of the regions is constructed, and A* is used to find the shortest path. The configuration obstacles are computed by considering one link at a time. The first link is considered, and feasible ranges of the first joint angle, θ_1, are computed. Next, the second link is taken into account. For each discretized value in feasible ranges of θ_1, feasible ranges of θ_2 are computed (Figure 34a). This process is repeated for
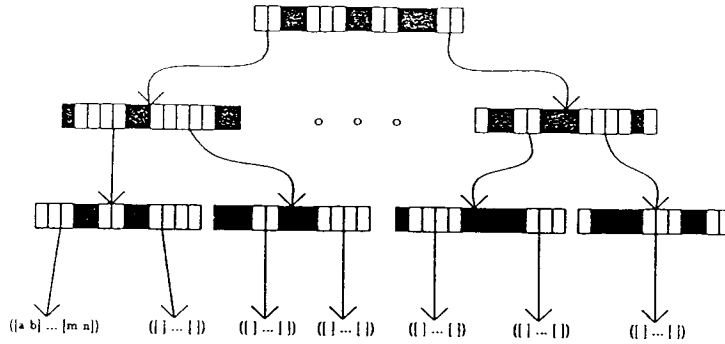
(a) Recursively generating the feasible ranges of the joint angles.
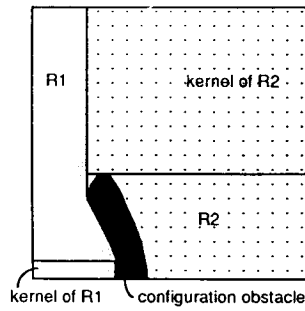
(b) Regions and kernels
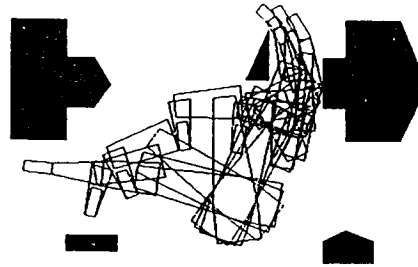
(c) A solution path

Figure 34. A general motion planner for a manipulator. Reprinted from *IEEE Journal of Robotics and Automation*, vol. RA-3, no. 3, pp. 224–238, Lozano-Pérez, T., "A simple motion planning algorithm for general manipulators," by permission of IEEE, Piscataway, N.J., Copyright, © 1987 IEEE.

all the remaining links. For polyhedral obstacles and manipulator links, it takes $O(r^{d-1}(mn)^2)$ time to build the configuration obstacles, where each θ_i is quantized into r values, d the number of degrees of freedom, m and n the numbers of face and edges of the manipulator links and obstacles, respectively. The free Cspace is then divided into maximal regions such that each region contains a *kernel*. A kernel is defined as the part of the region that can be reached from any points of the region by moving in a straight line parallel to one of the axes in the Cspace (Figure 34b). A collision-free path between two points within a region is found by first going to the kernel, moving along the kernel, then going to the goal. The connectivity among the regions is represented in the region graph. Finally, A* is used to find a solution.

This algorithm is general, i.e., applicable to any type of manipulators. There are two weak points of this algorithm. First, the paths found by this algorithm are not necessarily optimal since the kernels are used to move within regions. Second, the exhaustive nature of the algorithm makes it very slow. Consider, for example, an obstacle set and a manipulator each consisting of a set of polyhedra having a total of 30 faces and edges, i.e., $mn = 10^3$. Assume that $r = 100$, i.e., the angular resolution is 3.6 degrees. If it takes 10 integer operations to compute a contact condition, then the total number of integer operations required is 10^{11} for a 3-dof manipulator, i.e., 10^3 seconds or 17 minutes on a 100-MIPS computer. To reduce the computation time to a practical range, a coarse resolution of angles could be used at the expense of losing accuracy.
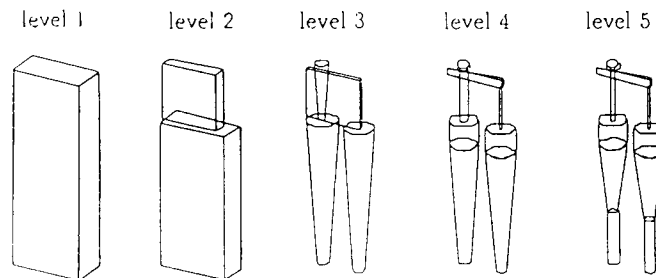
level 1   level 2   level 3   level 4   level 5

Figure 35. A hierarchical model of objects. Reprinted from *Proc. of IEEE Int. Conf. on Robotics and Automation*, pp. 330–340, Faverjon, B., "Hierarchical object models for efficient anti-collision algorithm," by permission of IEEE, Piscataway, N.J., Copyright, © 1989 IEEE.

Another option is to implement it on a parallel architecture to speed up the computation of the configuration space obstacles. Such an algorithm using the *Connection Machine* (a massively parallel SIMD machine consisting of $2^{16} = 65536$ 1-bit processors) is presented in Lozano-Pérez and O'Donnell [1991].

Herman [1986] developed a fast algorithm for a manipulator in 3D. The manipulator and its swept volume while following paths are approximated by primitive shapes such as spheres or cylinders, and the search for a collision-free path is done on the octree representation of the free space. Three search techniques, hypothesize and test, hill climbing, and A*, are used to generate the solution. First, an octant closest to the goal location is selected among the neighboring octants of the start location. Then the algorithm hypothesizes that a collision-free path is given by the straight line connecting the center of the selected octant and the center of the octant containing the start location. It approximates with a generalized cylinders (called cyl-spheres) the swept volume of the robot while following the straight-line path. If the swept volume intersects any of the octants occupied by the obstacles, the selected octant is abandoned, and the next best neighboring octant of the start location is selected. If the swept volume does not intersect any of the octants occupied by the obstacles, the robot moves to the selected neighboring octants. This process continues until the robot reaches

the goal location. Such a hill-climbing approach may lead the robot to a dead end. A* search is used to get the robot out of such situations. This algorithm works fast but should be used in relatively uncluttered environments due to its heuristic nature.

Faverjon [1986, 1989] uses hierarchical models of obstacles (Figure 35) and the swept volume of manipulator links to design a global path. The swept volume corresponding to the first joint angle is the volume the manipulator sweeps out when the first joint angle is fixed and when the rest of the joint angles are varied. The swept volume corresponding to the second joint angle is the volume the manipulator sweeps out when the first and second joint angles are fixed and when the rest of the joint angles are varied. The hierarchical models of objects and swept volumes of links are used to compute the configuration obstacles efficiently. For example, if the swept volume corresponding to the first joint angle does not intersect any obstacles, then the manipulator does not intersect the obstacles for all values of the joint angles $2, 3, \ldots, d$ as long as the first joint angle is fixed at the value used to generate the swept volume. The configuration space is then represented using an octree (in the example, the robot has 3 degrees of freedom), and A* search is used to find paths. This algorithm works well in situations that do not require a high-resolution octree to find a solution, i.e., the free space is not very narrow.
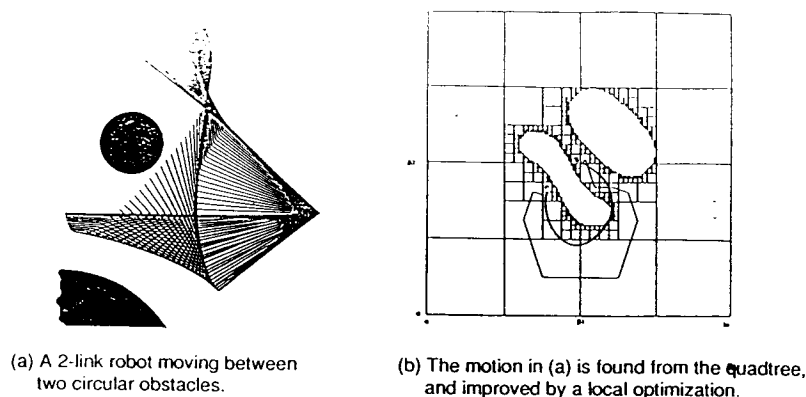
(a) A 2-link robot moving between two circular obstacles.

(b) The motion in (a) is found from the quadtree, and improved by a local optimization.

Figure 36. Manipulator motion planner using cell tree. Reprinted from *Proc. of IEEE Int. Conf. on Robotics and Automation*, pp. 1732–1737, Paden, B., Mees, A., and Fisher, M., "Path planning using a Jacobian-based freespace generation algorithm," by permission of IEEE, Piscataway, N.J., Copyright, © 1989 IEEE.

The Jacobian-based method of computing configuration obstacles is developed and used for MP of manipulators in Paden et al. [1989]. The Cspace representation is generated using the uniform bound on the Jacobian with l_x distance in the Cspace and a 2^d-tree. First, it tests whether the whole Cspace is free by computing the distance to obstacles with the manipulator in the configuration representing the center point of the Cspace. If it is not, the configuration space is divided into 2^d cubes, and each cube is tested and labeled as either free, not free, or not sure. Not-sure cubes are continually divided and tested up to a preset resolution limit. A feasible path can be searched in the resulting 2^d-tree (the authors use brush fire). For the 2-link problem in Figure 36, this algorithm takes 35 seconds on a 1.5-MIPS SUN computer to build the quadtree and under 1 second to search for a path. The main contribution of this paper is that it gives a simple way to compute a d-dimensional volume (not just a point or line) of collision-free parts of the Cspace. There are two weaknesses of this algorithm. First, the uniform bound on the Jacobian is so loose that cubes of big sizes are usually labeled as not sure. Second, it takes a long time to compute the

neighbor relations among the cubes in a 2^d-tree, especially for $d = 5$ or 6. Some improvements can be made to this algorithm such as using a nonuniform bound on the Jacobian $B(q)$ or dividing the Cspace into cubes of different sizes.

Kondo [1991] uses multiple-heuristic search strategies on a rectangular grid representing the Cspace. A set of parameterized heuristic functions is defined so that when A* search is performed to move the robot from the start to the goal, the robot has a preferential moving direction that is dependent on the parameters. The parameters are dynamically changed during the search based on how much progress the robot has made toward the goal. A bidirectional search is also used. This algorithm is fast because it minimizes the number of collision detection computations by limiting the search in promising parts of the Cspace. This algorithm solves 6-dof examples with a polyhedral robot in 3D with an average of 7000 collision detections and takes about 10 minutes on a 17-MIPS SUN computer. We note that this algorithm is very fast if the solution does not require a large backtracking motion. One drawback of this algorithm is that its resolution is limited by the size of available computer memory. This algorithm is res-

olution complete if the search is continued until all points on the grid are examined.

We note here some algorithms for computing the boundary equations of configuration obstacles, which can be used for object-dependent cell decomposition. The boundary equations of configuration obstacles for a planar manipulator amidst polygons are derived in Ge and McCarthy [1989]. The derivation of equations is based on the *Clifford algebra* [McCarthy et al. 1989]. This algorithm takes 1 second on a 10-MIPS Silicon Graphics computer to generate configuration obstacles for a 2-link robot moving among 7 polygonal obstacles. The boundary equations of configuration obstacles for stick figure manipulators in 3D polyhedral environments is presented in Hwang [1990]. It is based on the intersection condition between a line segment of the manipulator and a triangular face of a polyhedral obstacle. Because the boundary equations are highly nonlinear, most motion planners use object-independent cell decomposition.

Potential-Field Approach

There is no significant difference between the potential-field approaches for rigid robots and manipulators. In this section, we review local-motion planners developed for manipulators. They are developed for 2D environments, but can be generalized to 3D. Khatib [1985] uses an artificial-potential-repulsion approach to avoid imminent collisions among robot arms and obstacles. This algorithm is aimed at the local, short-term avoidance of obstacles in real time for moving robot arms rather than planning global paths. A repulsion force is generated by a potential field around each obstacle. When any link of the robot arm approaches an obstacle, the repulsive force pushes the link away from the obstacle. The potential used, P, is approximately inversely proportional to the square of the minimum distance, D, between the link and the obstacle, and becomes zero beyond a preset distance from the obstacle. The

force on the robot is calculated from the equation $F = -dP/dD^*dD/dx$ where x is the position vector of the robot. Appropriate torques at the joints of the robot to follow the externally specified global path are computed. The force from the artificial potential field is then taken into account to modify torques at the joints. This allows each link of the robot to follow the initially planned path closely while avoiding the obstacles. The role of the artificial potential field is to "bend" a given global trajectory around obstacles. Khatib's algorithm is significant in that the local-obstacle avoidance problem is implemented at low (control) level for real-time execution.

Newman and Hogan [1987] use an energy interpretation of the potential function for obstacle avoidance and acquisition of moving targets by a manipulator. The manipulator is driven solely by the force that is computed as the negative gradient of the potential. Two types of potentials are used: a goal potential driving the robot toward the goal position and *braking* potential stopping the manipulator at the goal or at the obstacle boundaries. If the goal position is moving, the goal potential is updated correspondingly. To have minimum-time solutions, the slopes of potentials are set to the maximum acceleration of the actuators. This algorithm guarantees time optimality for dynamically decoupled manipulators operating in obstacle-free regions. The algorithm is useful as a local-motion planner to compute force for each actuator. In Newman [1989], a similar algorithm is used to incorporate a *reflex-motion* planner in the control loop. The reflex-motion planner stays transparent until the robot is on a collision course.

Potential field is also used in Boissiere and Harrigan [1988] for real-time obstacle avoidance of a tele-operated Puma robot. When the robot is on a collision course while following the operator's command, a repulsive force is applied to modify the commanded path. This allows the human operator to concentrate on executing tasks rather than avoiding

obstacles and thus makes tele-operation much more efficient.

Khosla and Volpe [1988] use a superquadric potential function to remove spurious local potential minima at points other than the goal position. Superquadrics are a generalization of ellipsoid-shaped potential functions and can represent a much larger class of objects. The level curves of superquadrics approximate obstacles at close distances and become spheres far from obstacles. To the superquadric potential function is added a goal attraction potential, and the combined potential is used in path planning of planar manipulators. The potential for each link is computed at the point where the link is closest to obstacles, and a repulsive force is applied to the link at this point. The end effector moves in the direction minimizing the sum of the obstacle potential and the goal attraction potential. This algorithm again is essentially a local planner.

Mathematical Programming Approach

A local-collision avoidance algorithm for redundant (dof > 6) manipulators is developed in Maciejewski and Klein [1985]. The primary goal of the planner is to make the end effector follow a specified trajectory $x(t)$; $x(t)$ is typically a collision-free path for a point object, and thus collision between obstacles and the manipulator links are not considered when designing the initial path. Given $x(t)$, the values of joint variables are found using a generalized inverse from the Jacobian equation $\dot{x}(t) = J(\theta)\dot{\theta}(t)$. Then the joint variables are modified to move the point of the manipulator closest to obstacles away from the obstacles while the end effector is following $x(t)$. It may seem odd to design the path for the whole manipulator based on the path of its end effector. If a manipulator is highly redundant, however, its links can stay closely on the path the end effector is tracing (like a snake) and avoid collisions. In case a manipulator is not highly redundant, the motion cannot be planned by modifying the path for the manipulator tip.

Chen and Vidyasagar [1988] have developed an optimal trajectory planner for planar n-link manipulators. A grid of points is laid in the Cspace, and the points that result in collision are identified. Collision points occur in groups, since the mapping of obstacles from the world space to the Cspace is continuous. The collision points are approximated by ellipses. The equations of these ellipses are then used as constraints in the optimal-control formulation, which is solved numerically. This algorithm designs *globally* and *dynamically* optimal solutions among obstacles. Its main weakness is the large number of elliptical constraints needed to approximate configuration obstacles for a cluttered environment. The convergence rate of the numerical optimization in a high-dimensional Cspace (dof = 6) is also hard to predict. This algorithm should be used offline to dynamically optimize the motion of a manipulator engaged in a repetitive task, e.g., mechanical assembly. Speeding up the manipulator motion by a few seconds will result in a huge saving in manufacturing costs. A similar method is used to compute time-optimal trajectories of a manipulator that avoids the collision between the manipulator tip and obstacles [Eltimsahy and Yang 1988]. Collisions between manipulator links and obstacles are not considered.

Shiller and Dubowsky's algorithm plans globally time-optimal trajectories for a manipulator in the 2D work space (link-obstacle collisions considered) [Shiller and Dubowsky 1988]. A directed graph is constructed using the points of a uniform grid covering the work space. Adjacent points are connected by edges. The points that lie on the obstacles and in unreachable free space are deleted from the grid. Then, directed edges are drawn beginning from the start grid point toward the goal grid point. Edges making sharp turns or loops are not allowed. K shortest paths are selected from the directed graph. Each selected path is optimized using a numerical algorithm, and the minimum-time path is selected from the optimized paths. This approach does not take into account the manipula-
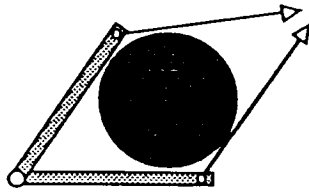
Figure 37. Two adjacent tip positions not reachable from each other.

tor kinematics fully. For example, there are cases where the manipulator tip may not be able to move from a point to an adjacent point directly, but can reach the adjacent point by changing to a different configuration (Figure 37). This happens because of the multiplicity of inverse kinematics solutions. This algorithm takes about 2 hours to solve a 3-link, 5-obstacle problem. The slow speed is typical of numerical optimization algorithms in a high-dimensional space. (When dynamics of the robot is included in the optimization, the number of dimensions doubles, since the time derivatives of configuration variables are also independent variables. Again, this algorithm has an application in offline optimization of repeated motions.)

Future Research Directions

MP of manipulators is essential for object manipulation, and a real-time algorithm is needed. Otherwise, after a command is given, robots have to sit idle while a collision-free motion is computed, resulting in inefficiency. In our view, the algorithm in Chen and Hwang [1992] is a near-optimal planner among algorithms implemented in serial computers, since it computes the Cspace information to a minimal amount needed to find a solution. It is also resolution complete and has a small memory requirement. We believe that a significant improvement over this algorithm is likely only by taking radically different approaches such as using parallel computers or knowledge-based methods. Future research in this direction is desirable.

There are other issues related to MP of manipulators, most importantly grasping and task constraints. When we plan motions for a manipulator, we actually plan motions for the ensemble of the manipulator and the object in its grasp. Thus, grasp configurations affect motion planning. On the other hand, MP is needed to verify that a grasp configuration is indeed reachable. This issue is considered in Lozano-Pérez et al. [1987], and more research is needed. Other constraints on manipulators arise for task-related reasons. Manipulators are often used to perform tasks involving interactions among objects such as hammering down a nail. This task has a constraint on the velocity of the hammer when it strikes the nail, among other constraints. Incorporation of task constraints in MP is a complex problem, involving kinematics/ dynamics of manipulators and objects, but nonetheless needed for robots performing any realistic task.

Lastly, we propose to generalize the point-to-point MP problem (moving the robot from one configuration to another) to the following problems: visit points, trace curves, and cover surfaces [Hwang et al. 1992]. These generalizations are useful for mobile robots, but needed far more for manipulators. Manipulators often perform operations other than transferring objects such as inspection of sample points, deburring and chamfering of sharp metal edges, imaging, painting, and cleaning. These operations require the tool in the manipulator hand to move along a curve or over a surface in a constrained manner. Examples of such constraints are the orientation of a deburring bit with respect to the part being deburred, stiffness of the manipulator arm while deburring, and the orientation and sweeping speed of a paint gun. On top of these constraints are the requirement of avoiding collisions between the manipulator and objects in the work space. These constraints usually do not completely specify the configuration of the manipulator, and algorithms for selecting a *good* configuration for every time instance are needed. To plan motion for these operations, the following three problems are defined.

(1) Given a set of world points to be visited by a set associated with a part of a manipulator (usually the tool in hand), a set of constraints associated with each of the points, and an index find an ordering of the points and manipulator motions to visit all the points according to the ordering that optimizes the index.

(2) Given a set of curves to be traced by a set associated with a part of a manipulator (usually the tool in hand), a set of constraints associated with each of the curves, and an index, find partitions of the curves, an ordering of the curve partitions, and motions to trace all the curve partitions according to the ordering that optimizes the index.

(3) Given a set of surfaces to be covered by a set associated with a part of a manipulator (usually the tool in hand), a set of constraints associated with each of the surfaces, and an index, find partitions of the surfaces, an ordering of the surface partitions, and motions to cover all surface partitions according to the ordering that optimizes the index.

We note that all these problems involve variations of the traveling salesman problem. These are well defined, challenging, and practical problems whose solutions will have a major impact on industry.

3.1.4 Multimover's Problem

The multimovers problem deals with MP of multiple robots. This problem arises in an automated factory where mobile robots bring parts from the warehouse to assembly stations (Figure 1). Each mobile robot must avoid other mobile robots as well as stationary obstacles in the factory. The MP of manipulators working in the same assembly station is also a multimovers problem. Still another example is the problem of rearranging furniture in a room. Given the current arrangement and a desired one, it is obvious that using a motion planner for the classical mover's

problem to move each piece of furniture would not solve the problem.

MP of multiple rectangles is shown to be PSPACE complete in Hopcroft et al. [1984b] and Hopcroft and Wilfong [1986]. Although an exact and efficient algorithm for the general multimover's problem is unlikely, several algorithms are available for some special cases. The multimover's problem can be considered in two different contexts. First, if there is a precedence ordering among robots, the problem becomes a series of single mover's problems in time-varying environments. The MP is done in decreasing order of precedence, and robots with higher precedence are regarded as moving obstacles for the robots with lower precedence. This is called a decentralized approach. Second, if there is no precedence, a centralized approach is used, wherein a single planner designs the paths for all the robots while optimizing some objective function. The first case amounts to a heuristic approximation of the second, with less computation at the expense of missing legal solutions in some cases. The multimover's problem is obviously much harder since the numbers of degrees of freedom is the sum of the numbers of degrees of freedom of each robot. This problem has received only moderate attention since an efficient exact algorithm for a single mover's problem is yet to be developed. Algorithms for this problem are developed for circular robots and manipulators and are surveyed in two subsections.

Circular Robots

MP of several circles among polygonal obstacles in 2D is reported in Schwartz and Sharir [1983b]. The cell decomposition method based on the critical curves [Schwartz and Sharir 1983a] is used to first solve the cases with two and three circular robots. Only two types of critical curves exist for two circular robots due to the symmetry of circles. For the case of three robots, critical curves for two robots R_1 and R_2 are computed while fixing the position of the remaining robot R_3. Then

the set of the critical positions of R_3 that cause discontinuity of the critical curves for R_1 and R_2 is identified. The connectivity graph of the regions separated by the critical curves is constructed, and a path is found from the graph. The complexities are $O(n^3)$ and $O(n^{13})$ for two and three robot cases, respectively. In case of k circular robots, the above algorithm is applied in a recursive manner. The paper demonstrates that exact algorithms for multimover's problems have high-complexities even for simple robots.

In Sharir and Sifrony [1988], a general technique of $O(n^2)$ is presented for MP of two robots each with two dof using a cell decomposition approach. Robots can be circles or manipulators. The algorithm decomposes the free Cspace of each robot into a collection of disjoint cells. Let $\{c_i\}$ and $\{c_j\}$ be the cells for the two robots, respectively. The collision-free part of the Cartesian product $c_i \times c_j$ is further decomposed into $O(1)$ 4D cells, and their adjacency relations are determined. Then the adjacency relations of the 4D cells from all $c_i \times c_j$ are computed, resulting in $O(n^4)$ cells. An $O(n^2)$ algorithm for motion planning is possible by limiting the computation to a *single* connected component of the configuration space containing the initial configurations of both robots. This paper also shows efficient ways to compute the free-configuration spaces for two cylindrical robots and two circular (or translating convex polygonal) robots.

Fast-motion planning of identical square robots in 2D is discussed in Buckley [1989]. This algorithm is designed for a specific application where the robots are feeding parts to an assembly table and where the robots themselves are the obstacles. A new method to assign priorities to robots is introduced to maximize the number of robots that can move in a straight line from the start to goal (called *linear* robots). This minimizes the number of such robots (called *complex* robots) for which expensive search of collision-free zigzag paths is necessary. Two rules of prioritization are derived from the start and the goal configurations of the robots. If the straight-line path of robot A between its start and goal position intersects the start position of robot B, then robot B should be moved first (is assigned a higher priority). If the straight-line path of robot A intersects the goal position of robot B, then robot A should be moved first. These rules allow robot A to move in a straight line. Using the priority relationships between pairs of robots, a priority graph is constructed. In this graph, a directed edge is drawn from robot A to B if robot A has a higher priority than robot B. If there are no cycles in the graph, then all the robots can move in straight lines in the order of the priority. If there are cycles in this directed graph, not all robots can travel in straight lines (Figure 38). A complex robot has to be introduced to break the cycles in the priority graph. The trajectory planners for the linear and complex robots have $O(m^2)$ and $O(m^4)$ time complexities, respectively (m is the number of robots). Both planners are based on the configuration space approach. The main advantage of this algorithm is that it is fast, e.g., 10 seconds to solve a nine-robot example of which two turn but to be complex robots. Buckley shows that even though the multimovers problem has a high complexity, an application-specific algorithm that runs in a practical time can be developed.

A decentralized approach is taken in Yeung and Bekey [1987] to plan paths for 2D circular robots. Each robot plans its own path using a visibility-graph-based algorithm. It attempts to reach its goal following the straight line path. If it hits an obstacle, it goes to the obstacle vertex closest to its goal. When a conflict occurs between robots, it is reported to a central coordinator called *blackboard*, and the blackboard issues priorities in replanning based on the current state and task.

Another decentralized algorithm is developed for MP of 2D circular robots of different sizes [Liu et al. 1989]. The initial path of each robot is planned separately using a quadtree representation of
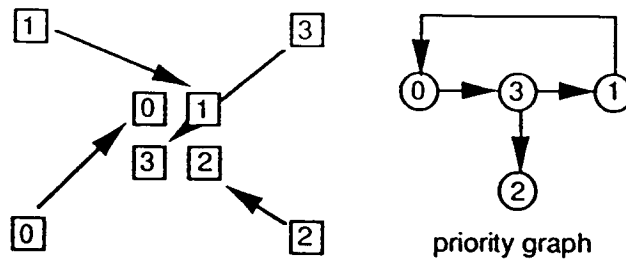
Figure 38. Not all four robots can go to their goal positions in straight lines, and the priority graph contains a cycle. Reprinted from *Proc. of IEEE Int. Conf. on Robotics and Automation*, pp. 322–326, Buckely, S. J., "Fast motion planning for multiple moving robots," by permission of IEEE, Piscataway, N.J.. Copyright, © 1989 IEEE.

obstacles. Intersections among the paths are detected, and those nodes that are neighbors of intersection nodes are considered as candidate free space where the robot should move to resolve the conflict. A search is conducted to select one among the candidate nodes. A Petri net formulation is used to resolve conflicts by globally modifying initial paths. It is implemented for a two-robot system, and more work is required for systems with several robots.

Manipulators

Fortune et al. [1986] report an algorithm for two planar manipulators in 2D using the critical-curve method. Each manipulator has one link that can rotate about and translate through a common point, i.e., it has a cylindrical geometry. They use *critical curves* [Schwartz and Sharir 1983a] to partition the free Cspace into cells, and they show that for a cylindrical manipulator (a manipulator consisting of a single link that can translate and rotate through a point), there are $O(n)$ number of critical curves of small algebraic degrees. It is further shown that the curves divide the configuration space of the first robot into $O(n^2)$ regions and that each of these regions is partitioned into $O(n)$ connected components by the critical curves of the second robot. They present exact algorithms for two separate cases: an $O(n^2 \log n)$ algorithm for the case when manipulator tips touch and move together and an $O(n^3)$ algorithm for the

case of independent motion. These algorithms can be used as submodules by a motion planner for manipulators having a cylindrical geometry.

A multimovers problem with 2-dof robots are considered in Erdmann and Lozano-Pérez [1986]. The robots can be either translating polygons or 2-link planar manipulators. They are prioritized, and when conflicts arise, the burden of avoidance is imposed on the robots with lower priorities. Thus, this algorithm solves many single mover's problem in a time-varying environment. This algorithm is useful for cases where the priority is evident, such as in assembly operations. Two separate cases are considered whose configuration spaces are 3D. First, polygonal robots are allowed only to translate at constant speeds. The configuration obstacles are polyhedra in $R^2 \times$ time space, and the search for solutions is done in a visibility graph. Second, robots are planar revolute links with two dof. The configuration space is $[0, 2\pi] \times [0, 2\pi] \times time$ for each robot, and the search for paths is done in the free Cspace. These algorithms are applications of the Cspace to cases with dof = 3. They are fast but need to be generalized to be useful in practical situations.

A real-time path planner for multi-robot systems among circular obstacles is presented in Freund and Hoyer [1988]. This algorithm can be used for circular robots or cylindrical manipulators with predefined precedence relationships. First, each robot travels in a straight line

in the Cspace. The configurations that make a robot barely touch the other robots are computed and used as the bounds on the configuration of the robot. These bounds are used to modify the control inputs in real time. This algorithm is highly successful in relatively simple environments. A real-time implementation is its strongest point (20 msec. on a microprocessor system for a 3-robot problem). An online algorithm is possible because of the simple geometries of robots and obstacles in 2D. It requires substantially more work to extend this approach to higher dof manipulators in 3D world, since the configuration obstacles are much more complex. On the other hand, this algorithm is well developed for mobile robots in 2D.

A real-time local-trajectory planner for cylindrical manipulators is developed in Chien et al. [1988]. The planner does not generate the whole trajectory at once, rather it does so incrementally. The obstacles and the robots' end effectors are represented as spheres. Then, each robot independently attempts to approach its goal in a straight line. Its next position, velocity, and acceleration (x, v, a) are computed based on the current x, v, a. Next, the predicted position of each robot is broadcast to all other robots. Possible interferences are then detected, and the trajectories are modified. This algorithm is not a global planner but is useful in resolving interference at a local level. A global planner that incorporates the geometry of all the links of the robots need to be used with this algorithm. The algorithm can be used for manipulators with simple shapes, but it will not easily extend to 3D manipulators, say, with 6 degrees of freedom. This algorithm is very similar to Freund and Hoyer [1988] in its use of decentralized approach; only the method of implementing the general principle is different.

In O'Donnell and Lozano-Pérez [1989], a trajectory-scheduling algorithm for two manipulators asynchronously operating in a common work space is developed. The initial path of each manipulator is computed in advance and is represented as a sequence of configurations. Then a rectangular grid called the *task completion diagram* (TC) is created. Each point on the grid denotes how far each manipulator has progressed toward its goal. The southwest corner of TC represents the state in which both manipulators are at their start positions, and the point at the northeast corner represents the state in which both manipulators are in their goal positions. As both manipulators proceed with their tasks, the point denoting the current state will move north and east in TC. Some points on the grid will correspond to a state in which the two manipulators collide. These points are identified using an algorithm that detects intersection between polyhedra. Next, a scheduling algorithm will try to find in the grid a sequence of points from the start state (southwest corner) to the goal state (northeast corner). To prevent the manipulators from going backwards, the point denoting the current state is allowed to move only to the north and to the east while avoiding the points involving collisions. Since the points involving collisions often form concave shapes, deadlock situations can occur while trying to move to the north and east. Southwest closures of the sets of collision points are used as forbidden zones to prevent deadlock situations (note backtracking is needed to resolve a deadlock). This algorithm has complexity of $O(n^2 \log n)$ where n is the grid size of each axis of TC. This algorithm is fast and is useful in a relatively sparse environment with a small number of robots.

Future Research Directions

Although the multimovers problem has a high complexity, many practical problems have multitudes of solutions, and suboptimal solutions usually suffice. For mobile robots in a factory floor, algorithms in Yeung and Bekey [1987] and Liu et al. [1989] are adequate. As mentioned in Section 3.1.2, MP of mobile robots with conflicting/common objectives needs more research. The MP of cooperating manipulators has very

important applications in a multimanipulator assembly work cell, handling of a large object with multiple manipulators, to name a few. Algorithms must run efficiently for 6-dof manipulators in 3D world and also incorporate constraints arising from task requirements. For example, lifting a large box with two manipulators requires exerting contact forces that form a stable closure and balancing the weight of the box. Formulating task requirements in terms of constraints on manipulator configurations and torque/force of actuators is an open area. As far as resolving conflicts due to collisions among 6-dof manipulator links are concern, an efficient heuristic algorithm seems possible (but does not exist yet).

3.2 Time-Varying Environment

When obstacles are moving in time, the problem space is one dimension higher than the Cspace of the corresponding stationary problem. A time-varying problem reduces to a stationary problem if there is no bound on the robot's velocity (just move the robot infinitely fast). We thus assume that it is bounded. In most algorithms, it is assumed that motions of obstacles are known for all time. Otherwise, robot motions have to be planned from the predicted motions of obstacles, and replanning is needed if the obstacle motions deviate from the prediction (see Kehtarnavaz and Li [1988] below). The time to reach the goal can be specified or used as a quantity to be minimized. As far as the complexity is concerned, it is shown to be NP-hard to plan a path for a point robot in 2D (with a bounded velocity) among translating obstacles [Canny and Reif 1987]. For a point robot in 3D it is PSPACE-hard [Reif and Sharir 1985].

Reif and Sharir [1985] also present an algorithm for the *asteroid avoidance* problem, which is the MP problem for a translating polytope robot with a bounded speed among polytope obstacles translating in fixed directions and velocities. The algorithm runs in $O(n \log n)$, $O(n^{2(k+2)}k)$ and $O((n + k)^{O(1)}) = O(n^{O(1)})$ time for

1D, 2D, and 3D world space, respectively. The n is the total number of vertices (edges) of k polygons (polyhedra). MP is done in the $d + 1$-dimensional Cspace $\times$ time space, wherein the Minkowski set difference is used to compute configuration obstacles. The concept of the *fundamental* and *normal* movements are introduced to plan paths. A fundamental movement is a *direct* movement (movement during which the robot touches obstacles only at the beginning and end of the movement) followed by a possible *contact* movement (movement on the surface of polyhedral obstacles beginning and ending at edges). A normal movement is a sequence of fundamental movements, where the robot changes its direction only on the obstacles and touches each obstacle at most once. We explain the algorithm for the 2D version (others are similar). Let $x_0/0$ and x_T/T be the start position/time and the goal position/time, and let V be the set of all obstacle vertices, x_0 and x_T. Let the time interval I_v^i be the set of time $v \in V$ can be reached from x_0 using at most i fundamental movements. Initially, $I_{x_0}^0 = [0, T]$, and $I_v^0 = \phi$ for all other $v \in V$. Inductively for some $i \geq 0$, let v^* be reachable from x_0 using at most i fundamental movements. Then for each $v \in V$, if there is a fundamental movement from v^* to v, we compute I_v^{i+1} by shifting the time interval I_v^i by the time needed for the fundamental movement. If T belongs to the time interval $I_{x_T}^{n+1}$ (n = number of obstacles), then the robot can reach the goal point in the specified time T. It is proven that such a sequence of fundamental movements is sufficient to find a solution if it exists. Fujimura and Samet [1989] implemented this algorithm in 2D by developing a method of computing reachable vertices from a given vertex using a direct movement.

MP of a point robot among translating polygonal obstacles is considered in Fujimura and Samet [1988]. The polyhedral obstacles in the 3-dimensional space-time is represented with an octree, and A* search is used to find a shortest path while enforcing maximum velocity,
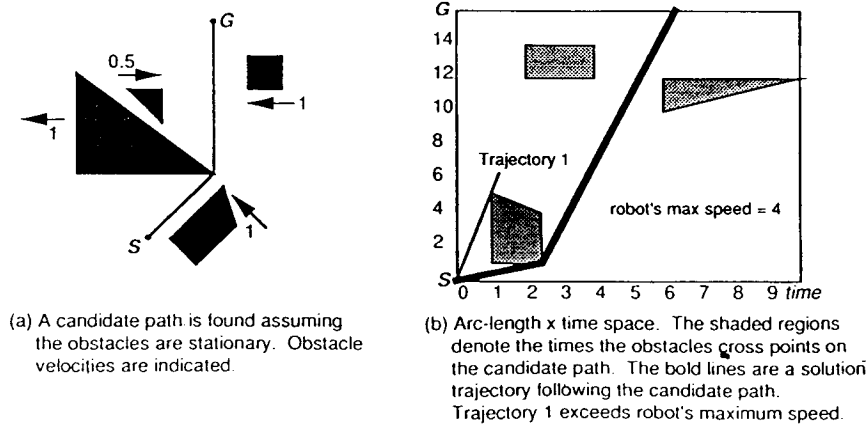
(a) A candidate path is found assuming the obstacles are stationary. Obstacle velocities are indicated

(b) Arc-length x time space. The shaded regions denote the times the obstacles cross points on the candidate path. The bold lines are a solution trajectory following the candidate path. Trajectory 1 exceeds robot's maximum speed

Figure 39. Path velocity decomposition of MP in a time-varying environment.

acceleration, and centrifugal-force constraints. Since the octree representation can change significantly even for small changes in the space-time obstacles, the uncertainty in the velocities of obstacles may result in different paths. This algorithm finds a shorter path than the visibility-graph-based algorithm in Erdmann and Lozano-Pérez [1986] for the same problem.

A heuristic algorithm is developed for the NP-hard problem of moving a point robot with a bounded velocity in the plane [Kant and Zucker 1986, 1988]. It is a two-level algorithm that decomposes the problem into path planning and velocity planning. A path is selected from the visibility graph that is constructed assuming the obstacles are stationary (Figure 39a). The selected path is given as a parametric curve whose parameter is arc length s along the path. Since the obstacles are moving, some points on this path will be occupied by obstacles in some time intervals. For each time instant, the points in the path occupied by obstacles are computed and represented as polygonal obstacles in the $s \times time$ space (Figure 39b). Another graph called the *directed-visibility graph* is constructed using the vertices of these polygons. (The robot can travel only in $+t$ direction in this graph.) Some edges of the directed visibility graph space will require the

robot to travel faster than its maximum speed. After these edges are pruned out, the best trajectory is selected from the remaining edges using A* or Dijkstra's algorithm. This approach is simple and effective if the obstacles have constant velocities. If there are uncertainties in the velocities of obstacles, this algorithm may fail because the paths from the visibility graph touch corners of obstacles. The algorithm is therefore complemented with a low-level avoidance module to modify the trajectory in the vicinity of obstacles. The derived trajectory is not optimal due to the decomposition of the problem into two levels.

Path planning of a point robot among moving circular obstacles in 2D is described in Kehtarnavaz and Li [1988]. The positions of obstacles are not known a priori and are predicted from the past positions using an autoregressive model. The forbidden regions are constructed at each sampling time from the set of line segments, each connecting the current and the next predicted position of an obstacle. The path for the robot at each sampling time is selected from the visibility graph. This algorithm solves a static problem for each time increment and resembles the logic humans use to walk through busy city sidewalks. When the obstacle motions are uncertain this algorithm is the best one can do.

Future Research Directions

Since MP in time-varying environments has a high complexity, application-specific heuristic algorithms need be developed. Two interesting areas of research are integration of a motion planner with sensing and incorporation of uncertainty in obstacle information. In real robot systems, it takes a finite amount of time to acquire information about motions of obstacles and to plan motion. Estimates of obstacle motions also tend to involve uncertainties. An analysis of the effect of sensing delays on the uncertainty of object models is needed. An algorithm must consider these factors to be robust and have a practical value.

3.3 Motion Planning with Constraints

Motion planning with constraints generally has a very high complexity (usually NP-hard or PSPACE-hard), and efforts to develop implementable algorithms are just beginning. Two commonly encountered types of constraints in motion planning are *holonomic* constraints and bounds on robot velocity (or acceleration). Holonomic constraints are constraints on the derivatives of configuration variables that cannot be integrated. For example, a wheeled vehicle can move to any position and orientation with a sequence of maneuvering moves, but its motion direction at any instant is constrained. As a result, there is a constraint on the curvature of paths for a wheeled vehicle. We briefly summarize the work on MP with these constraints.

The first result on motion with curvature constraints is presented in Dubins [1957]. It considers only obstacle-free cases and shows that the minimum-length paths consist of sequences of straight lines and maximum-curvature lines (curves). Fortune and Wilfong [1988] have presented a method to check the existence of a path with a curvature constraint among polygonal obstacles, but it does not generate the path. This algorithm runs in $2^{O(poly(m,n))}$ time and space where n is the number of vertices of obstacle polygons and where m is the number of bits used to specify the positions of the vertices. When the robot is given a network of line segments to follow such as on a factory floor, polynomial-time algorithms finding the shortest paths are available [Wilfong 1988a, 1989]. Jacobs and Canny [1989] have developed a configuration-space-based algorithm that computes paths that are approximately the shortest in polynomial time.

Some of the algorithms for MP in time-varying environments consider robots with velocity constraints [Reif and Sharir 1985; Kant and Zucker 1988], and the results are mentioned in Section 3.2. The kinodynamic motion planning deals with synthesizing robot motions subject to both kinematic constraints (such as avoiding obstacles) and dynamic constraints (such as bounds on the acceleration and velocity) [Canny et al. 1990]. It is first considered in O'Dúnlaing [1987], where a point robot with a bounded acceleration in 1D is studied. O'Dúnlaing shows that with a bound on the acceleration of a point robot, a minimum-acceleration trajectory from an initial pair of position and velocity to a goal pair is *bang-bang interpolant*, meaning that the magnitude of acceleration is constant, but its sign is reversed at most at one time; $O(n^2)$ and $O(n \log n)$ algorithms are presented for the motion planning of a point in 1D that evades two pursuing point obstacles, where n is the total number of times the obstacles change accelerations. Problems involving dynamics such as minimum-time and minimum-energy trajectory problems are extensively studied in the optimal-control literature [Athens and Falbs 1966; Bryson and Ho 1975].

A kinodynamic motion-planning problem for a point robot in 2D and 3D is studied in Canny et al. [1988]. An approximate time-optimal algorithm of $O(n^2 \epsilon^{-(3d+1)})$ complexity is developed using a nonlinear grid in the position velocity space (also called *phase space*). For the time-optimal problem, optimal solutions take on only one of three values

at each time instant: maximum acceleration, zero acceleration, or maximum deceleration. Thus, from a point in the position velocity grid, the robot can move to one of three different points in the next time instant. These transitions are represented by the edges of the grid. The time-optimal solution between two points in the phase space is found from the grid. The parameter ϵ denotes the goodness of approximation or grid spacing. This algorithm is extended to manipulators in Donald and Xavier [1989], and an exact algorithm is developed in Canny et al. [1990] for a point robot in 2D. This nonlinear grid can be used to find motions optimizing other measures, e.g., energy, by allowing the robot to take on many values of acceleration.

Future Research Directions

Constraints on robot motion arise from different sources. The first type of constraints comes from task requirements, which constrains the robot configuration and forces exerted by the robot. Research issues with these constraints are discussed in the future research section for manipulators. The second type of constraints comes from the anatomy of the robot. All physical robots have limitations on their capabilities such as the bounds on velocity and acceleration. These constraints are well characterized, but their nonlinearities prohibit elegant mathematical solutions. In the worst case, search methods can be used on a grid representing motions satisfying all kinds of nonlinear constraints, as done in Canny et al. [1988]. Remember, searching among all possibilities is the most general method of solving problems, and ever-increasing computer speeds enable more problems to be solved this way. We should start identifying problems with mathematical constraints that can be solved using a grid search. The third type of constraints comes from sensory requirements. Robots need to monitor the motions and the states of objects in the world in order to detect errors and reduce uncertainties in the object model.

Inclusion of sensory requirements in motion planning presents new constraints. This is an important area, and some results are available [Tarabanis et al. 1991].

3.4 Movable-Object Problem

In the movable-object problem, robots are allowed to move some of the objects in the environment while reaching the goal position. Immovable objects are called obstacles. The first complexity analysis of this problem has appeared in Wilfong [1988b]. It is shown that the problem is NP-hard when the final positions of the objects are unspecified and PSPACE-hard when specified. An $O(n^3 \log^2 n)$ algorithm is also presented for the case of one movable polygonal object. The algorithm partitions possible positions of each movable object into regions so that in each region the environment has essentially the same connectivity properties for the robot. Although the movable-object problem has a high theoretical complexity, it is often easier to solve than problems with stationary obstacles. This is because the robot can clear the objects in its way toward the goal. In light of this fact, a fast heuristic algorithm is developed in Chen and Hwang [1991]. In this algorithm, a global planner plans a plausible sequence of robot positions leading to the goal, and a local planner is used to move the robot from a position to the next in the sequence. The local planner allows the robot to push obstacles blocking its path.

There are algorithms that consider how to actually move objects with robots. The Handey system in Lozano-Pérez et al. [1987] and Lozano-Pérez et al. [1989] carries out the command *Move object To destination* with a manipulator. It consists of a range finder system for sensing, a model-based object locator, a manipulator motion planner for collision avoidance, and a grasping and regrasping module. It is designed for the assembly of planar-faced objects and has the ability to operate on a wide class of objects in a cluttered environment. The scale of this

system shows the complexity of building an actual robot system. A theoretical formulation of manipulation planning is presented in Alami et al. [1990]. In this algorithm, robot configurations of grasping movable objects are explicitly represented. The *manipulation graph* consists of *STABLE* and *GRASP* sets, which represent the set of stable configurations of movable objects and the set of a robot's collision-free configurations grasping movable objects. The manipulation graph is incrementally built and searched for a solution, which is a sequence of *transit* (robot moving without grasping an object) and *transfer* (robot moving while grasping an object) paths. To apply this algorithm to real applications, efficient ways of computing the sets *STABLE* and *GRASP* and limiting the size of the manipulation graph are needed.

The movable-object problem is actually a simple task-planning problem. In cluttered environments, a heuristic movable-object algorithm is likely to be preferred than an exact algorithm for the classical mover's problem. Readers interested in planners at a higher level than the movable-object problem should look at the work in assembly planning [Huang and Lee 1991; Hutchinson and Kak 1990; Lee and Shin 1990; Strip and Maciejewski 1990; Wilson 1992].

3.5 Comparison Tables

The algorithms surveyed above are compared in Tables 1–7. Each algorithm is denoted with the first two (or more) letters of the first author's name, followed by the first letters of the remaining authors and the year of publication. The *global/local* indicates whether an algorithm is a global or local planner, and *theo/simul/impl* indicates the algorithm is theoretical, simulated in computers, or implemented on actual robots. For gross-motion planning without uncertainty, a simulation is sufficient to demonstrate the efficiency and applicability of an algorithm. We still have indicated algorithms implemented on physical robots for the interest of indus-

try. The object models of robots and obstacles are shown in *robot shape* and *obstacle shape* columns. The world space dimensions (2D or 3D) can be inferred from the obstacle models. *Exact/heuristic* measures the degree of exactness of an algorithm. Rating 1 denotes the algorithms that are exact, i.e., they either find a solution or prove that there is no solution. Rating $1r$ and $1p$ are given to resolution-complete and probabilistically complete algorithms, respectively. Rating 2 is given to the heuristic algorithms that fail to find a solution for relatively small sets of pathological puzzle-like problems. Rating 3 is given to the heuristic algorithms that often fail to find a solution (these are usually very fast local algorithms).

4. CONCLUSIONS

A motion planner is an essential component of a robot that interacts with the environment; without it a human operator has to constantly specify the motion for the robot. A significant amount of research has been done on the development of efficient motion-planning algorithms. The motion-planning problem has been solved in a theoretical sense for subsets of the general problem, but existing exact algorithms have very high time complexities and often require discrete representations of space. Much more work needs to be done before practical algorithms are developed for the general motion-planning problem.

In stationary environments many efficient algorithms exist. For the case of point robots, algorithms based on the visibility graph or Voronoi diagram run in $O(n \log n)$ or $O(n^2)$ time. For the 3D classical mover's problem efficient exact algorithms are yet to be developed. For MP of manipulators, near-real-time, resolution-complete algorithms exist [Kondo 1991; Chen and Hwang 1992], but need to be integrated with grasping planners and task planners. Motion planning for time-varying cases, multimovers problems, and constrained cases have even higher complexities, and use

Table 1. Classical Mover's Problem

approach	algorithm	dof of robot	global/ local	theo/ simul/impl	robot shape	obstacle shape	exact/ heuristic	computation speed
skeleton	AlFKM90	3	global	theo	rectangle	polygon	1	-
	AvBF88	3	global	simul	polygon	polygon	1	M
	LiCa90	d	global	simul	polytope	polytope	1r	M
	LoWe79	2	global	simul	polygon	polygon	1	s
	KeSh88	3	global	impl	polygon	polygon	1	m
cell decomp.	Broo83	3	global	simul	polygon	polygon	3	m
	BrLo83	3	global	simul	polygon	polygon	1r	M
	Dona84	6	global	simul	polyhedron	polyhedron	1r	h
	GuSS88	2	global	theo	arbitrary	arbitrary	1	-
	KeOR87	5	global	theo	line	polyhedron	1	-
	KuZB85	3	global	simul	polygon	polygon	*3	m
	LeRDG90	3	global	simul	polygon	polygon	1r	s
	Madd86	3	global	simul	line	rectangle	1	m
	NoNA89	3	global	simul	polygon	polygon	2	m
	Nguy84	3	global	simul	polygon	polygon	2	m
	ScSh81	a	global	theo	polyhedron	polyhedron	1	h
	ScSh83a	3	global	theo	polygon	polygon	1	h
	ZhLa90	3	global	simul	polygon	polygon	1r	m
potential field	ChAh91	3	global	simul	polygon	polygon	2	m
	GiJo85	6	local	simul	polygon	polygon	1r	M
	HwAh89	6	global	simul	arbitrary	polyhedron	2	M
	Warr89	3	global	simul	polygon	polygon	3	M

*1. abbreviations

    theo/simul/impl category

      theo: theoretical algorithm

      simul: simulation on computers

      impl: implemented on actual robots

    exact/heuristic rating

      1: exact, finds a solution if exists.

      1r: resolution complete.

      1p: probabilistically complete.

      2: heuristic, find solutions except for very hard problems.

      3: heuristic, find solutions if free space is wide.

    computation speeds

      s: < 1 minute. m: 1 - 10 minutes. M: 10 - 60 minutes. h: > 1 hour.

of heuristics seems essential to obtain practical algorithms. We would like to conclude this survey by summarizing four components useful for developing efficient algorithms, which have been introduced by many researchers during the past seven years.

First, the complexity of the MP problem at hand needs to be examined and compared with available computing resources. There exist many complexity results for various cases of MP. If the complexity is very high, i.e., NP-hard or PSPACE-hard, exact algorithms should be sought for only when the input size of the MP problem (robot's degrees of freedom or number of obstacles) is small.

Otherwise a heuristic algorithm should be developed. Computing resources are limited by the available technology or for economic reasons. The accuracy and quality of motion required in the robot tasks should be used to determine the allowable degrees of inexactness and heuristics, which in turn determine the minimum computing resource. For example, to plan a shortest path for a submarine, one must settle for a heuristic algorithm since the 3D shortest-path problem is NP-hard.

Second, when selecting a spatial representation, the form of available object information in an actual implementation needs to be considered. For example, in a

Table 2. Point or Circular Robot

approach	algorithm	global/ local	theo/ simul/impl	obstacle shape	exact/ heuristic	computation speed
skeleton	AsAGH85	global	theo	polygon	1	s
	AtCh89	global	theo	polygon	1	s
	AtCG89	global	theo	line segment	1	s
	ClKV87	global	theo	rectangloid	1	-
	dReLW85	global	simul	rectangle	1	m
	ElGo88	global	theo	polygon	1	s
	GoSG90	global	theo	polygon	1	s
	LoWe79	global	simul	polygon	1	s
	MoGM87	global	simul	polygon	1	m
	OdYa82	global	simul	polygon	1	s
	Papa85	global	theo	polyhedra	1r	-
	RaIS88	global	simul	polygon	1	m
	ReSc88	global	theo	polyhedra	1	-
	ReSt85	global	theo	polygon	1	s
	ReSt88	global	theo	polyhedra	1	-
cell decomp.	GaMe86	global	simul	polygon	1r	m
	JuSh88	global	simul	polyhedra	1r	m
	KaDa86	global	simul	arbitrary, 2D	1r	s
	KrTh86	global	simul	polygon	1r	m
	RuWo87	global	simul	polygon	2	s
	SiWa86	global	simul	rectangle	2	s
potential field	KhTh87	local	impl	ellipse	3	s
	Kodi87	global	simul	sphere	1	s
	KrTh86	global	simul	polygon	1r	m
	RiKo89	global	simul	star	1	m
	Thor84	global	simul	polygon	1r	m
path on a polyhedron	ChHa90	global	theo	concave polyhedron	1	-
	HwCT89	global	theo	convex polyhedron	1	-
	MiMP87	global	theo	concave polyhedron	1	-
	Moun85	global	theo	convex polyhedron	1	-
	ORSB84	global	theo	concave polyhedron	1	-
	ShSc84	global	theo	convex polyhedron	1	-
weighted region	ClKV87	global	theo	polygon	1	-
	LeCY90	global	simul	rectangle	1	-
	MiPa87	global	theo	polygon	1	-
	RiRZM87	global	simul	polygon	1	m
partially known environment	Lume87	global	simul	arbitrary, 2D	1	s
	LuSk88	global	simul	arbitrary, 2D	1	s
	RaldS88	global	simul	polygon	1	s

mechanical assembly, object information is available in CAD models, which usually use constructive solid geometry. In this case, motion planners that use CSG models of objects are appropriate. If the robot has a range sensor, computation of distance may take as short a time as sampling a signal. Motion planning can be done directly using the depth map, and the conversion of the depth map to a polyhedral representation may not be needed. Algorithms that are slow due to distance computation may benefit from such a range sensor. Although many algorithms are developed in computer simulations, one should take into account how the obstacle information will be obtained in actual implementations.

Third, the minimum-work principle should be used, meaning computations should be done only if needed. This principle can be used in three areas of MP: hierarchical model of objects, multiresolution representation of the Cspace, and use of heuristics. Intersection detection and distance computation between objects are the two most used routines in MP (typically used tens of thousands

Table 3. Manipulator

approach	algorithm	dof of robot	global/local	theo/simul/impl	robot shape	obstacle shape	exact/heuristic	computation speed
skeleton	BaLa90	arbitrary	global	simul	polyhedron	arbitrary	1p	m
	ChHw92	arbitrary	global	simul	polyhedron	polyhedron	1r	m
	FaTo87	arbitrary	global	simul	polyhedron	polyhedron	1p	M
	HoJW85	arbitrary	global	theo	line	circle	1	-
	Lume86	3	global	simul	line	polyhedron	1	s
	Lume87	2	global	simul	line	arbitrary, 2D	1	s
	LuSu87	2	global	simul	line	arbitrary, 3D	1	s
cell decomp.	Broo83	6	global	impl	polyhedron	polyhedron	3	s
	Fave89	arbitrary	global	impl	polyhedron	polyhedron	2	m
	Herm86	arbitrary	global	impl	polyhedron	arbitrary	3	m
	Kond91	arbitrary	global	simul	polyhedron	polyhedron	1r	m
	Loza87	arbitrary	global	impl	polyhedron	polyhedron	1r	h
	PaMF89	arbitrary	global	simul	arbitrary	arbitrary	1r	h
potential field	BaLa90	arbitrary	global	simul	polyhedron	arbitrary	1p	m
	BoHa88	3	local	impl	polygon	polygon	3	s
	Khat85	arbitrary	local	impl	polyhedron	polyhedron	3	s
	KhVo88	arbitrary	local	simul	polygon	polygon	3	s
	NeHo87	arbitrary	local	impl	polygon	polygon	3	s
mathematical programming	ChVi88	arbitrary	global	simul	polygon	polygon	2	h
	ElYa88	2	global	simul	polyhedron	polyhedron	1	m
	MaKl85	arbitrary	global	simul	polyhedron	polyhedron	2	m
	ShDu88	arbitrary	global	simul	polygon	polygon	2	h

Table 4. Multimover's Problem

All are global algorithms.

approach	algorithm	dof of a robot	number of robots	theo/simul/impl	robot shape	obstacle shape	exact/heuristic	computation speed
predefined priority	ErLo86	2	arbitrary	simul	polygon,manip	polygon	2	m
	FrHo88	2	arbitrary	impl	point,manip	polygon	3	on-line
no predefined priority	Buck89	2	arbitrary	impl	square	none	2	s
	ChKL88	2	arbitrary	impl	manipulator	polyhedron	3	s
	FoWY86	2	2	simul	manipulator	polyhedron	1	s or m
	LiKNNA89	2	2	simul	circle	arbitrary	2	m
	ODLo89	arbitrary	2	simul	manipulator	polyhedron	2	m
	ScSh83b	2	arbitrary	theo	circle	polyhedron	1	h
	ShSi88	2	2	theo	circle,manip	polygon	1	-
	YeBe87	2	arbitrary	simul	circle	polyhedron	2	s or m

Table 5. Time-Varying Environment

All are global algorithms.
The robot is all a point, see note below.

approach	algorithm	dof of robot	thoe/simul/impl	obstacle shape	exact/heuristic	computation speed
skeleton	FuSa89	2	simul	polygon	1r	m
	KaZu88	2	simul	polygon	2	s or m
	KeLi88	2	simul	point	3	s
	ReSh85	2,3	theo	polytope	1	-
	CaRe85	2,3	theo	polytope	1	m or M
cell decomp.	FuSa88	2	simul	polygon	1r	m

Note: MP of a translating polytope robot among translating polytopes
   is the same as moving a point among polytope configuration obstacles.

Table 6. Motion Planning with Constraints

| constraint	algorithm	robot shape	theo/ simul/impl	description
curvature	Dubu57	point	thoe	Shows shortest paths consist of straight lines and maximum-curvature lines.
	FoWi88	point	simul	Checks the existence of a path satisfying curvature constraints.
	JaCa89	point	simul	Computes approximately the shortest path in polynomial time using the Cspace.
	Wilf89	rectangle	simul	Given a sequence of line segments for a wheeled vehicle to follow, computes the shortest path in polynomial time.
kinodynamic	ODun87	point	thoe	1D problem with a bounded acceleration, the robot avoids two point obstacles.
	CaDRX88	point	simul	Computes the minimum-time path using a grid, bounds on velocity and acceleration.
	DoXa89	manipulator	simul	Computes the minimum-time path using a grid, bounds on velocity and acceleration.

Table 7. Movable-Object Problem

| algorithm	work space dimension	robot shape	obstacle shape	description
AISL90	3D	manipulator	arbitrary	Formalize manipulation task, introduces STABLE and GRASP sets.
LoJMOGTL87	3D	manipulator	polyhedra	An actual system executing Move object O To destination D.
Wilf88	2D	rectangle	rectangle	Shows NP-hardness, $O(n \log n)$ for one movable object.

of times). Hierarchical representations of objects significantly speed up these computations [Faverjon 1989]. For example, if the two cuboids each containing an object do not intersect, the objects do not either (called the bounding-box method in computer graphics). Detail models of objects need to be considered only if coarser models fail to give necessary results. A representation of the Cspace should be built in multiple resolutions [Brooks and Lozano-Pérez 1983; Kambhampati and Davis 1986]. A coarse representation is easy to compute and needs less time to be searched. A finer resolution is needed only if a path cannot be found using a coarser representation. This is exactly the essence of the ICORS paradigm. Whenever there is a set of possible choices, develop *good* heuristics to order them so that the choice with the highest probability of yielding a solution is examined first. These heuristics often increase efficiency of algorithms.

Fourth, most robots operate in specific environments, and algorithms should be specialized to adapt to these environments. Also, robots have special geometries that can be exploited to develop fast algorithms. It would be an accomplishment to develop a general efficient algorithm, but such an algorithm will likely have high complexity. Application-specific algorithms will be more efficient without sacrificing performance.

We also have a suggestion for those who implement algorithms to demonstrate efficiency and performance. It has been difficult to compare performances of motion planners since they solve different examples on different computers. There is yet no set of benchmark problems that represent *realistic* and *non-pathological* motion-planning problems. Unless the work is theoretical, we urge motion-planning researchers to include at least one example satisfying the following criteria for a fair comparison.
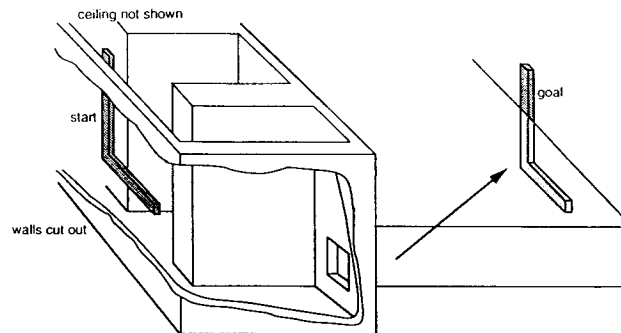
(a) To move the L-shaped robot, it requires an intelligent maneuvering at the lower left corner and through the hole. The space to the right of the robot at the start configuration represents a trap. To minimize the path length, the robot should take a short cut (arrow) rather than going around the lower right corner.
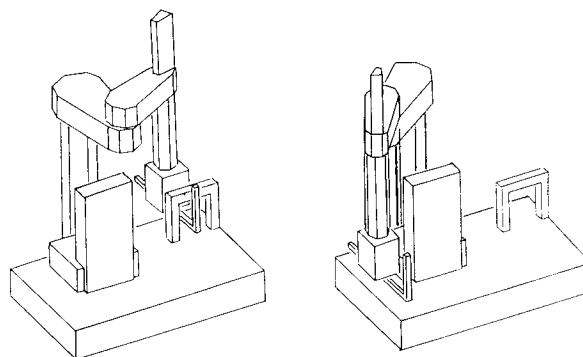
(b) The Adept robot has to bend its wrist to get the L-shaped object out of the wicket. It then has to bend its arm to avoid the middle tall block. Finally, it has to rotate its first link all the way to the left (a significant backtracking) before reaching the goal configuration

Figure 40. Benchmark motion-planning problems.

First, the number of obstacles should be at least 5 to 10, and some obstacles should be concave. Second, the solution path should be nontrivial and utilize all degrees of freedom available. Third, there should be a narrow space at some point along the solution path so that the problem cannot be solved with a coarse quantization of joint variables. Fourth, there should be a trap in the space so that some backtracking is required to find a solution. We present two benchmark problems for the classical mover's problem and MP of manipulators (Figure 40), meeting the criteria above. We have made an effort so that these problems are not pathological and likely to occur in practical situations.

REFERENCES

AHUJA, N., AND SCHACHTER, B. 1983. *Pattern Models.* Wiley, New York.

ALAMI, R., SIMÉON, T., AND LAUMOND, J. P. 1989. A geometric approach to planning manipulation tasks. The case of discrete placements and grasps. In *Proceedings of the 5th International Symposium of Robotics Research* (Tokyo, Aug. 28–31), MIT Press, Cambridge, Mass. pp. 453–463.

ALT, H., FLEISCHER, R., KAUFMANN, M., MEHLHORN, K., NÄHER, S., SCHIRRA, S., AND UHRIG, C.

1990. Approximate motion planning and the complexity of the boundary of the union of simple geometric figures. In *Proceedings of the 5th Annual ACM Symposium on Computational Geometry* (Berkeley, Calif., June 6–8). ACM, New York, pp. 281–289.

ASANO, T., ASANO, T., GUIBAS, L., HERSHBERGER, J., AND IMAI, H. 1985. Visibility-polygon search and Euclidean shortest path. In *The 26th Symposium on Foundations of Computer Science* (Portland, Oreg., Oct. 21–23) pp. 155–164.

ATALLAH, M. J., AND CHEN, D. Z. 1989. Optimal parallel algorithms for visibility of a simple polygon from a point. In *Proceedings of the 5th Annual ACM Symposium on Computational Geometry* (Berkeley, Calif., June 6–8). ACM, New York, pp. 114–123.

ATALLAH, M. J., COLE, R., AND GOODRICH, M. T. 1989. Cascading divide-and-conquer: A technique for designing parallel algorithms. *SIAM J. Comput. 18*, 3 (June), 499–532.

ATHENS, M., AND FALBS, P. L. 1966. *Optimal Control*. McGraw-Hill, New York.

AURENHAMMER, F. 1991. Voronoi diagrams—A survey of fundamental geometric data structure. *ACM Comput. Surv. 23*, 3 (Sept.), 345–405.

AVNAIM, F., BOISSONNAT, J. D., AND FAVERJON, B. 1988. A practical exact motion planning algorithm for polygonal objects amidst polygonal obstacles. In *Proceedings of the IEEE International Conference on Robotics and Automation* (Philadelphia, Apr. 24–29). IEEE, New York, pp. 1656–1661.

BARR, A., AND FEIGENBAUM, E. A. 1981. *The Handbook of Artificial Intelligence*. William Kaufmann, Los Altos, Calif.

BARRAQUAND, J., AND LATOMBE, J. C. 1990. A Monte-Carlo algorithm for path planning with many degrees of freedom. In *Proceedings of the IEEE International Conference on Robotics and Automation* (Cincinnati, May 13–18). IEEE, New York, pp. 1712–1717.

BOBROW, J. E., DUBOWSKY, S., AND GIBSON, J. S. 1985. Time-optimal control of robotic manipulators along specified paths. *Int. J. Robotics Res. 4*, 3 (Fall), 3–17.

BOISSIERE, P. T., AND HARRIGAN, R. W. 1988. Telerobotic operation of conventional robot manipulators. In *Proceedings of the IEEE International Conference on Robotics and Automation* (Philadelphia, Apr. 24–29). IEEE, New York, pp. 576–583.

BRANICKY, M., AND NEWMAN, W. 1990. Rapid computation of configuration obstacles. In *Proceedings of the IEEE International Conference on Robotics and Automation* (Cincinnati, May 13–18). pp. 304–310.

BROOKS, R. A. 1983. Solving the Findpath problem by good representation of free space. *IEEE Trans. Syst., Man, and Cybernetics SMC-13*, 3 (Mar./Apr.), 190–197.

BROOKS, R. A., AND LOZANO-PÉREZ, T. 1983. A subdivision algorithm in configuration space for Findpath with rotation. In *The International Joint Conference on Artificial Intelligence* (Karlsruhe, Germany, Aug. 8–12). William Kaufmann, Inc., Los Altos, Calif., pp. 799–806.

BRYSON, A. E., JR., AND HO, Y. C. 1975. *Applied Optimal Control*. Hemisphere Publishing, Washington, D.C.

BUCKLEY, S. J. 1989. Fast motion planning for multiple moving robots. In *Proceedings of the IEEE International Conference on Robotics and Automation* (Scottsdale, Ariz., May 14–19). pp. 322–326.

CANNY, J. F. 1988. *The Complexity of Robot Motion Planning*. The MIT Press, Cambridge, Mass.

CANNY, J. F. 1987. A new algebraic method for robot motion planning and real geometry. In *Proceedings of the 28th Annual Symposium on Foundations of Computer Science* (Los Angeles, Oct. 12–14). IEEE, Washington, D.C., pp. 39–48.

CANNY, J. F., AND DONALD, B. 1987. Simplified Voronoi diagram. In *Proceedings of the 3rd Annual ACM Symposium on Computational Geometry* (Waterloo, Ontario, June 8–10). ACM Press, New York, pp. 153–161.

CANNY, J. F., AND LIN, M. C. 1900. An opportunistic global path planner. In *Proceedings of the IEEE International Conference on Robotics and Automation* (Cincinnati, May 13–18). IEEE, New York, pp. 1554–1561.

CANNY, J. F., AND REIF, J. 1987. New lower bound techniques for robot motion planning problems. In *Proceedings of the 28th Annual Symposium on Foundations of Computer Science* (Los Angeles, Oct. 12–14). IEEE, New York, pp. 49–60.

CANNY, J. F., DONALD, B., REIF, J., AND XAVIER, P. 1988. On the complexity of kinodynamic planning. In *Proceedings of the 29th Annual Symposium on Foundations of Computer Science* (White Plains, New York, Oct. 24–26). IEEE, New York, pp. 306–315.

CANNY, J. F., REGE, A., AND REIF, J. 1990. An exact algorithm for kinodynamic planning in the plane. In *Proceedings of the 6th Annual ACM Symposium on Computational Geometry* (Berkeley, Calif., June 6–8). ACM, New York, pp. 271–280.

CHATILA, R. 1982. Path planning and environment learning in a mobile robot system. In *Proceedings of the European Conference on Artificial Intelligence* (Orsay, France, July 12–14). pp. 211–215.

CHATILA, R., AND LAUMOND, J. P. 1985. Position referencing and consistent world modeling for mobile robots. In *Proceedings of the IEEE International Conference on Robotics and Automation* (St. Louis). IEEE, New York, pp. 138–145.

CHATTERGY, R. 1985. Some heuristics for the navigation of a robot. *Int. J. Robotics Res. 4*, 1 (Spring), 59–66.

CHEN, J., AND HAN, Y. 1990. Shortest paths on a polyhedron. In *Proceedings of the 6th Annual ACM Symposium on Computational Geometry* (Berkeley, Calif., June 6–8). ACM, New York, pp. 360–369.

CHEN, P. C., AND HWANG, Y. K. 1992. SANDROS: A motion planner with performance proportional to task difficulty. In *Proceedings of the IEEE International Conference on Robotics and Automation* (Nice, France, May 12–14). IEEE, New York, pp. 2346–2353.

CHEN, P. C., AND HWANG, Y. K. 1991. Practical path planning among movable obstacles. In *Proceedings of the IEEE International Conference on Robotics and Automation* (Sacramento, Apr. 7–12). ACM, New York, pp. 444–449.

CHEN, Y. C., AND VIDYASAGAR, M. 1988. Optimal trajectory planning for planner n-link revolute manipulators in the presence of obstacles. In *Proceedings of the IEEE International Conference on Robotics and Automation* (Philadelphia, Apr. 24–29). IEEE, New York, pp. 202–208.

CHEUNG, E., AND LUMELSKY, V. 1988. Motion planning for robot arm manipulators with proximity sensing. In *Proceedings of the IEEE International Conference on Robotics and Automation* (Philadelphia, Apr. 24–29). IEEE, New York, pp. 740–745.

CHEW, L. P. 1985. Planning the shortest path for a disc in $O(n^2 \log n)$ time. In *Proceedings of the 1st Annual ACM Symposium on Computational Geometry* (Baltimore, June 5–7). ACM, New York, pp. 214–220.

CHIEN, Y. P., KOIVO, A. J., AND LEE, B. H. 1988. On-line generation of collision free trajectories for multiple robots. In *Proceedings of the IEEE International Conference on Robotics and Automation* (Philadelphia, Apr. 24–29). IEEE, New York, pp. 209–211.

CHUANG, J., AND AHUJA, N. 1991a. Path planning using the Newtonian potential. In *Proceedings of the IEEE International Conference on Robotics and Automation* (Sacramento, Apr. 7–12). IEEE, New York, pp. 558–563.

CHUANG, J., AND AHUJA, N. 1991b. Skeletonization using a generalized potential field model. In *The 8th Israeli Symposium on Artificial Intelligence and Computer Vision* (Dec. 30–31).

CLARKSON, K. L., KAPOOR, S., AND VAIDYA, P. M. 1987. Rectilinear shortest paths through polygonal obstacles in $O(n(\log n)^2)$ time. In *Proceedings of the 3rd Annual ACM Symposium on Computational Geometry* (Waterloo, Ontario, June 8–10). ACM, New York, pp. 251–257.

COLLINS, G. 1975. Quantifier elimination for real closed fields by cylindrical algebraic decomposition. In *The 2nd GI Conference on Automata Theory and Formal Languages*, vol. 33. Springer-Verlag, New York, pp. 134–183.

CORMEN, T. H., LEISERSON, C. E., AND RIVEST, R. L. 1990. *Introduction to Algorithms*. McGraw-Hill, New York, pp. 916–963.

DE REZENDE, P. J., LEE, D. T., AND WU, Y. F. 1985. Rectilinear shortest paths with rectangular barriers. In *Proceedings of the 1st Annual ACM Symposium on Computational Geometry* (Baltimore, June 5–7). ACM, New York, pp. 204–213.

DIJKSTRA, E. W. 1959. A note on two problems in connection with graphs. *Numerische Mathematik 1*, 269–271. In English.

DONALD, B. 1984. Motion planning with six degrees of freedom, Tech. Rep. AI-TR-791, Artificial Intelligence Lab., Massachusetts Inst. of Technology, Cambridge, Mass.

DONALD, B., AND JENNINGS, J. 1991. Sensor interpretation and task-directed planning using perceptual equivalence class. In *Proceedings of the IEEE International Conference on Robotics and Automation* (Sacramento, Apr. 7–12). IEEE, New York, pp. 190–197.

DONALD, B., AND XAVIER, P. 1989. A provably good approximation algorithm for optimal time trajectory planning. In *Proceedings of the IEEE International Conference on Robotics and Automation* (Scottsdale, Ariz., May 14–19). IEEE, New York, pp. 958–963.

DRYSDALE, R. L. 1979. Generalized Voronoi diagrams and geometric searching. Tech. Rep. STAN-CS-79-705, Stanford Univ., Stanford, Calif.

DUBINS, L. E. 1957. On curves of minimal length with a constraint on average curvature and with prescribed initial and terminal positions and tangents. *Amer. J. Math. 79*, 497–516.

ELGINDY, H., AND GOODRICH, M. T. 1988. A linear algorithm for computing the visibility polygon from a point. *J. Alg. 2*, 186–197.

ELTIMSAHY, A. H., AND YANG, W. S. 1988. Near Minimum-time control of robotic manipulator with obstacles in the workspace. In *Proceedings of the IEEE International Conference on Robotics and Automation* (Philadelphia, Apr. 24–29). IEEE, New York, pp. 358–363.

ERDMANN, M., AND LOZANO-PÉREZ, T. 1986. On multiple moving objects. In *Proceedings of the IEEE International Conference on Robotics and Automation* (San Francisco, Apr. 7–10). IEEE, New York, pp. 1419–1424.

FAVERJON, B. 1989. Hierarchical object models for efficient anti-collision algorithm. In *Proceedings of the IEEE International Conference on Robotics and Automation* (Scottsdale, Ariz., May 14–19). IEEE, New York, pp. 333–340.

FAVERJON, B. 1986. Object level programming of industrial robots. In *The IEEE International Conference on Robotics and Automation* (San

Francisco, Apr. 7-10). IEEE, New York, pp. 1406-1412.

FAVERJON, B., AND TOURNASSOUD, P. 1987. A local approach for path planning of manipulators with a high number of degrees of freedom. In *Proceedings of the IEEE International Conference on Robotics and Automation* (Raleigh, N. Carol., Mar. 31-Apr. 3). IEEE, New York, pp. 1152-1159.

FORTUNE, S., AND WILFONG, G. 1988. Planning constrained motion. In *The Symposium on the Theory of Computer Science* (Chicago). pp. 445-459.

FORTUNE, S., WILFONG, G., AND YAP, C. 1986. Coordinated motion of two robot arms. In *Proceedings of the IEEE International Conference on Robotics and Automation* (San Francisco, Apr. 7-10). IEEE, New York, pp. 1215-1223.

FREUND, E., AND HOYER, H. 1988. Real-time pathfinding in multirobot systems including obstacle avoidance. *Int. J. Robotics Res.* 7, 1 (Feb.), 42-70.

FUJIMURA, K., AND SAMET, H. 1989. Time minimal paths among moving obstacles. In *Proceedings of the IEEE International Conference on Robotics and Automation* (Scottsdale, Ariz., May 14-19). IEEE, New York, pp. 1110-1115.

FUJIMURA, K., AND SAMET, H. 1988. Path planning among moving obstacles using spatial indexing. In *Proceedings of the IEEE International Conference on Robotics and Automation* (Philadelphia, Apr. 24-29). IEEE, New York, pp. 1662-1667.

GAW, D., AND MEYSTEL, A. 1986. Minimum-time navigation of an unmanned mobile robot in a 2-1/2D world with obstacles. In *Proceedings of the IEEE International Conference on Robotics and Automation* (San Francisco, Apr. 7-10). IEEE, New York, pp. 1670-1677.

GE, Q., AND MCCARTHY, J. M. 1989. Equations for boundaries of joint obstacles for planar robots. In *Proceedings of the IEEE International Conference on Robotics and Automation* (Scottsdale, Ariz., May 14-19). IEEE, New York, pp. 164-169.

GEWALI, L., MENG, A., MITCHELL, J. S. B., AND NTAFOS, S. 1988. Path planning in $0/1/\infty$ weighted regions with applications. In *Proceedings of the 4th Annual ACM Symposium on Computational Geometry* (Urbana, Ill., June 6-8). ACM, New York, pp. 266-278.

GILBERT, E. G., AND FOO, C. P. 1990. Computing the distance between general convex objects in three-dimensional space. *IEEE Trans. Robotics Auto.* 6, 1 (Feb.), 53-61.

GILBERT, E. G., AND JOHNSON, D. W. 1985. Distance functions and their applications to robot path planning in the presence of obstacles. *IEEE J. Robotics Auto.* RA-1, 1, 21-30.

GILBERT, E. G., JOHNSON, D. W., AND KEERTHI, S. S. 1988. A fast procedure for computing the distance between complex objects in three-

dimensional space. *IEEE J. Robotics Auto.* RA-4, 2 (Apr.), 193-203.

GOODRICH, M. T., SHAUCK, S. B., AND GUHA, S. 1990. Parallel method for visibility and shortest path problems in a simple polygons. In *Proceedings of the 6th Annual ACM Symposium on Computational Geometry* (Berkeley, Calif., June 6-8). ACM, New York, pp. 73-82.

GUIBAS, L. J., SHARIR, M., AND SIFRONY, S. 1988. On the general motion planning problem with two degrees of freedom. In *Proceedings of the 4th Annual ACM Symposium on Computational Geometry* (Urbana, Ill., June 6-8). ACM, New York, pp. 289-298.

HERMAN, M. 1986. Fast, three-dimensional, collision-free motion planning. In *Proceedings of the IEEE International Conference on Robotics and Automation* (San Francisco, Apr. 7-10). IEEE, New York, pp. 1056-1063.

HOGAN, N. 1985. Impedance control: An approach to manipulation: Part III—Application. *ASME J. Dynamic Syst. Meas. Control.* 107 (Mar.), 17-24.

HOPCROFT, J., AND ULLMAN, J. D. 1979. *Introduction to Automata Theory, Languages and Computations.* Addison-Wesley, Reading, Mass.

HOPCROFT, J., AND WILFONG, G. T. 1986. Reducing multiple object motion planning to graph searching. *SIAM J. Comput.* 15, 3 (Aug.), 768-785.

HOPCROFT, J., JOSEPH D., AND WHITESIDE, S. 1985. On the movement of robot arms in 2-dimensional bounded regions. *SIAM J. Comput.* 14, 2 (May), 315-333.

HOPCROFT, J., JOSEPH, D., AND WHITESIDE, S. 1984a. Movement problems for 2-dimensional linkages. *SIAM J. Comput.* 13, 3 (Aug.), 610-629.

HOPCROFT, J., SCHWARTZ, J. T., AND SHARIR, M. 1984b. On the complexity of motion planning for multiple independent objects; PSPACE-hardness of the "Warehouseman's Problem." *Int. J. Robotics Res.* 3, 4 (Winter), 76-88.

HUANG, Y. F., AND LEE, C. S. G. 1991. A framework of knowledge-based assembly planning. In *Proceedings of the IEEE International Conference on Robotics and Automation* (Sacramento, Apr. 7-12). IEEE, New York, pp. 599-604.

HUTCHINSON, S. A., AND KAK, A. C. 1990. Spar: A planner that satisfies operational and geometric goals in uncertain environments. *AI Mag.* 11, 1 (Spring), 31-61.

HWANG, Y. K. 1990. Boundary equations of configuration obstacles for manipulators. In *Proceedings of the IEEE International Conference on Robotics and Automation* (Cincinnati, May 13-18). IEEE, New York, pp. 298-303.

HWANG, Y. K., AND AHUJA, N. 1992. Potential field approach to path planning. *IEEE Trans. Robotics Auto.* 8, 1 (Feb.), 23-32.

HWANG, Y. K., AND AHUJA, N. 1989. Robot path planning using a potential field representation. In *The IEEE Computer Society Conference on Computer Vision and Pattern Recognition* (San Diego, June 4–8). IEEE, New York, pp. 569–575.

HWANG, Y. H., CHANG, R. C., AND TU, H. Y. 1989. Finding all shortest path edge sequences on a convex polyhedron. In *Lecture Notes in Computer Science, Algorithms and Data Structures Workshop*, vol. 332, Springer-Verlag, New York.

HWANG, Y. K., CHEN, P. C., AND XAVIER, P. G. 1992. Test suites for motion planning. Internal Rep., Sandia National Laboratories, Albuquerque, New Mex.

JACOBS, P., AND CANNY, J. 1989. Planning smooth paths for mobile robots. In *Proceedings of the IEEE International Conference on Robotics and Automation* (Scottsdale, Ariz., May 14–19). IEEE, New York, pp. 2–7.

JONES, S. T. 1980. Solving problems involving variable terrain. Part 1: A general algorithm. *Byte 5*, 2.

JUN, S., AND SHIN, K. G. 1988. A probabilistic approach to collision-free robot path planning. In *Proceedings of the IEEE International Conference on Robotics and Automation* (Philadelphia, Apr. 24–29). IEEE, New York, pp. 220–227.

KAMBHAMPATI, S., AND DAVIS, L. S. 1986. Multiresolution path planning for mobile robots. *IEEE J. Robotics Auto. RA-2*, 3 (June), 135–145.

KANT, K., AND ZUCKER, S. W. 1988. Planning collision-free trajectories in time-varying environments: A two-level hierarchy. In *Proceedings of the IEEE International Conference on Robotics and Automation* (Philadelphia, Apr. 24–29). IEEE, New York, pp. 1644–1649.

KANT, K., AND ZUCKER, S. W. 1986. Toward efficient trajectory planning: The path-velocity decomposition. *Int. J. Robotics Res. 5*, 1 (Spring), 72–89.

KE, Y. 1989. An efficient algorithm for link distance problems. In *Proceedings of the 5th Annual ACM Symposium on Computational Geometry* (Saarbruchen, West Germany, June 5–7). ACM, New York, pp. 69–78.

KE, Y., AND O'ROURKE, J. 1988. Lower bounds on moving a ladder in two and three dimensions. In *Discrete and Computational Geometry*, vol. 3. Springer-Verlag, New York, pp. 197–217.

KE, Y., AND O'ROURKE, J. 1987. Moving a ladder in three dimensions: Upper and lower bounds. In *Proceedings of the 3rd Annual ACM Symposium on Computational Geometry* (Waterloo, Ontario, June 8–10). ACM, New York, pp. 136–145.

KEDEM, K., AND SHARIR, M. 1988. An automatic motion planning system for a convex polygonal mobile robot in 2-D polygonal space. In *Proceedings of the 4th Annual ACM Symposium on*

Computational Geometry (Urbana, Ill., June 6–8). ACM, New York, pp. 329–340.

KEDEM, K., AND SHARIR, M. 1985. An efficient algorithm for planning collision-free motion of a convex polygonal object in 2-dimensional space amidst polygonal obstacles. In *Proceedings of the 1st Annual ACM Symposium on Computational Geometry* (Baltimore, June 5–7). ACM, New York, pp. 75–80.

KEHTARNAVAZ, N., AND LI, S. 1988. A collision-free navigation scheme in the presence of moving obstacles. In *The International Conference on Computer Vision*. IEEE Computer Society, Los Angeles, pp. 808–813.

KEIL, J. M., AND SACK, J. R. 1985. Minimum decomposition of polygonal objects. In *Computational Geometry*. Elsevier Science Publishers, North Holland, Amsterdam, pp. 197–216.

KHATIB, O. 1985. Real-time obstacle avoidance for manipulators and mobile robots. In *Proceedings of the IEEE International Conference on Robotics and Atomation* (St. Louis, Missouri). IEEE, New York, pp. 500–505.

KHATIB, O., AND MAMPEY, L. M. 1978. Fonction decision-commande d'un robot manipulateur. Rep. 2/7156. DERA/CERT, Toulouse, France.

KHERADPIR, S., AND THORP, J. S. 1987. Real-time control of robot manipulators in the presence of obstacles. *IEEE Int. J. Robotics Auto. RA-4*, 6 (Dec.), 687–698.

KHOSLA, P., AND VOLPE, R. 1988. Superquadric artificial potentials for obstacle avoidance and approach. In *Proceedings of the IEEE International Conference on Robotics and Automation* (Philadelphia, Apr. 24–29). IEEE, New York, pp. 1778–1784.

KEIRSEY, D. M., AND MITCHELL, J. S. B. 1984. Planning strategic paths through variable terrain data. In *Proceedings of SPIE Applications of Artificial Intelligence* vol. 485, SPIE, Bellingham, Washington, pp. 172–179.

KIRKPATRICK, D. G. 1979. Efficient computation of continuous skeletons. In *The 20th Symposium on the Foundations of Computer Science* (San Juan, Puerto Rico, Oct. 29–31). pp. 18–27.

KOCH, E., YEN, C., HILLEL, G., MEYSTEL, A., AND ISIK, C. 1985. Simulation of path planning for a system with vision and map updating. In *Proceedings of the IEEE International Conference on Robotics and Automation* (St. Louis, Missouri). IEEE, New York, pp. 146–160.

KODITSCHEK, D. E. 1989. Robot planning and control via potential functions. In *Robotics Review*, vol. 1, O. Khatib, J. Graig, and T. Lozano-Pérez, Eds. MIT Press, Cambridge, Mass.

KODITSCHEK, D. E. 1987. Exact robot navigation by means of potential functions: Some topological considerations. In *Proceedings of the IEEE International Conference on Robotics and Automation* (Raleigh, N. Carol, Mar. 31–Apr. 3). IEEE, New York, pp. 1–6.

KONDO, K. 1991. Motion planning with six degrees of freedom by multistrategic, bidirectional heuristic free space enumeration. *IEEE Trans. Robotics Auto. 7*, 3 (June), 267-277.

KROGH, B. H., AND THORPE, C. E. 1986. Integrated path planning and dynamic steering control for autonomous vehicles. In *Proceedings of the IEEE International Conference on Robotics and Automation* (San Francisco, Apr. 7-10). IEEE, New York, pp. 1664-1669.

KUAN, D. T., ZAMISKA, J. C., AND BROOKS, R. A. 1985. Natural decomposition of free space for path planning. In *Proceedings of the IEEE International Conference on Robotics and Automation* (St. Louis, Missouri). IEEE, New York, pp. 168-173.

LATOMBE, J. C. 1991. *Robot Motion Planning.* Kluwer Academic Publishers, Boston/ Dordrecht/London.

LEE, D. T. 1978. Proximity and reachability in the plane. Ph.D. dissertation, Univ. of Illinois, Urbana-Champaign, Ill.

LEE, D. T., AND DRYSDALE, R. L. 1981. Generalization of Voronoi diagram in the plane. *SIAM J. Comput. 10*, 73-83.

LEE, S., AND SHIN, Y. G. 1990. Disassembly planning based on subassembly extraction. In *Proceedings of the IEEE International Conference on Robotics and Automation* (Cincinnati, May 13-18). IEEE, New York, pp. 1606-1613.

LEE, D. T., CHEN, T. H., AND YANG, C. D. 1990. Shortest rectilinear paths among weighted obstacles. In *Proceedings of the 6th Annual ACM Symposium on Computational Geometry* (Berkeley, Calif., June 6-8). ACM, New York, pp. 301-310.

LENGYEL, J., REICHERT, M., DONALD, B. R., AND GREENBERG, D. P. 1990. Real-time robot motion planning using rasterizing computer graphics hardware. *Comput. Graph. 24*, 4 (Aug.), 327-335.

LIN, M. C., AND CANNY, J. F. 1991. A fast algorithm for incremental distance calculation. In *Proceedings of the IEEE International Conference on Robotics and Automation* (Sacramento, Apr. 7-12). IEEE, New York, pp. 1008-1014.

LIU, Y. H., KURODA, S., NANIWA, T., NOBORIO, H., AND ARIMOTO, S. 1989. A practical algorithm for planning collision-free coordinated motion of multiple mobile robots. In *Proceedings of the IEEE International Conference on Robotics and Automation* (Scottsdale, Ariz., May 14-19). IEEE, New York, pp. 1427-1432.

LOZANO-PÉREZ, T. 1987. A simple motion-planning algorithm for general robot manipulators. *IEEE J. Robotics Auto. RA-3*, 3 (June), 224-238.

LOZANO-PÉREZ, T., AND O'DONNELL, P. A. 1991. Parallel robot motion planning. In *Proceedings of the IEEE International Conference on Robotics and Automation* (Sacramento, Apr. 7-12). IEEE, New York, pp. 1000-1007.

LOZANO-PÉREZ, T., AND WESLEY, M. A. 1979. An algorithm for planning collision-free paths among polyhedral obstacles. *Commun. ACM 22*, 10 (Oct.), 560-570.

LOZANO-PÉREZ, T., JONES, J. L., MAZER, E., O'DONNELL, P. A. 1989. Task-level planning of pick-and-place robot motions. *IEEE Comput. 22*, 3 (Mar.), 21-29.

LOZANO-PÉREZ, T., JONES, J. L., MAZER, E., O'DONNELL, P. A., GRIMSON, E. L., TOURNASSOUD, P., AND LANUSSE, A. 1987. Handey: A robot system that recognizes, plans, and manipulates. In *Proceedings of the IEEE International Conference on Robotics and Automation* (Raleigh, N. Carol., Mar. 31-Apr. 3). IEEE, New York, pp. 843-849.

LUMELSKY, V. J. 1987. Effect of kinematics on motion planning for planar robot arms moving amidst unknown obstacles. *IEEE J. Robotics Auto. RA-3*, 3 (June), 207-223.

LUMELSKY, V. 1986. Continuous motion planning in unknown environment for a 3D cartesian robot arm. In *Proceedings of the IEEE International Conference on Robotics and Automation* (San Francisco, Apr. 7-10). IEEE, New York, pp. 1050-1055.

LUMELSKY, V., AND SKEWIS, T. 1988. A paradigm for incorporating vision in the robot navigation function. In *Proceedings of the IEEE International Conference on Robotics and Automation* (Philadelphia, Apr. 24-29). IEEE, New York, pp. 734-739.

LUMELSKY, V., AND SUN, K. 1987. Gross motion planning for a simple 3D articulated robot arm moving amidst unknown arbitrarily shaped obstacles. In *Proceedings of the IEEE International Conference on Robotics and Automation* (Raleigh, N. Carol., Mar. 31-Apr. 3). IEEE, New York, pp. 1929-1934.

MACIEJEWSKI, A. A., AND KLEIN, C. A. 1985. Obstacle avoidance for kinematically redundant manipulators in dynamically varying environments. *Int. J. Robotics Res. 4*, 3 (Fall), 109-117.

MADDILA, S. R. 1986. Decomposition algorithm for moving a ladder among rectangular obstacles. In *Proceedings of the IEEE International Conference on Robotics and Automation* (San Francisco, Apr. 7-10). IEEE, New York, pp. 1413-1418.

MCCARTHY, J. M., GE, Q., AND BODDULURI, R. M. C. 1989. The analysis of cooperating planar robot arms in the image space of the workpiece. *Int. J. Robotics Res.*

MITCHELL, J. S. B., AND PAPADIMITRIOU, C. H. 1987. The weighted region problem. In *Proceedings of the 3rd Annual ACM Symposium on Computational Geometry* (Waterloo, Ontario, June 8-10). ACM, New York, pp. 30-38.

MITCHELL, J. S. B., MOUNT, D. M., AND PAPADIMITRIOU, C. H. 1987. The discrete

geodesic problem. *SIAM J. Comput. 16*, 4 (Aug.), 647–668.

MITCHELL, J. S. B., ROTE, G., AND WOEGINGER, G. 1990. Minimum-link paths among obstacles in the plane. In *Proceedings of the 6th Annual ACM Symposium on Computational Geometry* (Berkeley, Calif., June 6–8). ACM, New York, pp. 63–72.

MIYAZAKI, F., AND ARIMOTO, S. 1984. Sensory feedback based on the artificial potential for robots. In *Proceedings of the 9th Triannual World Congress of International Factory Automation* (Budapest, July 2–6). Pergamon Press, New York, pp. 2381–2386.

MONTGOMERY, M., GAW, D., AND MEYSTEL, A. 1987. Navigation algorithm for a nested hierarchical system of robot path planning among polyhedral obstacles. In *Proceedings of the IEEE International Conference on Robotics and Automation* (Raleigh, N. Carol., Mar. 31–Apr. 3). IEEE, New York, pp. 1612–1622.

MOUNT, D. M. 1985. On finding shortest paths on convex polyhedra. Tech. Rep. 1495, Dept. of Computer Science, Univ. of Maryland, Baltimore.

NEWMAN, W. 1989. Automatic obstacle avoidance at high speeds via reflex control. In *Proceedings of the IEEE International Conference on Robotics and Automation* (Scottsdale, Ariz.). IEEE, New York, pp. 1104–1109.

NEWMAN, W., AND HOGAN, N. 1987. High speed robot control and obstacle avoidance using dynamic potential function. In *Proceedings of the IEEE International Conference on Robotics and Automation* (Raleigh, N. Carol., Mar. 31–Apr. 3). IEEE, New York, pp. 14–24.

NGUYEN, V. D. 1984. The Findpath problem in the plane. AI Memo 760, Artificial Intelligence Lab., Massachusetts Inst. of Technology, Cambridge, Mass.

NOBORIO, H., NANIWA, T., AND ARIMOTO, S. 1989. A feasible motion planning algorithm for a mobile robot on a quadtree representation. In *Proceedings of the IEEE International Conference on Robotics and Automation* (Scottsdale, Ariz., May 14–19). IEEE, New York, pp. 327–332.

O'DONNELL, P. A., AND LOZANO-PÉREZ, T. 1989. Deadlock-free and collision-free coordination of two robot manipulators. In *Proceedings of the IEEE International Conference on Robotics and Automation* (Scottsdale, Ariz., May 14–19). IEEE, New York, pp. 484–489.

O'DÚNLAING, C. 1987. Motion planning with inertial constraints. *Algorithmica 2*, 4, 431–475.

O'DÚNLAING, C., AND YAP, C. K. 1985. A retraction method for planning the motion of a disc. *J. Algor. 6*, 1(Mar.), 104–111.

OOMMEN, B. J., IYENGAR, S. S., RAO, N. S. V., AND KASHYAP, R. L. 1987. Robot navigation in unknown terrains using learned visibility graphs. Part I: The disjoint convex obstacle case. *IEEE Int. J. Robotics Auto. RA-3*, 6 (Dec.), 672–680.

O'ROURKE, J., SURI, S., AND BOOTH, H. 1984. Shortest paths on polyhedral surfaces. Tech. Rep. The Johns Hopkins Univ., Baltimore.

PADEN, B., MEES, A., AND FISHER, M. 1989. Path planning using a Jacobian-based freespace generation algorithm. In *Proceedings of the IEEE International Conference on Robotics and Automation* (Scottsdale, Ariz. May 14–19). IEEE, New York, pp. 1732–1737.

PAPADIMITRIOU, C. H. 1985. An algorithm for shortest-path motion in three dimensions. *Inf. Process. Lett. 20*, 5 (June), 259–263.

PAVLOV, V. V., AND VORONIN, A. N. 1984. The method of potential functions for coding constraints of the external space in an intelligent mobile robot. *Soviet Auto. Cont. 6*.

PREPARATA, F. P., AND SHAMOS, M. I. 1985. *Computational Geometry, An Introduction.* Springer-Verlag, New York.

QUEK, F. K. H., FRANKLIN, R. F., AND PONT, F. 1985. A decision system for autonomous robot navigation over rough terrain. In *Proceedings of SPIE Applications of Artificial Intelligence* (Boston).

RAO, N., IYENGAR, S., AND DESAUSSURE, G. 1988. The visit problem: Visibility graph-based solution. In *Proceedings of the IEEE International Conference on Robotics and Automation* (Philadelphia, Apr. 24–29). IEEE, New York, pp. 1650–1655.

REIF, J. ,H. 1979. Complexity of the mover's problem and generalizations, extended abstract. In *Proceedings of the IEEE Symposium on Foundations of Computer Science* (San Juan, Puerto Rico, Oct. 29–31), IEEE, New York, pp. 421–427.

REIF, J. H., AND SHARIR, M. 1985. Motion planning in the presence of moving obstacles. In *Proceedings of the 26th Annual IEEE Symposium on Foundations of Computer Science* (Portland, Oreg., Oct. 21–23). IEEE, New York, pp. 144–154.

REIF, J. H., AND STORER, J. A. 1988. 3-dimensional shortest paths in the presence of polyhedral obstacles. In *Proceedings of the IEEE Symposium on Foundations of Computer Science.* (White Plains, New York, Oct. 24–26), IEEE, New York, pp. 85–92.

REIF, J. H., AND STORER, J. A. 1985. Shortest paths in Euclidean space with polyhedral obstacles. Tech. Rep. CS-85-121, Computer Science Dept., Brandeis Univ., Waltham, Mass.

RICHBOURG, R. F., ROWE, N. C., ZYDA, M. J., AND McGHEE, R. B. 1987. Solving the global, two-dimensional routing problem using Snell's Law and A* search. In *Proceedings of the IEEE International Conference on Robotics and Automation* (Raleigh, N. Carol., Mar. 31–Apr. 3). IEEE, New York, pp. 1631–1636.

RIMON, E., AND KODITSCHEK, D. E. 1989. The construction of analytic diffeomorphism for exact robot navigation on star worlds. In *Proceedings of the IEEE International Conference on Robotics and Automation* (Scottsdale, Ariz., May 14–19). IEEE, New York, pp. 21–26.

RIMON, E., AND KODITSCHEK, D. E. 1988. Exact robot navigation using cost functions: The case of distinct spherical boundaries in E^n. In *Proceedings of the IEEE International Conference on Robotics and Automation* (Philadelphia, Apr. 24–29). IEEE, New York, pp. 1791–1796.

RUEB, K. D., AND WONG, A. K. C. 1987. Structuring free space as a hypergraph for roving robot path planning and navigation. *IEEE Trans. Patt. Anal. Machine Intell. PAMI-9*, 2 (Feb.), 263–273.

SCHWARTZ, J. T., AND SHARIR, M. 1983a. On the piano movers' problem: I. The case of a two-dimensional rigid polygonal body moving amidst polygonal barriers. *Commun. Pure Appl. Math. 36*, 3(May), 345–398.

SCHWARTZ, J. T., AND SHARIR, M. 1983b. On the piano movers' problem: III. Coordinating the motion of several independent bodies amidst polygonal barriers. *Int. J. Robotics Res. 2*, 3 (Fall), 46–75.

SCHWARTZ, J. T., AND SHARIR, M. 1981. On the piano movers' problem: II: Techniques for computing topological properties of real algebraic manifolds. Report No. 39, Courant Inst. of Mathematical Sciences. New York Univ.

SCHWARTZ, J. T., AND YAP, C. K. 1987. *Advances in Robotics, Vol. I, Algorithmic and Geometric Aspects of Robotics*. Erlbaum, Hillsdale, New Jersey.

SHAMOS, M. I., AND HOEY, D. 1975. Closest point problems. In *Proceedings of the 16th IEEE Symposium on Foundations of Computer Science* (Berkeley, Calif., Oct. 13–15), IEEE, New York, pp. 151–162.

SHARIR, M. 1987. Efficient algorithms for planning purely translational collision-free motion in two and three dimensions. In *Proceedings of the IEEE International Conference on Robotics and Automation* (Raleigh, N. Carol., Mar. 31–Apr. 3). IEEE, New York, pp. 1326–1331.

SHARIR, M., AND SCHORR, A. 1986. On shortest paths in polyhedral spaces. *SIAM J. Comput. 15*, 1(Feb.), 193–215.

SHARIR, M., AND SCHORR, A. 1984. On shortest paths in polyhedral spaces. In *Proceedings of the 16th Symposium on the Theory of Computing*. American Computing Machinery, pp. 144–153.

SHARIR, M., AND SIFRONY, S. 1988. Coordinated motion planning for two independent robots. In *Proceedings of the 4th Annual ACM Symposium on Computational Geometry* (Urbana, Ill., June 6–8). ACM, New York, pp. 319–328.

SHILLER, Z., AND DUBOWSKY, S. 1988. Global time optimal motions of robotic manipulators in the presence of obstacles. In *Proceedings of the IEEE International Conference on Robotics and Automation* (Philadelphia, Apr. 24–29). IEEE, New York, pp. 370–375.

SHIN, K. G., AND MCKAY, N. D. 1984. Open-loop minimum-time control of mechanical manipulators and its application. In *Proceedings of the American Control Conference* (San Diego, June 6–8). IEEE, New York, pp. 1231–1236.

SINGH, S., AND WAGH, M. D. 1987. Robot path planning using intersecting convex shapes. *IEEE J. Robotics Auto. RA-3*, 2 (Apr.), 101–108.

STRIP, D. R., AND MACIEJEWSKI, A. A. 1990. Archimedes: An experiment in automating mechanical assembly. In *The 11th International Conference on Assembly Automation* (Dearborn, Mich.). pp. MS90–839.

SURI, S. 1986. A linear time algorithm for minimum link paths inside a simple polygon. *Comput. Vision, Graph. Image Proc. 35*, 99–110.

TANNENBAUM, A., AND YOMDIN, Y. 1987. Robotic manipulators and the geometry of real semialgebraic sets. *IEEE J. Robotics Auto. RA-3*, 4 (Aug.), 301–307.

TARABANIS, K., TSAI, R. Y., AND ALLEN, P. K. 1991. Automated sensor planning for robotic vision task. In *Proceedings of the IEEE International Conference on Robotics and Automation* (Sacramento, Apr. 7–12). IEEE, New York, pp. 76–83.

TARSKI, A. 1951. *A Decision Method for Elementary Algebra and Geometry*, 2nd ed. University of California Press, Berkeley, Calif.

THORPE, C. E. 1984. Path relaxation: Path planning for a mobile robot. In *Proceedings of the AAAI* (Austin, Tex., Aug. 6–10). Morgan Kaufmann Publishers, Inc. Los Altos, Calif., pp. 318–321.

WARREN, C. W. 1989. Global path planning using artificial potential fields. In *Proceedings of the IEEE International Conference on Robotics and Automation* (Scottsdale, Ariz., May 14–19). IEEE, New York, pp. 316–321.

WELZL, E. 1985. Constructing the visibility graph for n line segments in $O(n^2)$ time. *Inf. Process. Lett. 20*, 4(May), 167–171.

WILFONG, G. 1989. Shortest path for autonomous vehicles. In *Proceedings of the IEEE International Conference on Robotics and Automation* (Scottsdale, Ariz., May 14–19). IEEE, New York, pp. 15–20.

WILFONG, G. 1988a. Motion planning for an autonomous vehicle. In *Proceedings of the IEEE International Conference on Robotics and Automation* (Philadelphia, Apr. 24–29). IEEE, New York, pp. 529–533.

WILFONG, G. 1988b. Motion planning in the presence of movable obstacles. In *Proceedings of the 4th Annual ACM Symposium on Computational Geometry* (Urbana, Ill., June 6–8). ACM, New York, pp. 279–288.

WILSON, R. H. 1992. On geometric assembly planning. Tech. Rep. STAN-CS-92-1416, Dept. of Computer Science, Stanford Univ., Stanford, Calif.

YAP, C. K. 1985. An $O(n \log n)$ algorithm for the Voronoi diagram of a set of simple curve segments. Rep. No. 43, Courant Inst. Robotics Laboratory, New York Univ.

YEUNG, D. Y., AND BEKEY, G. A. 1987. A decentralized approach to the motion planning prob-

lem for multiple mobile robots. In *Proceedings of the IEEE International Conference on Robotics and Automation* (Raleigh, N. Carol., Mar. 31–Apr. 3). IEEE, New York, pp. 1779–1784.

ZHU, D., AND LATOMBE, J. C. 1990. Constraint reformulation in a hierarchical path planner. In *Proceedings of the IEEE International Conference on Robotics and Automation* (Cincinnati, May 13–18). IEEE, New York, pp. 1918–1923.